CONTAINED MODES
IN INHOMOGENEOUS PLASMAS
AND THEIR INTERACTION
WITH HIGH ENERGY PARTICLES

by

CATERINA RICONDA

Laurea in Fisica, Università di Torino, Italy (1991)

Submitted to the Department of Physics
in Partial Fulfillment of the
Requirements for the
Degree of

DOCTOR OF PHILOSOPHY

at the

MASSACHUSETTS INSTITUTE OF TECHNOLOGY

February 1997

Signature of Author: _____

Department of Physics
December 1996

Certified by: _____

Bruno Coppi
Professor of Physics
Thesis Supervisor

Accepted by: _____

George Koster
Chairman,
Graduate Thesis Committee

CONTAINED MODES
IN INHOMOGENEOUS PLASMAS
AND THEIR INTERACTION
WITH HIGH ENERGY PARTICLES

by

CATERINA RICONDA

Submitted to the Department of Physics
in partial fulfillment of the requirements for the
Degree of Doctor of Philosophy in Physics at the
Massachusetts Institute of Technology

December 1996

ABSTRACT

In experiments with fusing plasmas, enhanced emission at the harmonics of the ion cyclotron frequency of the fusion products has been observed. In this thesis a model is developed that explains the main characteristics of the emission, in particular the fact that the radiation peaks occur at frequencies corresponding to harmonics of the α (or D) cyclotron frequency, Ω_α, at the outer edge of the plasma column. Our results indicate also a transition to a continuum spectrum at high frequencies that is consistent with the experiments.

The modes corresponding to the discrete spectrum, are localized near the plasma edge. The radial containment is in fact a fundamental characteristic of our model, since only contained modes can generate sufficient growth of the mode to justify the detected emission power levels. The instability evolves on a time scale that is shorter than the slowing-down time of α-particles, and so the distribution

function for the interacting particles, which are trapped particles near the outer edge of the plasma, can be described as strongly anisotropic in velocity space and having energies close to their value at birth from the fusion reaction. The contained mode is a solution to the ideal MHD equations, extended to include the Hall term, so the frozen-in law is replaced by the more general Ohm's equation $\vec{E} + \vec{v} \times \vec{B} = (1/en)\vec{J} \times \vec{B}$. We focus on quasi-flute modes with a high poloidal number, that are generalizations, to the case of an inhomogeneous plasma, of the magnetosonic-whistler modes. The wavevector has a small component parallel to the magnetic field, $k_{\parallel}$. The sensitivity of the localization of the mode to $k_{\parallel}$ effects increases with frequency, and the interval over which modes can be excited extends toward the center of the plasma column. This suggest a mechaninsm for the transition to a continuum spectrum, since more α-particles can interact with the mode. The growth rate can be evaluated using a full toroidal calculation for the particle dymanics. The growth rate depends linearly on the α-particle density, and can be of the order of the bounce frequency of the interacting α-particles.

Thesis Supervisor: Professor Bruno Coppi

3

TABLE OF CONTENTS

ACKNOWLEDGMENTS

I wish to express my gratitude to my advisor, Prof. Bruno Coppi for his constant advice, guidance and criticism. From him I learned a style of doing physics. His way of always focusing on the essence of a problem and his curiosity and open mind with respect to new results and problems in plasma physics have been a constant source of inspiration. Of course the process of learning has its harsh moments, but we know that "πάθηι μάθος".

I would also like to thank Prof. John Belcher and Prof. Thomas Greytak for their patience and kindness.

It is a pleasure to thank prof. Francesco Pegoraro for his willingness to discuss my research over the past five years. I cannot count the number of times when, being stuck on a problem, a discussion with him would give me new insight into it. He was the first person from whom I learned plasma physics as an undergraduate and his ability as a lecturer is evidenced by the fact that I decided to pursue this studies. He has also been a constant source of moral support and pleasant conversations.

I would like to express my gratitude to Gregg Penn, with whom I've worked in the past two years. With him I've spent long hours of discussion writing, and research. He is a great person, and has always been ready to help me when I needed it.

A very special thanks goes to Neer Asherie. The initial motivation for the work presented in this thesis came in part from him, and he made my first years at M.I.T. more "endurable" thanks to his openness, enthusiasm, readiness to share thoughts and physics' insights. I am deeply indebted to him.

My warmest thanks go to my husband, Ruben Levi, that has been a constant source of support and companionship, and as a former M.I.T. student himself, helped me a lot in dealing with the intricacies of M.I.T. His patience and his

understanding have been most valuable during this years. In particular I would like to thank him because without him I would never have scheduled a day for my thesis defense.

I wish to thank Franceso Rubini, with whom I spent a summer working in Pisa, for a fruitful collaboration and for his ironic attitude towards life.

I am grateful to Peter Catto, for his encouragement and for sharing with me some of his insight in physics. He's really a great teacher.

I wish to thank all the people in my group for sharing many years of meetings and discussions, Linda Sugiyama, Bill Daughton, George Svolos, Francesca Bombarda, Paolo Detragiache, Giuseppe Bertin, Franco Carpignano, Riccardo Betti for his encouragement, and particularly Stefano Migliuolo for his constant support, and for many useful conversations. I also wish to thanks Marika Contos for her patience.

During my stay at M.I.T. I have learned a great deal of physics during the classes and in conversation with many professors, among which I would like to mention: Mehran Kardar, John Tonry, Sergei Krasheninnikov, Alan Guth, Abraham Bers. A special thanks goes to Prof. Tonry for giving me further motivation to study physics while I was recitation instructor for his class, thanks to his rigorous and at the same time playful approach.

I also wish to thank Prof. George Koster for his great job as graduate program coordinator, and for his patience and attention to my needs.

I wish to express my gratitude to Peggy Berkovitz, Pat Solakoff, and all the women in the physics department with whom I interacted thanks to our monthly meetings. It's a nice way of getting together and it was always an opportunity I was looking forward to. Thanks to Raissa for being in charge of the organization.

In particular I would like to thank Peggy for..., how should I put it, for being Peggy!

I am very grateful to Beth Soll, for her classes and for her great sense of music. I really learned a lot from her.

6

Finally I would like to thank all my friends without whom I would not have been able to survive the cold Boston environment.

In particular, I would like to thank Patricia for many conversations during which we discovered a shared attitude towards life, as well as a deep understanding of each other. Einat for her enthusiasm, for many laughs and for her unwavering solidarity. Peter for his readiness to help me with my English, and for sharing the troubles of being a graduate student. Pablo and Maria for a longtime friendship.

Among the friends with whom I spent many lunches and coffee breaks, I would like to thank: Anne for teaching me how to be a "survivor", Marta for her sweetness, Paola for her energy and sharp mind, Vittorio for his calmness, Vincenzo for being such a talker, Sandra for always being there, Lorenzo for his contradictions, Felix for his good mood, Gilad for conversations about life and physics, and coffees at the CTP, Luca for his style, Domenico for his depth, Mark for his sense of humor, Franco for his orderliness, Maylise for her openness, Chahab for his generosity, and Raissa for not being a nerd.

Finally, I would like to thank the ASSTP (Associazione per lo Sviluppo Scientifico e Tecnologico del Piemonte), and the Physics Department at M.I.T. for financial support.

Chapter 0.

Introduction

Fusion reactions in plasmas produce a considerable population of high energy particles that can interact with the background thermal plasmas both by collisions and by collective modes. In 1991, two plasma discharges were produced by the JET (Joint European Torus) machine in England in which deuterium (D) and tritium (T) were the component nuclei. In fact this was the first time that a well confined plasma made of these two elements could be investigated. It is hoped that the reaction between deuterium and tritium will form the basis of a working fusion reactor:

$$D + T \rightarrow \ ^4He[3.56MeV] + n[14.03MeV]$$
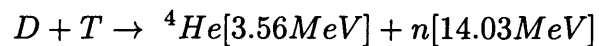
The α-particles [^4He] produced by the above reaction give rise to many interesting physical phenomena that have not yet been fully explored experimentally as well as theoretically. One such phenomenon is the emission of radiation at the cyclotron harmonics of the α-particles well above the thermal emission level, and thus called anomalous ion cyclotron emission (ICE). The detected spectrum[1,2] shows peaks at

the harmonics of $\Omega_\alpha = q_\alpha B(R)/m_\alpha$ for the lower harmonics, while above a critical harmonic number the spectrum becomes a continuum, that is, there is a superposition of the peaks. We recall that the magnetic field in a toroidal confinement device goes roughly as the inverse of the major radius of the torus so that the magnetic field is considerably lower at the outer edge with respect to the inner edge. The peaks of the cyclotron frequency are detected for values of Ω_α that correspond to values of the magnetic field B at the outer edge of the plasma column. This observation was quite unexpected as the bulk of the α-particle population is produced at the center of the plasma column.

Subsequently other experiments have been performed that included deuterium and tritium as fuel and that have detected anomalous ion cyclotron emission. These experiments were carried out in the TFTR[3,4,5] (Tokamak Fusion Test Reactor) machine at Princeton : a summary of the typical parameters for the D-T discharges in TFTR and in JET, as well as the main experimental results involving ion cyclotron emission, is given in appendix A.

The theory developed in this thesis explains the main features of these observations and indicates the possibility of extracting significant information about the fusion product population distribution, both in velocity space and over the plasma cross section. In addition, it is pointed out that α-particle transport may be influenced through coupling with externally applied modes having frequencies in the range considered, and thus this theory has relevance for the problem of ash control and removal.

Although the motivation to investigate a theoretical model describing the anomalous ion cyclotron emission came primarily from laboratory plasma experimental results, this problem is by no means restricted only to the laboratory. In fact wave fluctuations and the ion distribution function in the solar wind bow shock have been detected [28], that can excite an analogous mechanism of instability as the one examined in this thesis. Recently, a similar process has also been associated to cyclotron instability at the supernova shock[29].

9

In this thesis we study the mechanism that is thought to lie behind the observed anomalous cyclotron emission, and we explain the spectrum by considering a resonant interaction between fusion produced α-particles and a contained[6,7] compressional-whistler mode.

The first part of the thesis focuses on studying those modes the plasma can support that can be destabilized by hot particles[8,9], that is, which have frequencies in a range that can resonate with the α-particle cyclotron frequency at the outer edge of the plasma column, leading to a positive growth rate.

We find that for a realistic plasma configuration a broad class of modes that are radially localized exist, due to the presence of magnetic field and density gradients. By this we mean that we find a solution for the perturbed fields not travelling radially, $f(r)g(\theta, \zeta, t)$, such that $f(r)$ is a function of the minor radius of the torus, and goes to zero at the center of the colunm and at $r = a$, where a is the minor radius of the torus. The dispersion relation of these modes is very similar to that of the magnetosonic-whistler mode and becomes exactly that in the limit of a homogeneous plasma. We call this mode a "contained" mode and this solution can be described as a toroidal shell centered about the value r_{mode} that we call the radius of localization. We find that r_{mode} is close to the edge of the plasma; that is, the mode is spatially localized near the periphery of the plasma column. This feature is one of the strongholds of this analysis as this result can be correlated to the fact that the observed emission spectrum is seen as coming from the outer edge of the plasma.

The existence of these contained modes however is not enough to explain the spectrum. A driving mechanism must be found to produce emission at $\omega \sim \ell\Omega_\alpha$. There must be some source of "free energy"[10] that is released from the particles to the modes leading to exponential growth of the mode amplitude, to explain the detected power level well above the thermal emission. Velocity space anisotropy in the α-particles distribution function is the likely source of instability.

Only those particles which intersect the region where the mode is localized can resonate with the mode, and thus drive the emission. By studying the single

particle orbits we find that only trapped particles with large radial excursions can reach the mode, and these particles intersect the mode layer on the outer edge of the plasma, as explained in Chap. 4. Finally the growth rate γ is calculated in the framework of a linearized Vlasov-Maxwell theory.

The structure of this thesis is as follows: in Chapter 1 we identify for the sake of illustration the relevant mode in the homogeneous limit, the magnetosonic-whistler mode, and we look at the ions and electrons dynamics as well as at the field polarization and dispersion relation.

In Chapter 2 we find the mode equation for the contained magnetosonic-whistler mode, for the case of an inhomogeneous plasma. This equation is obtained by solving the extended magnetohydrodynamics (MHD) equations, including the Hall term in Ohm's law for the perturbed magnetic field. We focus on the case of a cold plasma in the frequency range $\omega \sim \ell\Omega_i$, considering a mode that is propagating mainly in the poloidal direction, perpendicular to the equilibrium magnetic field. We consider an equilibrium magnetic field configuration that corresponds to sheared field in a straight cylinder; this assumption corresponds to keeping the lowest order term in the inverse aspect ratio in a toroidal configuration. For the case of the high poloidal numbers that are of relevance to our problem, the first order toroidal corrections can easily be incorporated into the solution, and do not substantially alter the structure of the mode [6]. At first, we solve the mode equation neglecting propagation along the equilibrium magnetic field lines. This is justified by the fact that for frequencies of the order of the first harmonics of the cyclotron frequency the structure of the mode is not affected by parallel propagation as long as $k_\parallel \ll k_\perp$. The solution of the mode is studied analytically and then a numerical solution is obtained.

In Chapter 3 we show that if we look at higher frequencies, and thus at higher poloidal numbers, even for the case $k_\parallel \ll k_\perp$, propagation along the magnetic field lines becomes important: in this case it is said that the whistler part of the spectrum dominates, and a new class of localized solutions is identified.

In Chapter 4 we examine the single particle orbits for energetic α-particles in a toroidal configuration, to identify the class of fusion products that can reach the mode and thus have resonant interaction. We identify the region of parameters in phase space that defines that class.

In Chapter 5 we model the resonant α-particle distribution function, for a typical production rate. The model depends on the results of the analysis of Chapter 4, and includes general principles that impose constraints on the distribution function. Averaging of the distribution function over the periodic particle orbits is included.

In Chapter 6 we study the dependence of the growth rate on the ratio between the α-particles density and the electron density, n_α/n_e, in the framework of the linearized Maxwell-Vlasov equations.

In chapter seven we perform the calculation for the growth rate by using the ratio $n_\alpha/n_e \ll 1$ as an expansion parameter. We include in the calculation finite Larmor radius effects as well as the drifts due to the curvature and the gradient of the magnetic field, and we consider a gyrokinetic formulation.

Finally, in chapter eight we summarize our conclusions.

Chapter 1.

The Magnetosonic-Whistler Mode

We are interested in a mode that can interact with high energy fusion products giving rise to instability for frequencies that correspond to harmonics of the energetic particles' cyclotron frequency. For this reason we look at a mode whose frequency can be comparable to Ω_i and which allows for radially confined solutions. To this end, we examine the magnetosonic-whistler mode; it is well known that in a configuration with inhomogeneous magnetic field, density and temperature, it is possible to find radially localized solutions[6] for the perturbed fields. At the high frequencies under consideration, contained solutions exist for those modes which have high poloidal mode numbers and which propagate mainly in the perpendicular direction with respect to the equilibrium magnetic field,

The existence of contained modes is essential to justify the possibility of having a significant interaction of fusion products with magnetosonic-whistler modes, giving rise to a positive growth rate and subsequent emission. We note that if we were to consider a travelling wave in the radial direction, after a time $\sim a/\left(\frac{\partial \omega}{\partial k}\right)$ the wave would convect out of the plasma. This time scale however is short compared

to the inverse growth rate, so that the instability would not have time to grow. We can see this by comparing γ versus v_A/a, taking characteristic plasma parameters as reproduced in Table A-I: $\gamma/\Omega_i \sim n_\alpha/n_e \sim 10^{-3}$ while $v_A/(a\Omega_i) \sim 6 \times 10^{-2}$ so that $\gamma << v_A/a$. As a consequence only a localized solution will allow the development of the instability. Localization can also explain why emission is detected as coming from the outer edge of the plasma column.

We look at the homogeneous case as an illustration of the mode solution which we shall consider later. We refer to a collisionless, homogeneous, magnetized, cold plasma.

Section 1-1. The Magnetosonic Mode.

We first give a brief derivation for the magnetosonic wave that allows for an immediate visualization of the polarization and dispersion relation of the mode and of the role of the perturbed current and velocities for the different species in the plasma.

Let us consider a constant magnetic field in the z direction, $\vec{B}_0 = B_0\hat{z}$. We look for a perturbation of the form:

$$\vec{E}_1(t,y) = \vec{E}_1 e^{-i\omega t + ik_\perp y} \tag{1.1.1}$$

and we consider a range of frequencies such that $\Omega_e >> \omega > \Omega_i$, $\omega_{pi} >> \Omega_i$, and $\omega_{pe} \sim \Omega_e$. We consider a two fluid model, with electrons and one ions species. Each species satisfies the momentum equation:

$$-i\omega\vec{v}_{s1} = \frac{q_s}{m_s}\left(\vec{E}_1 + \vec{v}_{s1} \times \vec{B}_0\right) \tag{1.1.2}.$$

By neglecting the electron inertia we obtain:

$$v_{elx} = \frac{E_{1y}}{B_0} \tag{1.1.3}$$

$$v_{ely} = -\frac{E_{1x}}{B_0} \tag{1.1.4}.$$

14

These equations can be solved self-consistently with the relevant Maxwell's equations for an electromagnetic wave, where we can neglect the displacement current $(\omega \ll kc)$.

$$\vec{\nabla} \times \vec{E}_1 = i\omega \vec{B}_1 \qquad (1.1.5)$$

$$\vec{\nabla} \times \vec{B}_1 = \mu_0 \vec{j}_1 \qquad (1.1.6)$$

Here $\vec{j}_1 = \Sigma_s n_s q_s \vec{v}_{s1}$. Combining equations (1.1.5) and (1.1.6) we obtain:

$$\vec{\nabla}(\vec{\nabla} \cdot \vec{E}_1) - \nabla^2 \vec{E}_1 = i\omega \mu_0 \vec{j}_1 \qquad (1.1.7).$$

For a mode propagating in the y direction, the y component of Eq. (1.1.7) gives $J_{1y} = 0$ so that

$$v_{i1y} = v_{e1y} = -\frac{E_{1x}}{B_0} \qquad (1.1.8)$$

By substituting this into Eq. (1.1.2) we obtain

$$v_{i1x} = 0 \qquad (1.1.9).$$

Another form for v_{i1y} comes from the y component of Eq. (1.1.2), giving:

$$v_{i1y} = \frac{q_i E_{1y}}{-i\omega m_i} \qquad (1.1.10)$$

Thus the perturbed current, in the x direction, is carried only by the electrons. This current generates a perturbed magnetic field that is parallel to the equilibrium magnetic field. By equating Eq. (1.1.8) and (1.1.10) we have that the polarization of the mode is

$$E_{1y} = i\frac{\omega}{\Omega_i} E_{1x} \qquad (1.1.11).$$

We thus see that for $\omega > \Omega_i$, the projection of the perturbed electric field along the same direction of propagation of the wave becomes important and as the frequency grows becomes the largest component.

By taking the x component of Eq. (1.1.7) combined with Eq. (1.1.3), we obtain:

$$-i\frac{k_\perp^2}{\omega}E_{1x} = -\mu_0\frac{en_e}{B_0}E_{1y} \tag{1.1.12}$$

that combined with Eq. (1.1.11) gives the dispersion relation:

$$\omega^2 = k_\perp^2 v_A^2 \tag{1.1.13}$$

where $v_A^2 = B_0^2/(m_i n_i \mu_0)$.

We can summarize by saying that the magnetosonic wave is a wave propagating in the perpendicular direction to the equilibrium magnetic field, and is elliptically polarized with the largest component of the electric field along the direction of propagation of the wave, for frequencies above the ion cyclotron frequency. The perturbed current is zero in the direction of propagation of the wave and the electrons' motion is dominated by the $\vec{E} \times \vec{B}$ drift. The perturbed magnetic field has only one component, $B_{1\parallel}$, along the equilibrium magnetic field.

By the same procedure used to obtain equation (1.1.13) we can find the dispersion relation for the case of two ion species[1], for example Deuterium (D) and Tritium (T):

$$\omega^2 \frac{\omega^2 - \bar{\bar{\Omega}}^2}{\omega^2 - \Omega_{hy}^2} = k^2 \bar{v}_A^2 \tag{1.1.14}$$

Here $\bar{v}_A^2 = D_H(\alpha_D\Omega_D + \alpha_T\Omega_T)$, $D_H = B_0/(\mu_0 n_e q_e)$ $\Omega_{hy}^2 = \Omega_D\Omega_T(\bar{\bar{\Omega}}/\bar{\Omega})$, $\bar{\Omega} = \alpha_D\Omega_D + \alpha_T\Omega_T$, $\bar{\bar{\Omega}} = \alpha_D\Omega_T + \alpha_T\Omega_D$, $\alpha_D = n_D/n_e$, $\alpha_T = n_T/n_e$. A graphical display of Eq. (1.1.14) is given in Fig [1.1].

We note that if we consider for completeness a multi species plasma in order to include an impurity species, the main effect is to include a new cutoff and a new resonance, well below the frequency of interest for us, and instead of $\bar{v}_A$ we have ,

with I referring to the impurity species and Z_I to its charge, $v_{AI}^2 = D_H(\alpha_D\Omega_D + \alpha_T\Omega_T + Z_I\alpha_I\Omega_I)$, where $\alpha_I = n_I/n_e$. The relevant dispersion relation is given by:

$$\frac{\omega^2}{k_\perp^2 v_{AI}^2}\frac{\omega^2 - \Omega_1^2}{\omega^2 - \Omega_3^2}\frac{\omega^2 - \Omega_2^2}{\omega^2 - \Omega_4^2} = 1 \qquad (1.1.15)$$

where

$v_{AI}^2 = D_H(\alpha_D\Omega_D + \alpha_T\Omega_T + Z_I\alpha_I\Omega_I)$,

$D_H = B_0/(\mu_0 n_e q_e)$,

$\alpha_i = n_i/n_e, i = D, T, I$

$\bar{\Omega} = \alpha_D\Omega_D + \alpha_T\Omega_T$,

$\bar{\bar{\Omega}} = \alpha_D\Omega_T + \alpha_T\Omega_D$,

$Z_I = $ average charge of impurities,

$\Omega_{1,2} = [\Omega_S + (\Omega_S^2 - 4\Omega_M^2)^{1/2}]/2$,

$\Omega_S = \bar{\bar{\Omega}} + \Omega_I + Z_I\alpha_I(\Omega_D + \Omega_T - \Omega_I)$,

$\Omega_M^2 = \Omega_I\bar{\bar{\Omega}} + Z_I\alpha_I\Omega_D\Omega_T$,

Ω_3^2 and Ω_4^2 are the solutions of the equation

$$\omega^4 - \omega^2\frac{\Omega_{hy}^2\bar{\Omega} + \Omega_I^2\bar{\Omega} + Z_I\alpha_I\Omega_I(\Omega_D^2 + \Omega_T^2)}{\alpha_D\Omega_D + \alpha_T\Omega_T + Z_I\alpha_I\Omega_I}$$
$$+ \frac{\Omega_I\Omega_{hy}^2\Omega_M^2\bar{\Omega}}{\bar{\bar{\Omega}}(\alpha_D\Omega_D + \alpha_T\Omega_T + Z_I\alpha_I\Omega_I)} = 0$$

Figure [1.2] is a graphical display of Eq. (1.1.15) in which we have taken realistic values of the relevant parameters taken from Table I and we have assumed that the impurity species is partially ionized oxigen ($Z_I = 4.9$). It is evident from this that the new resonance and cutoff related to the presence of impurities are well below the ion cyclotron frequency. The introduction of this new cutoff and resonance should be considered in studying the corresponding contained mode for the purpose of analyzing the spectrum for frequencies below Ω_α as the observed emission shows some peaks in this range.

Section 1-2. The Magnetosonic-Whistler Mode

In the previous section we considered a mode propagating in the perpendicular direction respect to the equilibrium magnetic field, that is assumed to be in the z direction. Let us now consider a mode that is propagating at an arbitrary angle respect to the z axis. We will later focus on the limit of interest for us, that is $k_\parallel / k_\perp \ll 1$. We look at a perturbation of the form

$$\sim e^{-i\omega t + i\vec{k}\cdot\vec{x}} \tag{1.2.1}$$

where $\vec{k} = k_\perp \hat{y} + k_\parallel \hat{z}$.

We can find the dispersion relation for this mode by considering, as in the previous section, Eq.s (1.1.2) and (1.1.7). The electron dynamics is still dominated by the $\vec{E} \times \vec{B}$ drift, so that we can consider the electron velocity as given by Eq.s (1.1.3) and (1.1.4). For the ions we consider instead:

$$v_{i1x} = \frac{iq_i}{\omega m_i}\left[\frac{E_{1x} + (i\Omega_i/\omega)E_{1y}}{1 - \Omega_i^2/\omega^2}\right] \tag{1.2.2}$$

$$v_{i1y} = \frac{iq_i}{\omega m_i}\left[\frac{-iE_{1x}(\Omega_i/\omega) + E_{1y}}{1 - \Omega_i^2/\omega^2}\right] \tag{1.2.3}$$

$$v_{i1z} = \frac{iq_i}{\omega m_i}E_{1z} \tag{1.2.4}$$

We can now calculate the perturbed current and obtain two coupled equations for E_{1x} and E_{1y}. Since we are in the limit $\omega \ll \omega_{pe}$ the E_{1z} term decouples, as it is shown also in Fig. (1.3).

$$-\frac{c^2 k_\parallel^2}{\omega^2}E_{1y} = \frac{j_{1y}}{i\omega\epsilon_0} = \frac{\omega_{pi}^2}{\omega^2 - \Omega_i^2}E_{1y} + i\left(\frac{\Omega_i}{\omega}\frac{\omega_{pi}^2}{\omega^2 - \Omega_i^2} - \frac{\omega_{pe}}{\omega\Omega_e}\right)E_{1x} \tag{1.2.5}$$

$$-\frac{c^2 k^2}{\omega^2}E_{1x} = \frac{j_{1x}}{i\omega\epsilon_0} = \frac{\omega_{pi}^2}{\omega^2 - \Omega_i^2}E_{1x} - i\left(\frac{\Omega_i}{\omega}\frac{\omega_{pi}^2}{\omega^2 - \Omega_i^2} - \frac{\omega_{pe}}{\omega\Omega_e}\right)E_{1y} \tag{1.2.6}$$

We can solve for this equations and obtain:

18

$$\left(\frac{c^2 k_\parallel^2}{\omega^2} + \frac{\omega_{pi}^2}{\omega^2 - \Omega_i^2} \right) \left(\frac{c^2 k^2}{\omega^2} + \frac{\omega_{pi}^2}{\omega^2 - \Omega_i^2} \right) - \frac{\omega}{\Omega_i} \frac{\omega_{pi}^2}{\omega^2 - \Omega_i^2} = 0 \qquad (1.2.7)$$

Here we have used quasi-neutrality to substitute $\omega_{pi}^2/(\omega\Omega_1) = -\omega_{pe}/(\omega\Omega_e)$. We can expand Eq.(1.2.7) and explicitly write the equation for ω that is a fourth order equation.

$$\omega^4 - \omega^2 \left[k^2 v_A^2 + k_\parallel^2 v_A^2 \left(1 + \frac{k^2 v_A^2}{\Omega_i^2} \right) \right] + (k_\parallel v_A)^2 (k^2 v_A^2) = 0 \qquad (1.2.8)$$

We find two roots by solving Eq. (1.2.8) for ω^2, and we use $k^2 k_\parallel^2 \sim k_\perp^2 k_\parallel^2$ since $k_\perp \gg k_\parallel$. One root is given by $\omega^2 = k_\parallel^2 v_A^2$, and the other, that is the one of interest, is

$$\omega^2 = k_\perp^2 \left(v_A^2 + k_\parallel^2 D_H^2 \right) \qquad (1.2.9)$$

where $D_H = B_0/(\mu_0 n_e q_e) = v_A^2/\Omega_i$.

In the limit of $k_\parallel = 0$, Eq. (1.2.9) reproduces the usual dispersion relation for magnetosonic waves, Eq. (1.1.13). If we consider frequencies such that $\omega \sim \ell\Omega_i$, with ℓ an integer number, Eq. (1.2.9) is approximatly given by:

$$\omega^2 = k_\perp^2 v_A^2 + k_\parallel^2 v_A^2 \ell^2.$$

We thus see that in this range of frequencies even for $k_\perp/k_\parallel \ll 1$ the whistler correction can give a significant contribution.

To generalize Eq. (1.2.9) to the case of a two ion species plasma we have to substitute v_A with $\bar{v}_A$, as defined in Section [1.1], and ω^2 with the right hand side of Eq. (1.1.14). Analogously we can include impurities as a third species. A schematic representation of the magnetosonic-whistler mode is presented in Fig. (1.3). As we said before E_{1z} can be neglected and we can obtain the same result by using the extended MHD equations that include the Hall term in Ohm's law instead of the two fluids approach. This will be more convenient when we study the case of an inhomogenous plasma in Chapter 2.
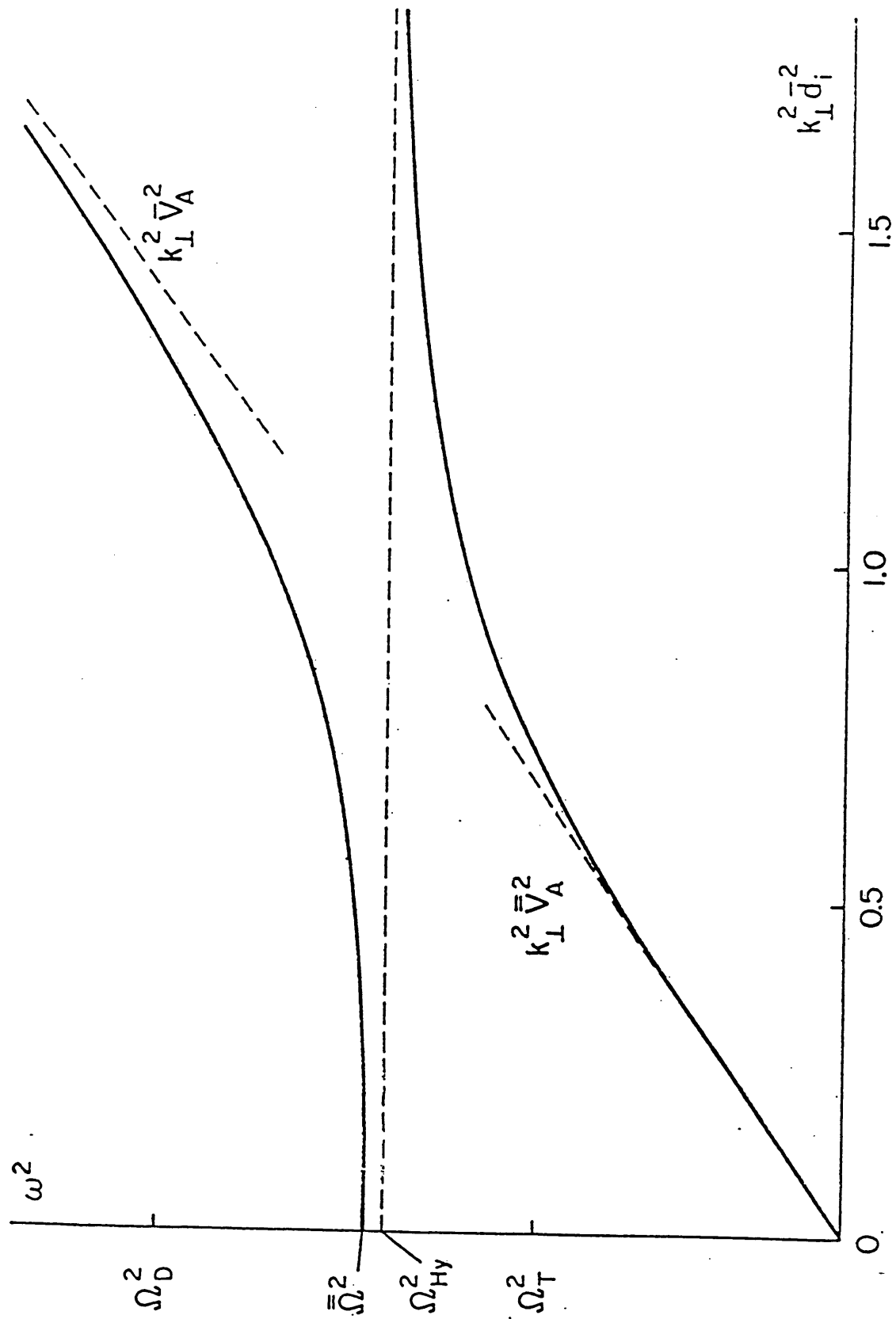
Figure 1.1 The dispersion relation for the magnetosonic mode for the case of two ion species.
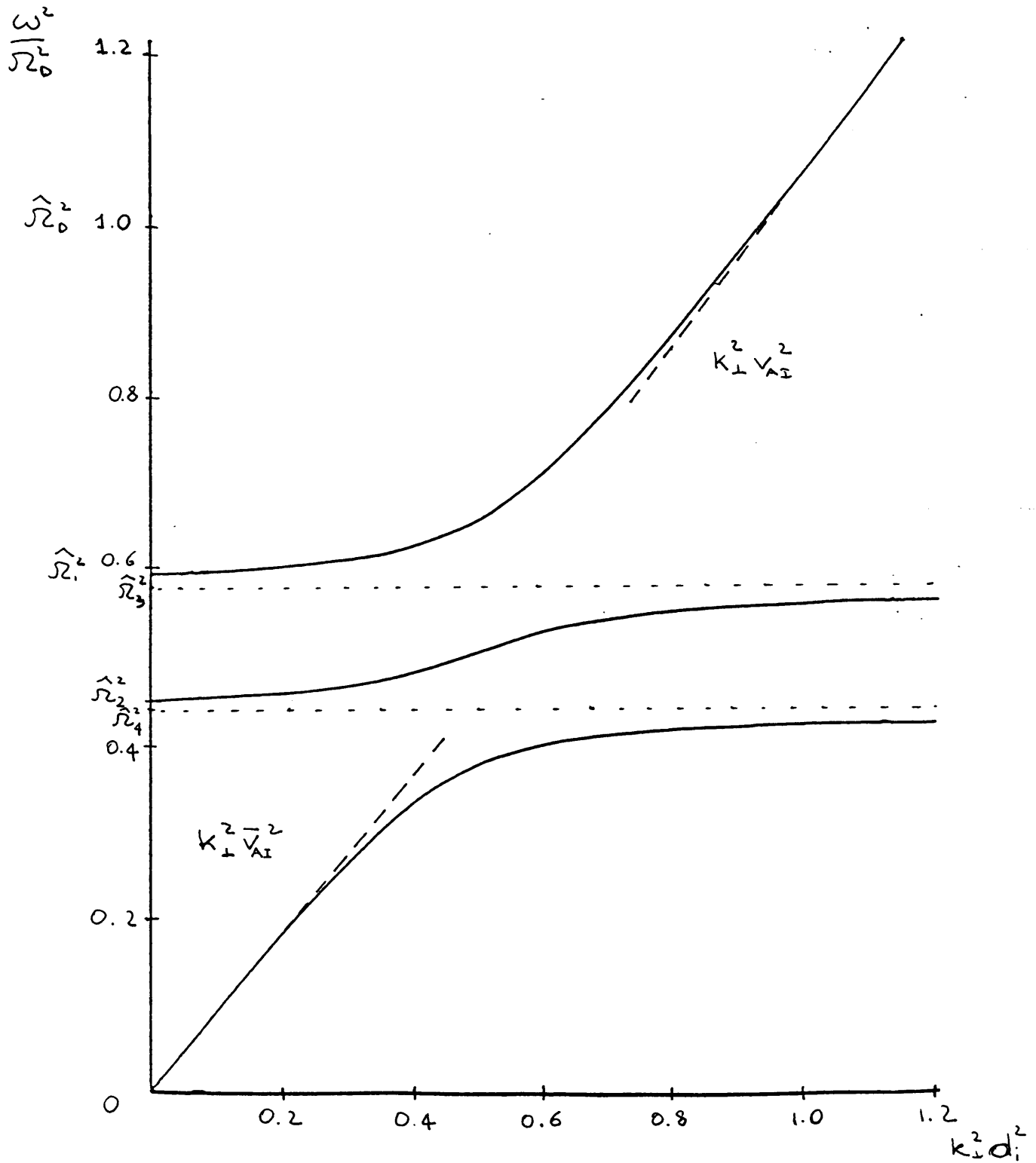
Figure 1.2 The dispersion relation for the magnetosonic mode for the case of three ion species, where one of the species is given by impurities with charge $Z_I = 4.9$
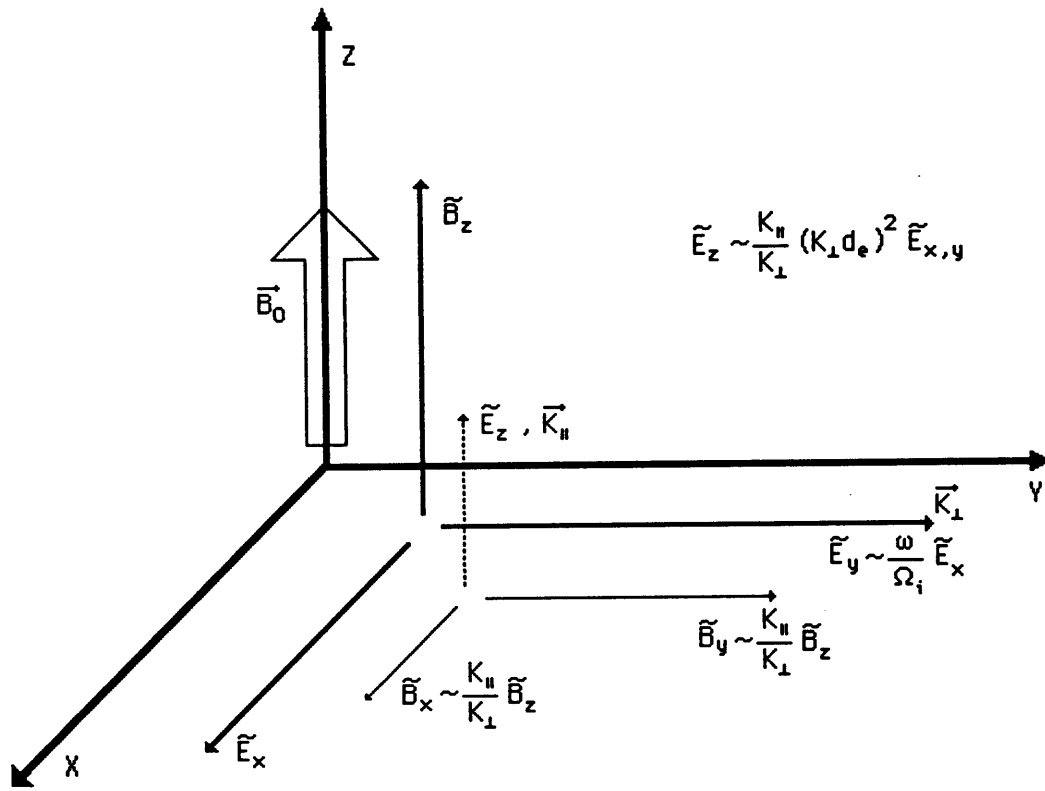
Figure 1.3 A schematic representation of the magnetosonic-whistler mode, in the limit $k_\perp/k_\parallel \ll 1$. The dispersion relation of this mode is $\omega^2 = k_\perp^2 (v_A^2 + k_\parallel^2 D_H^2)$. For $k_\parallel \to 0$ the perturbed magnetic field has only a parallel component.

Chapter 2.

The Mode Structure.

A Contained-Interactive Mode.

In this chapter we derive the differential equations that govern the behavior of the perturbed fields in an inhomogeneous plasma focusing on those solutions that in the limit of a homogeneous plasma reduce to magnetosonic-whistler waves as described in Chapter 1. In Section 2.1 we derive the differential for the contained magnetosonic-whistler mode. In Section 2.2 we solve this equation in the limit of a mode that does not propagate along the equilibrium magnetic field ($k_\parallel = 0$). We examine this case for the sake of clarity and since it is the relevant solution for frequencies that correspond to the lowest harmonics of the cyclotron frequencies. In Chapter 3 we analyze how this solution is affected by propagation along the equilibrium magnetic field.

Since the relevant frequencies are in the range $\omega \sim \ell\Omega_i$, where ℓ is an integer, we will look at modes rapidly varying along the poloidal direction. In addition, $\omega \ll \Omega_e$. We consider an inhomogeneous, collisionless, cold plasma with one

main ion species and use the extended magnetohydrodynamics (MHD) equations, that include the Hall term as the first relevant correction to the frozen-in law for frequencies comparable to the ion cyclotron frequency. The cold plasma assumption is justified by the fact that $k_\perp \rho_i << 1$ for the modes of interest. The relevant values of $k_\perp$ are given by $\omega \sim k_\perp v_A \sim \ell \Omega_i$. By using this we can show that $k_\perp \rho_i \sim \ell v_{\text{th}i}/v_A$. If we consider $T_i \simeq 10$ keV, $B \simeq 1$ T and $n_e \simeq 10^{13}$ cm^{-3} we have $v_{\text{th}i}/v_A \simeq 3 \times 10^{-2}$.

Section 2-1. The Mode Equation.

Let consider the following set of equations[26]:

$$\frac{\partial}{\partial t}n + \vec{\nabla}\cdot(n\vec{V}) = 0 \qquad (2.1.1)$$

$$nm_i\frac{\partial}{\partial t}\vec{V} = \vec{J}\times\vec{B} \qquad (2.1.2)$$

$$\vec{E} + \vec{V}\times\vec{B} = \frac{1}{en}(\vec{J}\times\vec{B}) \qquad (2.1.3)$$

$$\vec{\nabla}\times\vec{E} = -\frac{\partial}{\partial t}\vec{B} \qquad (2.1.4)$$

$$\vec{\nabla}\times\vec{B} = \mu_0\vec{J} \qquad (2.1.5)$$

$$\vec{\nabla}\cdot\vec{B} = 0 \qquad (2.1.6)$$

We recall that the term that appears on the right hand side of Ohm's law, Eq. (2.1.3), is the so called Hall term. We look at an equilibrium situation where $\vec{V}_0 = 0$, $\vec{E}_0 = 0$ and we consider a magnetic field configuration represented by

$$\vec{B}_0 = B_{z0}(r)\vec{e}_z + B_{\theta0}(r)\vec{e}_\theta \qquad (2.1.7)$$

It is convenient to introduce the following set of coordinates:

$$\vec{e}_{\parallel} = \frac{\vec{B}_0}{|\vec{B}_0|}, \qquad \vec{e}_r, \qquad \vec{e}_{\perp} = \frac{\vec{B}_0 \times \vec{e}_r}{|\vec{B}_0|} \qquad (2.1.8)$$

We solve the linearized equations for a perturbation of the form

$$\vec{B}_1 = \vec{B}_1(r) \exp(-i\omega t - im\theta + ik_z z)$$

Without loss of generality, we consider $\omega > 0$. Defining the k-vector as $\vec{k} = -(m/r)\vec{e}_\theta + k_z\vec{e}_z$, the appropriate components for our set of coordinates are $k_{\parallel} = \vec{k} \cdot \vec{e}_{\parallel}$ and $k_{\perp} = \vec{k} \cdot \vec{e}_{\perp}$.

Since the main component of $\vec{B}_1$ is in the parallel direction, we solve for the parallel component of the perturbed magnetic field, $B_{1\parallel}$. It is customary to introduce $\vec{V}_1 = -i\omega\vec{\xi}_1$. We obtain by linearizing Eq. (2.1.2) the following equation relating $\vec{\xi}_1$ and $\vec{B}_1$:

$$\vec{\xi}_1 = \frac{1}{\mu_0 \rho_0 \omega^2} \left[\vec{\nabla}(\vec{B}_0 \cdot \vec{B}_1) - (\vec{B}_0 \cdot \vec{\nabla})\vec{B}_1 - (\vec{B}_1 \cdot \vec{\nabla})\vec{B}_0 \right] \qquad (2.1.9)$$

where $\rho_0 = m_i n_{i0}$. The second equation for $\vec{\xi}_1$ and $\vec{B}_1$ comes from taking the curl of the linearized form of Eq. (2.1.4):

$$\vec{E}_1 - i\omega\vec{\xi}_1 \times \vec{B}_0 = \frac{1}{en} \left(\vec{J}_1 \times \vec{B}_0 + \vec{J}_0 \times \vec{B}_1 \right) \qquad (2.1.10)$$

which combined with Eq. (2.1.2) yields

$$\vec{B}_1 = -\vec{B}_0(\vec{\nabla} \cdot \vec{\xi}_1) + (\vec{B}_0 \cdot \vec{\nabla})\vec{\xi}_1 - (\vec{\xi}_1 \cdot \vec{\nabla})\vec{B}_0 + i\frac{\omega m_i}{e}(\vec{\nabla} \times \vec{\xi}_1) \qquad (2.1.11)$$

By introducing the configuration of the field given by Eq. (2.1.7) we can solve for $B_{1\parallel}$; note that Eq. (2.1.1) is not used, because it is not necessary to solve for n_1.

Rewriting Eq. (2.1.10) and Eq. (2.1.12) by components, and defining $\eta = B_{\theta 0}/B_{\zeta 0}$ we find:

25

$$\xi_{1r} = \frac{B_0}{\mu_0 \rho_0 \omega^2} \left[\frac{dB_{1\parallel}}{dr} - ik_\parallel B_{1r} + \frac{\eta^2}{r(1+\eta^2)} B_{1\parallel} + \frac{2\eta}{r(1+\eta^2)} B_{1\perp} \right] \quad (2.1.12)$$

$$\xi_{1\perp} = \frac{B_0}{\mu_0 \rho_0 \omega^2} \left[i\left(k_\perp B_{1\parallel} - k_\parallel B_{1\perp} \right) - \frac{B_{1r}}{(1+\eta^2)} \left(\frac{\eta}{r} + \frac{d\eta}{dr} \right) \right] \quad (2.1.13)$$

$$\xi_{1\parallel} = 0 \quad (2.1.14)$$

$$B_{1r} = k_\parallel B_0 \left(i\xi_{1r} + \frac{\omega}{\Omega_i} \xi_{1\perp} \right) \quad (2.1.15)$$

$$B_{1\perp} = ik_\parallel B_0 \left(\xi_{1\perp} + i\frac{\omega}{\Omega_i} \xi_{1r} \right) + \frac{B_0}{(1+\eta^2)} \left(\frac{d\eta}{dr} - \frac{\eta}{r} \right) \left(i\xi_{1r} + \frac{\omega}{\Omega_i} \xi_{1\perp} \right) \quad (2.1.16)$$

$$B_{1\parallel} = -ik_\perp B_0 \left(\xi_{1\perp} + i\frac{\omega}{\Omega_i} \xi_{1r} \right) + \frac{2\eta^2}{(1+\eta^2)} B_0 \frac{\xi_{1r}}{r}$$
$$- \frac{B_0}{r} \frac{d}{dr}(r\xi_{1r}) + i\frac{\omega}{\Omega_i} \frac{1}{r} \frac{d}{dr}\left(r\xi_{1\perp} B_0 \right) \quad (2.1.17)$$

In the limit of $k_\parallel \ll k_\perp$, $\eta \ll 1$, $B_{1\parallel}$ and $\xi_{1\perp}$ are the main components.

Since $\vec{B}_1$ is constrained by the condition by $\vec{\nabla} \cdot \vec{B} = 0$, we find it more convenient to replace Eq. (2.1.17) with:

$$\vec{\nabla} \cdot \vec{B}_1 = \frac{1}{r} \frac{d}{dr}(rB_{1r}) + ik_\parallel B_{1\parallel} + ik_\perp B_{1\perp} = 0 \quad (2.1.18)$$

We will now derive a mode equation for $B_{1\parallel}$ starting from Eq. (2.1.18) by solving for $B_{1\perp}$ and B_{1r} in terms of $B_{1\parallel}$ and $dB_{1\parallel}/(dr)$ only. We obtain from Eqs. (2.1.12) through (2.1.16) an equation for B_{1r}:

$$iB_{1r}S = P_r B_{1\parallel} + Q_r \frac{dB_{1\parallel}}{dr} \quad (2.1.19)$$

26

where

$$S = \left(1 - \frac{k_{\parallel}^2 v_A^2}{\omega^2}\right)^2 - \frac{k_{\parallel}^4 v_A^4}{\omega^2 \Omega_i^2} + \frac{4\eta}{r(1+\eta^2)} \frac{k_{\parallel} v_A^2}{\omega \Omega_i}$$

$$- \frac{2\eta^2 v_A^2}{r^2(1+\eta^2)^2 \omega^2}\left[1 + \frac{k_{\parallel}^2 v_A^2}{\omega^2}\left(1 - \frac{\omega^2}{\Omega_i^2}\right)\right]$$

$$+ \frac{2\eta v_A^2}{r(1+\eta^2)^2 \omega^2}\frac{d\eta}{dr}\left[1 - \frac{k_{\parallel}^2 v_A^2}{\omega^2}\left(1 - \frac{\omega^2}{\Omega_i^2}\right)\right] \qquad (2.1.20)$$

$$Q_r = -\frac{k_{\parallel} v_A^2}{\omega^2}\left[1 - \frac{k_{\parallel}^2 v_A^2}{\omega^2}\left(1 - \frac{\omega^2}{\Omega_i^2}\right)\right] \qquad (2.1.21)$$

$$P_r = -\frac{k_{\parallel} k_{\perp} v_A^2}{\omega \Omega_i} + \frac{2\eta}{(1+\eta^2)}\frac{k_{\perp}}{r}\frac{v_A^2}{\omega^2}\frac{k_{\parallel}^2 v_A^2}{\omega^2}\left(1 - \frac{\omega^2}{\Omega_i^2}\right)$$

$$- \frac{\eta}{(1+\eta^2)}\frac{k_{\parallel}}{r}\frac{v_A^2}{\omega^2}\left[1 - \frac{k_{\parallel}^2 v_A^2}{\omega^2}\left(1 - \frac{\omega^2}{\Omega_i^2}\right)\right] \qquad (2.1.22)$$

The equation for $B_{1\perp}$ is given by:

$$B_{1\perp} S = P_{\perp} B_{1\parallel} + Q_{\perp}\frac{dB_{1\parallel}}{dr} \qquad (2.1.23)$$

where

$$Q_{\perp} = -\frac{k_{\parallel} v_A^2}{\omega \Omega_i}$$

$$+ \frac{\eta v_A^2}{r(1+\eta^2)\omega^2}\left[1 + \frac{k_{\parallel}^2 v_A^2}{\omega^2}\left(1 - \frac{\omega^2}{\Omega_i^2}\right)\right]$$

$$- \frac{v_A^2}{r(1+\eta^2)\omega^2}\frac{d\eta}{dr}\left[1 - \frac{k_{\parallel}^2 v_A^2}{\omega^2}\left(1 - \frac{\omega^2}{\Omega_i^2}\right)\right] \qquad (2.1.24)$$

$$P_{\perp} = -\frac{v_A^2 k_{\perp} k_{\parallel}}{\omega^2}\left[1 - \frac{k_{\parallel}^2 v_A^2}{\omega^2}\left(1 - \frac{\omega^2}{\Omega_i^2}\right)\right]$$

$$+ \frac{\eta v_A^2}{r\omega\Omega_i}\frac{(k_{\perp} - \eta k_{\parallel})}{(1+\eta^2)} - \frac{d\eta}{dr}\frac{1}{(1+\eta^2)}\frac{k_{\perp} v_A^2}{\omega \Omega_i}$$

$$+ \frac{\eta^3 v_A^2}{r^2(1+\eta^2)\omega^2}\left[1 + \frac{k_{\parallel}^2 v_A^2}{\omega^2}\left(1 - \frac{\omega^2}{\Omega_i^2}\right)\right]$$

$$- \frac{\eta^2 v_A^2}{r(1+\eta^2)^2 \omega^2}\frac{d\eta}{dr}\left[1 - \frac{k_{\parallel}^2 v_A^2}{\omega^2}\left(1 - \frac{\omega^2}{\Omega_i^2}\right)\right] \qquad (2.1.25)$$

and where S is the same as before. To obtain the mode equation we use Eqs. (2.1.19), (2.1.23) and (2.1.18) to find:

$$\frac{d^2 B_{1\parallel}}{dr^2} + \left[\frac{1}{rQ_r}\frac{d}{dr}(rQ_r) + \frac{(P_r - k_\perp Q_\perp)}{Q_r} - \frac{1}{S}\frac{dS}{dr}\right]\frac{dB_{1\parallel}}{dr} \qquad (2.1.26)$$

$$+ \left[\frac{1}{rQ_r}\frac{d}{dr}(rP_r) - \frac{(Sk_\parallel + P_\perp k_\perp)}{Q_r} - \frac{P_r}{Q_r S}\frac{dS}{dr}\right] B_{1\parallel} = 0$$

We are interested in the limit where $k_\parallel \ll k_\perp$ and $\eta \ll 1$, so we explicitly evaluate the various terms in the previous equation neglecting all the η corrections and keeping only the leading order corrections in $k_\parallel / k_\perp$.

$$\frac{1}{rQ_r}\frac{d}{dr}(rQ_r) = \frac{1}{r(v_A^2 + k_\parallel^2 D_H^2)}\frac{d}{dr}\left[r(v_A^2 + k_\parallel^2 D_H^2)\right] + \mathcal{O}\left(\frac{1}{r}\frac{k_\parallel^2 v_A^2}{\omega^2}\right)$$

$$\frac{(P_r - k_\perp Q_\perp)}{Q_r} \sim \mathcal{O}\left(\frac{\eta}{r}\right)$$

$$\frac{1}{S}\frac{dS}{dr} \sim \mathcal{O}\left(\frac{1}{r}\frac{k_\parallel^2 v_A^2}{\omega^2}\right)$$

$$\frac{1}{rQ_r}\frac{d}{dr}(rP_r) = \frac{k_\perp \omega}{v_A^2 + k_\parallel^2 D_H^2 - k_\parallel^2 D_H^2 \frac{\Omega_i^2}{\omega^2}}\frac{d}{dr}(D_H) + \mathcal{O}\left(\frac{\eta}{r^2}\right)$$

$$\frac{Sk_\parallel + P_\perp k_\perp}{Q_r} = k_\perp^2 - \frac{\omega^2}{\left(v_A^2 + k_\parallel^2 D_H^2 - k_\parallel^2 D_H^2 \frac{\Omega_i^2}{\omega^2}\right)}$$

$$+ k_\parallel^2 \left(1 + \frac{v_A^2}{\left(v_A^2 + k_\parallel^2 D_H^2 - k_\parallel^2 D_H^2 \frac{\omega^2}{\Omega_i^2}\right)}\right)$$

$$+ \mathcal{O}\left(\frac{k_\parallel^2}{k_\perp^2}\frac{\omega}{\Omega_i}\frac{1}{k_\perp r}\right) + \mathcal{O}\left(\frac{\eta}{r^2}\right)$$

28

$$\frac{P_r}{Q_r S}\frac{dS}{dr} \sim \mathcal{O}\left(\frac{k_\parallel^2}{k_\perp^2}\frac{\omega}{\Omega_i}\frac{k_\perp}{r}\right) + \mathcal{O}\left(\frac{\eta}{r^2}\right)$$

We see that for frequencies $\omega \sim p\Omega_i = pv_A^2/D_H$ we can neglect quantities on the order of $k_\parallel^2 D_H^2/(p^2 v_A^2) = k_\parallel^2 d_i^2/p^2$ while keeping corrections on the order of $k_\parallel^2 D_H^2/v_A^2$. For $k_\parallel^2 << k_\perp^2$, the mode equation for $B_{1\parallel}$ reduces to:

$$\frac{1}{r\left(v_A^2 + k_\parallel^2 D_H^2\right)}\frac{d}{dr}\left[r\left(v_A^2 + k_\parallel^2 D_H^2\right)\frac{dB_{1\parallel}}{dr}\right]$$

$$+ \left[\frac{\omega^2}{v_A^2 + k_\parallel^2 D_H^2} - k_\perp^2 + \frac{\omega k_\perp}{v_A^2 + k_\parallel^2 D_H^2}\frac{d}{dr}(D_H)\right]B_{1\parallel}$$

$$+ \mathcal{O}\left(k_\parallel^2 B_{1\parallel}, \frac{k_\parallel^2 k_\perp D_H^2}{rpv_A^2}B_{1\parallel}, \frac{\eta}{r^2}B_{1\parallel}\right)$$

We can thus write the final form for our equation as:

$$\frac{d}{dr}\left[r\left(v_A^2 + k_\parallel^2 D_H^2\right)\frac{dB_{1\parallel}}{dr}\right] \qquad (2.1.27)$$

$$+ \left[r\omega^2 + \omega\frac{d}{dr}(rk_\theta D_H) - k_\theta^2 r(v_A^2 + k_\parallel^2 D_H^2)\right]B_{1\parallel} = 0$$

where $k_\theta = -m/r$. Here $D_H \propto B_0/n(r)$, so that the spatial derivative of D_H is proportional to the density gradient.

The Hall term is responsible for the appearance in this equation of the quantity $k_\parallel^2 D_H^2$ and the term which is linear in both D_H and k_θ. The term linear in k_θ is related to inhomogeneity and is absent in the case of a homogenous plasma, as is clear from Eq. (2.1.27).

Section 2-2. The Contained-Interactive Magnetosonic Mode

For the sake of simplicity we neglect at first the term $k_\parallel^2 D_H^2$ and, using the fact that $D_H = v_A^2/\Omega_i$, the mode equation reduces to:

$$\frac{1}{rv_A^2}\frac{d^2}{dr^2}\left(rv_A^2 B_{1\parallel}\right) + \left[\frac{\omega^2}{v_A^2} + \frac{\omega^2}{v_A^2 r}\frac{d}{dr}\left(\frac{rk_\theta v_A^2}{\omega\Omega_i}\right) - k_\theta^2\right] B_{1\parallel} = 0 \qquad (2.2.1)$$

Note that the effect of the Hall term still appears through the term linear in k_θ, that breaks the symmetry in the $\pm$ poloidal direction. Subsequently we define $b_1 = B_{1\parallel}\sqrt{rv_A^2}$ and we obtain the following equation:

$$\frac{d^2 b_1}{dr^2} + \left[\frac{\omega^2}{v_A^2} + \frac{\omega}{v_A^2 r}\frac{d}{dr}\left(\frac{rk_\theta v_A^2}{\Omega_i}\right) - k_\theta^2\right. \qquad (2.2.2)$$
$$\left. - \frac{1}{4}\left(\frac{1}{rv_A^2}\frac{d\,rv_A^2}{dr}\right)^2 - \frac{1}{2}\frac{d}{dr}\left(\frac{1}{rv_A^2}\frac{d\,rv_A^2}{dr}\right)\right] b_1 = 0$$

Defining Δ as the typical scale of variation of b_1, as given by the solution of Eq. (2.2.2). In this equation, the first term scales with $1/\Delta^2$ and the last two terms as $1/r^2$. Since we look for a localized solution, we can consider the limit where $1/\Delta^2 >> 1/r^2$ and neglect the last two terms. The existence of such a solution will be verified *a posteriori.*

With these assumptions the equation for b_1 is:

$$\frac{d^2 b_1}{dr^2} - V_{\text{eff}}(r,\omega)b_1 = 0 \qquad (2.2.3)$$

where

$$V_{\text{eff}} \equiv -\frac{\omega^2}{v_A^2} - \frac{\omega}{v_A^2 r}\frac{d}{dr}\left(\frac{rk_\theta v_A^2}{\Omega_i}\right) + k_\theta^2$$

To find a localized solution, we Taylor expand this effective potential around its minimum, that we call r_{mode}. Eq. (2.2.3) thus becomes

$$\frac{d^2 b_1}{dr^2} - \left\{V_{\text{eff}}(r_{\text{mode}},\omega) + \frac{d^2 V_{\text{eff}}(r_{\text{mode}},\omega)}{dr^2}\frac{(r - r_{\text{mode}})^2}{2}\right\} b_1 = 0 \qquad (2.2.4)$$

By doing this we approximate our equation with the Hermite equation. The solutions will be localized around the surface $r = r_{\text{mode}}$ and have the form:

$$b_1(r) = b_1 H_s \left(\frac{r - r_{\text{mode}}}{\Delta} \right) \exp \left(-\frac{(r - r_{\text{mode}})^2}{2\Delta^2} \right) \qquad (2.2.5)$$

where s is the positive integer index of the eigenfunction and the functions H_s are Hermite polynomials. We recall that as traditionally studied in quantum mechanics the Hermite equation represent the solution to the harmonic oscillator and can be satisfied only for discrete values of the energy. In our case instead this condition defines the dispersion relation for the mode, that is, $\omega(k)$ that will be dependent on the positive integer index of the eigenfunction.

The solution of Eq. (2.2.4) is expressed in the form of Eq. (2.2.5) in terms of two unknowns, the localization of the mode, r_{mode}, and the width of the mode, Δ. These unknowns, together with the dispersion relation, can be found by substituting $b_1(r)$ as given by Eq. (2.2.5) in Eq. (2.2.4), and by imposing the condition that r_{mode} is a minimum of the effective potential, V_{eff}. Thus the equations determining r_{mode}, ω, and Δ are given by:

$$\frac{dV_{\text{eff}}(\omega, r_{\text{mode}})}{dr} = 0 \qquad (2.2.6)$$

$$V_{\text{eff}}(\omega, r_{\text{mode}}) = -(2s + 1)/\Delta^2 \qquad (2.2.7)$$

$$\frac{d^2 V_{\text{eff}}(\omega, r_{\text{mode}})}{dr^2} = 2/\Delta^4 \qquad (2.2.8)$$

We solve for these simultaneous equations by expanding ω in powers of $1/m$ since we are interested in high poloidal numbers. We consider the orderings $\omega = \omega_0 + \delta\omega_s + O(\omega/m^2)$, and $r_{\text{mode}} = r_0 + \delta r + O(r/m^2)$, and we introduce the length scale $d_i = v_A/\Omega_i = c/\omega_{pi}$; d_{i0} is this quantity evaluated at $r = 0$.

Since we will find that the solutions can be very different for positive or negative $k_\perp$, we write explicitly $m = \sigma_m |m| = \pm|m|$. The lowest order frequency ω_0 is defined by the dispersion relation obtained by setting $V_{\text{eff}}(\omega_0, r_0) = 0$, which can be rewritten as

$$\omega_0 = \frac{|m|v_A}{r}\left[1 - \sigma_m d_i \frac{n'}{n}\frac{\omega_0 r}{|m|v_A}\right]^{1/2}\Bigg|_{r=r_0} \tag{2.2.9}$$

Recall that we impose the condition that ω_0 is positive. Combining Eq. (2.2.9) together with $V'_{\text{eff}}(\omega_0, r_0) = 0$, r_0 satisfies the equation:

$$2 + r\frac{n'}{n} + \sigma_m d_i \left(\frac{rn'}{n}\right)'\left[1 - \frac{n'}{n}\frac{2 + rn'/n}{(rn'/n)'}\right]^{1/2}\Bigg|_{r=r_0} = 0 \tag{2.2.10}$$

and the width of the mode is given by

$$\frac{1}{\Delta^4} = \frac{m^2}{r^4}\left(3 - \frac{r^2}{2}\frac{1}{N}\frac{d^2 N}{dr^2}\right) \tag{2.2.11}$$

where $N = n\left(1 + \frac{d_{i0}^2 n'}{rn}\frac{n_0}{n}\frac{m\Omega_i}{\omega}\right)\Bigg|_{r=r_0}$.

From these quantities we can evaluate the next higher order correction to the frequency,

$$\delta\omega_s = -\frac{(2s+1)}{\Delta^2}\left(\frac{\partial V_{\text{eff}}(\omega_0, r_0)}{\partial \omega_0}\right)^{-1} \propto \frac{\omega}{m} \tag{2.2.12}$$

The solution is not greatly affected by δr corrections since $\delta r << \Delta$.

This set of coupled equations can be easily solved and a summary of the solutions is reproduced in Table 2-I, for typical parameters and density profiles. Before examining these solutions however, we wish to study these equations comparing them with the ideal MHD case, that is without the Hall term, to show how including this term in Eq. (2.1.3) changes significantly the perturbed field solutions. To do so we approximate these equations by expanding in the small parameter d_i/a around the ideal MHD solution . The ideal MHD solution is independent of σ_m and is given by

$$\omega_{\text{MHD}} = \frac{|m|v_A}{r}\Bigg|_{r=r_{\text{MHD}}}$$

where r_{MHD} is the solution of

$$r_{\text{MHD}} = -2\frac{n}{n'}\bigg|_{r=r_{\text{MHD}}}$$

It becomes apparent that for realistic values of d_i/a we need to keep second order terms in the expansion. We can thus rewrite Eq. (2.2.9) and Eq. (2.2.10) for $\omega_0/\omega_{\text{MHD}}$ and $r_0 - r_{\text{MHD}}$ as

$$\frac{\omega_0}{\omega_{\text{MHD}}} = 1 + \left[-\frac{r_0 - r_{\text{MHD}}}{r} + \left(\frac{r_0 - r_{\text{MHD}}}{r} \right)^2 \left(1 + \frac{r^2 n''}{4n} + \frac{r(rn'/n)''}{2(rn'/n)'} \right) \right]_{r=r_{\text{MHD}}}$$

(2.2.13)

$$r_0 - r_{\text{MHD}} = -\sigma_m d_i + \frac{d_i^2}{r} \left(2 + \frac{r}{2} \frac{(rn'/n)''}{(rn'/n)'} \right)\bigg|_{r=r_{\text{MHD}}}$$

(2.2.14)

In equation (2.2.14), since d_i is a positive quantity, the sign of $r_0 - r_{\text{MHD}}$ will be opposite to the sign of m, σ_m. To be specific, this means that for positive m we have $r_0 < r_{\text{MHD}}$, indicating a shift towards the inside of the plasma. Let us define L by $2 + \frac{r(rn'/n)''}{2(rn'/n)'}\big|_{r=r_{\text{MHD}}} \equiv \frac{r_{\text{MHD}}}{L}$, so that Eq. (2.2.14) can be rewritten as

$$r_0 - r_{\text{MHD}} = -\sigma_m d_i \left[1 - \sigma_m \frac{d_i}{L} \right]$$

(2.2.15)

This equation can have two solutions, corresponding respectively to positive and negative σ_m. However we see that if d_i is above a critical value $\sim L$, the second order corrections are as important as the first order corrections. If $\sigma_m < 0$, we find that for sufficiently large values of d_i, there is no value of r for which the effective potential has a minimum, so we do not have a contained solution. This behavior is quite general, with some variations in the numerical value of $d_{i0\,\text{crit}}$, the local maximum of d_{i0} taken as a function of r_0, according to the particular density profile considered. Typically, $d_{i0\,\text{crit}} \simeq L/4$.

To illustrate this behavior, we consider density profiles having the form $n = n_0[1 - (r/a)^2]^\nu$, where a is the minor radius of the plasma column. For these profiles we find $r_{\text{MHD}}/a = 1/\sqrt{1+\nu}$ and $d_{i0\,\text{crit}}/a = \frac{1}{4\sqrt{1+\nu}}\left(\frac{\nu}{2+\nu}\right)^{1+(\nu/2)}$. In the particular case of $\nu = 1/2$, which is consistent with the JET data[2], $r_{\text{MHD}}/a =$

$\sqrt{2/3} \simeq 0.82$ and $d_{i0\,\text{crit}}/a \simeq 0.027$. In Fig. (2-1), we plot the dependence of mode localization on d_{i0}, showing the difference between the linear approximation and the exact solution for the $\nu = 1/2$ case. The value of $d_{i0\,\text{crit}}/a$ for this case is also indicated. The experimental value of d_{i0}/a taken from JET parameters, as given in Table A-I, is $\simeq 0.063$.

With this value of d_{i0} there are no localized solutions for $m < 0$, which means that confined solutions exist only for modes whose poloidal motion is in the same direction as the ion gyromotion in a field aligned with the z-axis. Confined solutions do occur for $m > 0$, such that the radial width of the mode varies inversely with the square root of m whereas the radius of localization is independent of m. For the parameters considered, the modes are localized close to the edge of the plasma column and we find $r_0/a \simeq 0.76$, consistent with experimental results.

In Table 2-I, we summarize the values for ω_0, r_0 and Δ obtained by solving Equations (2.2.9), (2.2.10) and (2.2.11) for the JET and TFTR experimental parameters. We notice that since d_{i0}/a for TFTR is $\lesssim d_{i0\,\text{crit}}/a$ we have two solutions for $m > 0$, $m < 0$.

Numerical solutions of Eq. (2.2.3) have been performed and they are shown in Figures [2.2] to [2.5] for lowest radial eigenmodes in the cases $m = 10, 40, -40, 100$ using parameters from table A-I as above. In the graphs ω has been normalized to Ω_i, and the radius is normalized to a. We note that in the case of negative m the solution is not localized, as expected from the previous analysis.

TABLE 2-I - Relevant parameters and mode solution for JET and TFTR

JET	**TFTR**
$\epsilon \simeq 0.3$	$\epsilon \simeq 0.35$
$d_{i0}/a \simeq 0.063$	$d_{i0}/a \simeq 0.028$
$\nu \simeq 1/2$	$\nu \simeq 1$
$r_{\mathrm{MHD}}/a \simeq 0.82$	$r_{\mathrm{MHD}}/a \simeq 0.71$
$L/a \simeq 0.13$	$L/a \simeq 0.16$
$d_{i0\,\mathrm{crit}}/a \simeq 0.027$	$d_{i0\,\mathrm{crit}}/a \simeq 0.034$

MODE SOLUTIONS:

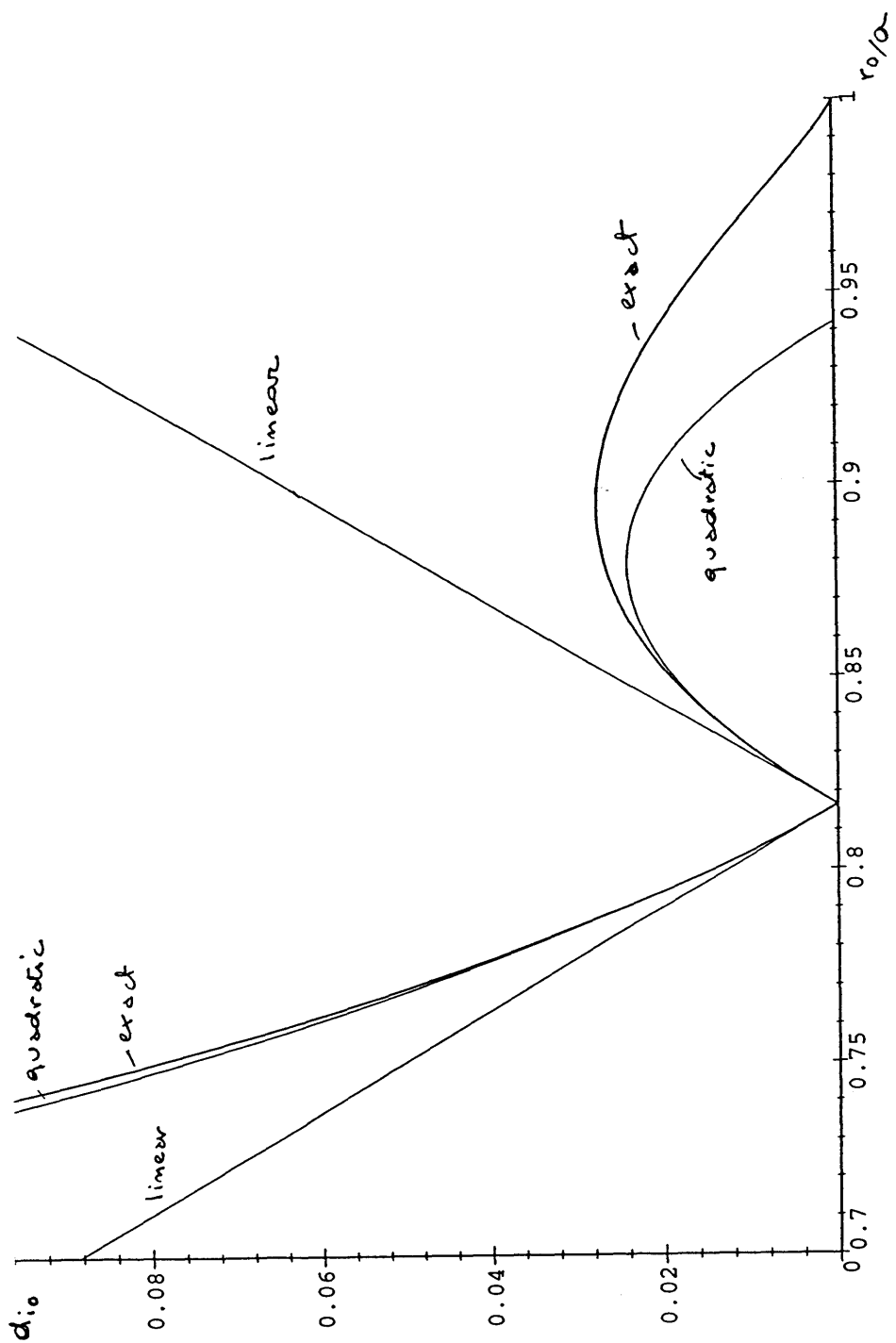| **JET**	**TFTR**	**TFTR**
$m > 0$	$m > 0$	$m < 0$
$r_0/a \simeq 0.76$	$r_0/a \simeq 0.67$	$r_0/a \simeq 0.77$
$\omega/m\Omega_i \simeq 0.11$	$\omega/m\Omega_i \simeq 0.059$	$\omega/m\Omega_i \simeq -0.052$
$|m|^{1/2}\Delta/a \simeq 0.48$	$|m|^{1/2}\Delta/a \simeq 0.47$	$|m|^{1/2}\Delta/a \simeq 0.59$
$\delta\omega/\Omega_i \simeq 0.13$	$\delta\omega/\Omega_i \simeq 0.058$	$\delta\omega/\Omega_i \simeq 0.047$

Figure 2.1 The dependence of the mode localization r_0/a on the parameter $d_{i0}/a = c/(\omega_{pi}a)$, showing the difference between the linear approximation and the exact solution. The density profile is taken as $n = n_0(1 - (r/a)^2)^{1/2}$. On the y-axis is d_{i0}/a, on the x-axis is r_0/a.
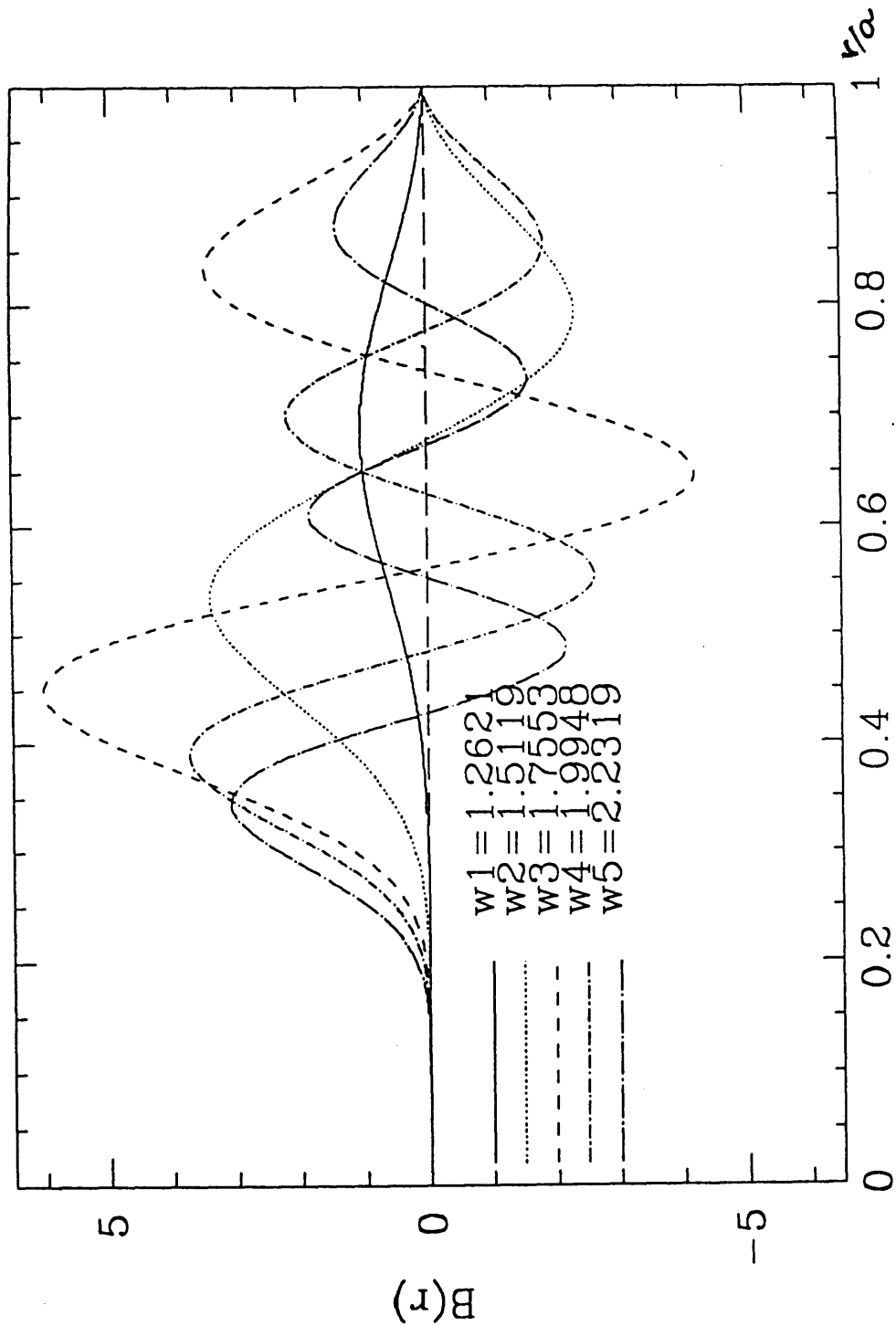
Figure 2.2 The radial dependence of the contained mode for $m = 10$. In the figure the first five eigenmodes are plotted (s=1...5). The frequency ω_s is normalized to Ω_i and the radius is normalized to a.

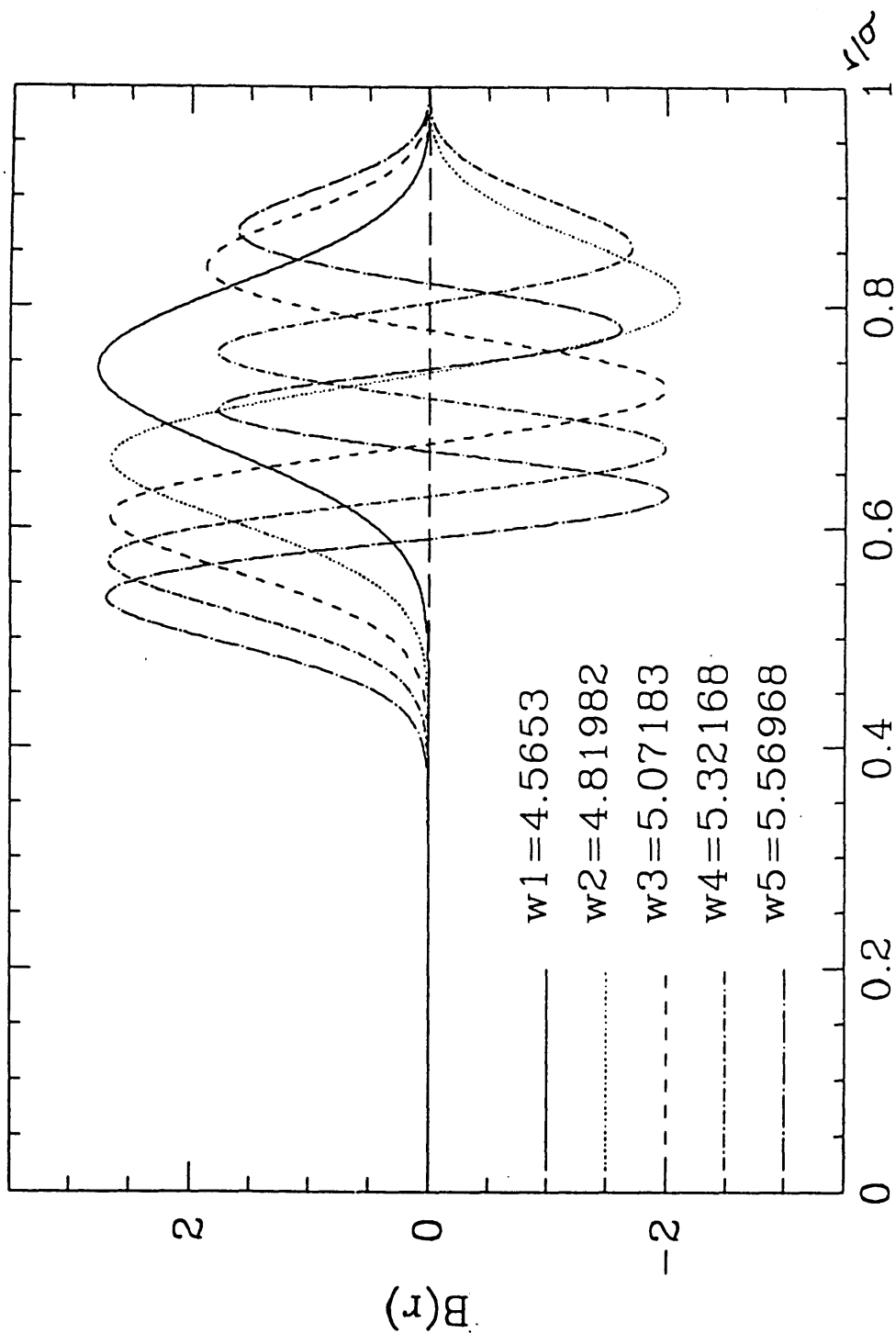**Figure 2.3** The radial dependence of the contained mode for $m = 40$. In the figure the first five eigenmodes are plotted (s=1...5). The frequency ω_s is normalized to Ω_i and the radius is normalized to a.
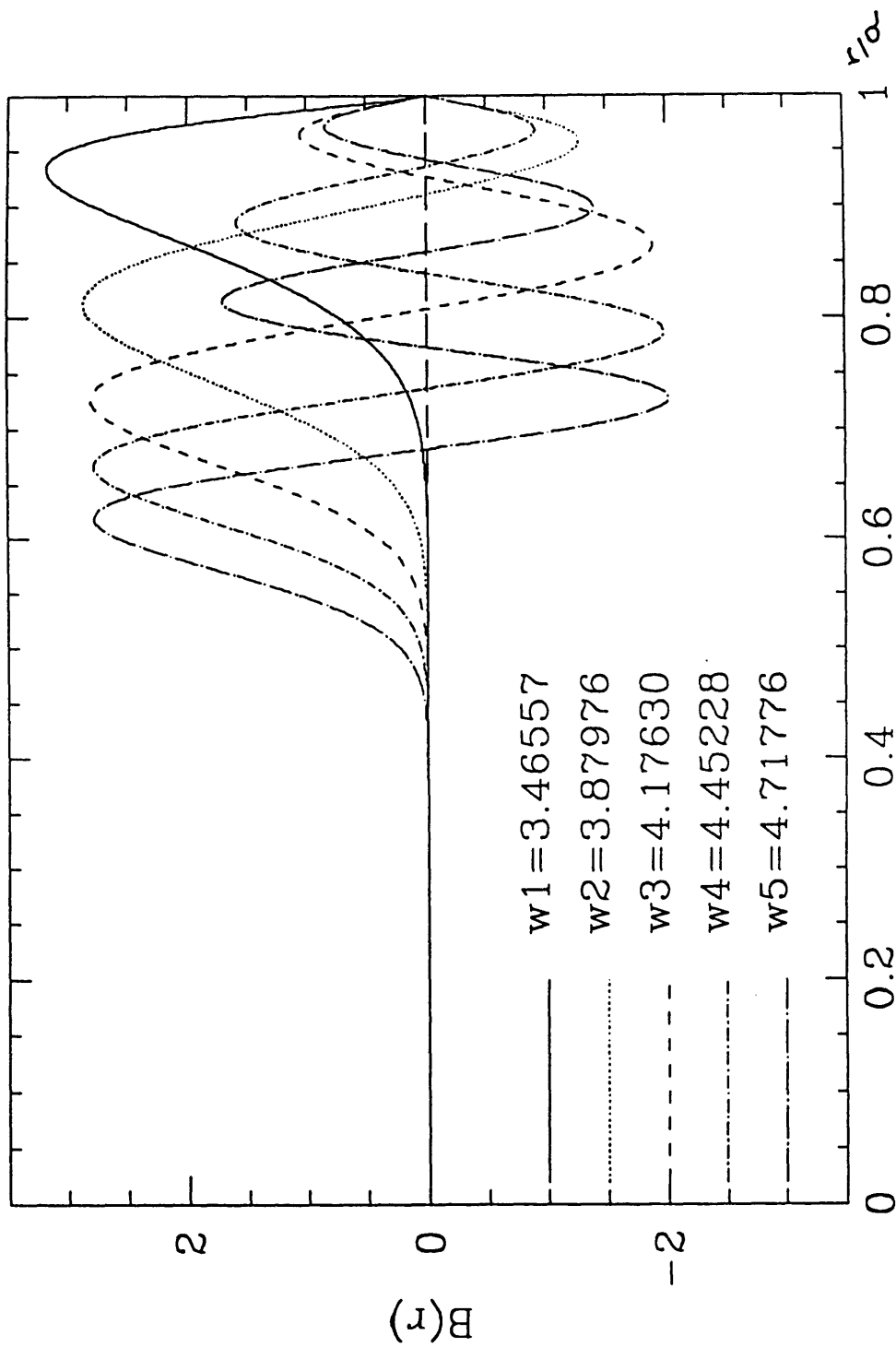
Figure 2.4 The radial dependence of the contained mode for $m = -40$. In the figure the first five eigenmodes are plotted (s=1...5). The frequency ω_s is normalized to Ω_i and the radius is normalized to a. We notice that in this case the solution is not localized.
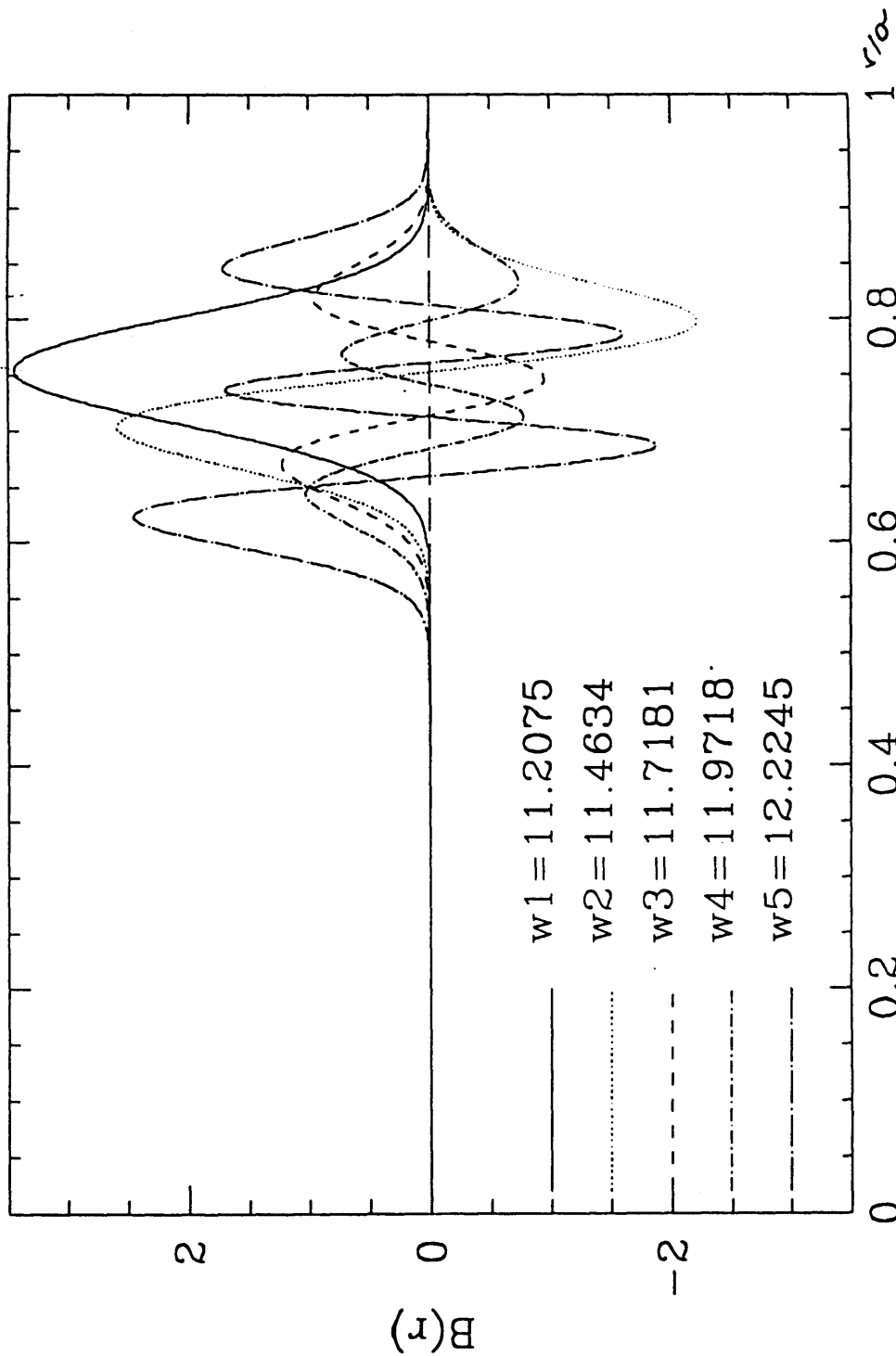
Figure 2.5 The radial dependence of the contained mode for $m = 100$. In the figure the first five eigenmodes are plotted (s=1...5). The frequency ω_s is normalized to Ω_i and the radius is normalized to a.

40

Chapter 3.

The Whistler Contribution to the Contained Mode

In this chapter we study Eq. (2.1.27) for the containde magnetosonic-whistler mode. This equation can be analyzed by using the same technique described in the previous chapter to study Eq. (2.2.1), and will thus admit solutions of the form of Eq. (2.2.5) but with different values of r_{mode}, Δ and a different dispersion relation. Particularly we find that the fact that we can have different points of localization of the mode can be related to the observed spectrum. To understand this we recall that the observed frequencies are selected by resonant interaction with the α-particles, as detailed in Chapters 6 and 7. Thus to explain the spectrum of the instability, we can consider first a single resonance with a harmonic of the cyclotron frequency, defined by $\omega \sim \ell \Omega_i(R)$, where R is measured at the point of interaction of the particle with the mode, and where ℓ is an integer. Note that while the mode characteristics have been calculated in the cylindrical limit, the particle resonance terms incorporate toroidal effects, because of the local nature

of the interaction and because of the importance of toroidal effects on particle orbits. The region of interaction must be contained within the mode layer defined by $r_0 - \Delta < r < r_0 + \Delta$, and is expected to be localized around the outer edge of the mode layer, where $R \simeq R_0 + r$ and where the trapped energetic particles are located. Due to the spread of values of Ω_i within the region of interaction between energetic particles and the mode, the resonance condition determines the mode frequency within a band of frequencies. In the limit considered in Chapter 2, where all of the modes were localized about the same radius r_0, this broadening of the frequency spectrum is proportional to the mode width Δ, restricting our attention to a sufficiently small region of interaction at the outer edge ($\cos \theta \sim 1$), so that $R = R_0 + r$ is a valid approximation. As the poloidal number m increases, Δ decreases and the mode becomes more sharply localized, so that at first glance we would expect a more peaked spectrum for the higher harmonics. On the other hand, the experimental observations show the opposite trend. There are many effects in addition to Δ that can be responsible for the width of the peaks, such as the Doppler effect and the presence of frequency shifts due to the drift velocity and variations in the poloidal angle. However we can show that a crucial role is played by the fact that, as the harmonic number increases above some value ($\ell > \ell_{\text{trans}}$), the whistler part of the spectrum significantly affects the localization of the mode.

Section 3-1. The Localization of the Whistler Mode

We define

$$k_\parallel \equiv -\frac{m}{R_0 q(r)}\left(1 - \frac{n_0}{m}q(r)\right) \tag{3.1.1}$$

We recall that in the case where $k_\parallel$ can be neglected, modes with different values of m are localized around the same radius r_0, defined by Eq. (2.2.10) (up to $O(1/m)$). When the full mode equation is considered[7,9] we find an additional shift in the mode localization, so that $r_{\text{mode}} \neq r_0$ (even neglecting terms $O(1/m)$) for different values of m and n^0. This shift in mode localization lifts the degeneracy in the

interacting mode frequencies which resulted from the equivalence of the relevant value of $\Omega_i(R)$ for different modes. For sufficient values of $D_H/(a^2\Omega_i)$, this will be a major contribution to the transition to a continuum.

Defining the quantity $b_1 = B_{1\parallel}/\sqrt{r(v_A^2 + k_\parallel^2 D_H^2)}$ and neglecting terms of order $(k_\parallel/k_\perp)^2(\omega/\Omega_i)^2$ the mode equation for b_1 becomes:

$$\frac{d^2 b_1}{dr^2} + \left\{ \frac{1}{v_A^2 + k_\parallel^2 D_H^2}\left[\omega^2 + \omega k_\theta \frac{d}{dr}(D_H)\right] - k_\theta^2 \right\} b_1 = 0 \tag{3.1.2}$$

where $k_\theta = -\frac{m}{r}$, $m > 0$ and with $q(r) \equiv rB_{z0}(r)/(R_0 B_{\theta 0}(r))$, and $D_H \equiv B/\mu_0 n_e e$.

To identify the value of m (i.e. ℓ) for which the whistler part of the spectrum becomes relevant, we study analytically the simplified case where:

$$\frac{d^2 b_1}{dr^2} + \left(\frac{\omega^2}{v_A^2 + k_\parallel^2 D_H^2} - k_\theta^2 \right) b_1 = 0 \tag{3.1.3}$$

It is convenient to define

$$G^2(r) \equiv \frac{m^2}{R_0^2} d_i^2 \frac{1}{q(r)^2}\left(1 - \frac{n_0}{m} q(r) \right)^2 = \frac{k_\parallel^2 D_H^2}{v_A^2} \tag{3.1.4}$$

where $d_i = c/\omega_{pi} = D_H/v_A$. The lowest order (in $1/m$) the equations for ω_{mode} and r_{mode} are:

$$\omega_{\text{mode}} = \frac{m v_A}{r_{\text{mode}}}\left(1 + G^2(r_{\text{mode}}) \right)^{1/2} \tag{3.1.5}$$

$$r_{\text{mode}} = -2\frac{n}{n'} \left. \frac{\left[1 + G^2(r)\left(1 + \frac{\hat{s}}{1 - \frac{n^0}{m}q(r)}\right)\right]}{1 + 2G^2(r)} \right|_{r=r_{\text{mode}}} \tag{3.1.6}$$

where $\hat{s} = rq'/q$.

We examine Eq. (3.1.5) and Eq. (3.1.6) in two different regimes, where

$$i)\quad |1 - n^0 q/m| << 1, \quad \text{and} \quad ii)\quad |1 - n^0 q/m| \sim 1$$

43

Let us consider this two cases separately

i) Quasi-Flute Mode

In this case the mode is localized near the mode rational surface r_s, defined by $q(r_s) = m/n^0$. Therefore we can approximate

$$G^2 \simeq \frac{d_i^2}{R_0^2} \left(\frac{m\hat{s}}{qr} \right)^2 (r - r_s)^2$$

and

$$1 + \frac{\hat{s}}{1 - n^0 q/m} \simeq \frac{r_s}{r_s - r}$$

We regard the terms proportional to G^2 as perturbations to the ideal MHD mode solution

$$r_{\mathrm{MHD}} = -2 \frac{n}{dn/dr} \bigg|_{r=r_{\mathrm{MHD}}}$$

and we define $\delta r_w \equiv r_{\mathrm{mode}} - r_{\mathrm{MHD}}$; we find that for $|1 - n^0 q/m| << 1$

$$\frac{\delta r_w}{r_{\mathrm{MHD}}} \simeq \frac{1}{(1 + (2n/n')')} \frac{m^2 d_i^2}{R_0^2} \frac{\hat{s}}{q^2} \left(1 - \frac{n^0 q}{m} \right) \bigg|_{r=r_{\mathrm{MHD}}} \tag{3.1.7}$$

The quantity δr_w scales linearly with $(1 - n^0 q/m)$ in this range, where q is evaluated at r_{MHD}. If we consider as an example the set of parameters for JET given in table A-I, $d_i/R_0 = 0.021$.

ii) Oscillatory Mode (along the field)

In this case, the mode is localized "far" from the mode rational surface $r = r_s$. Therefore, $1 + \hat{s}/(1 - \frac{n^0 q}{m})$ is a quantity of order unity, and the term

$$\frac{\left[1 + G^2(r) \left(1 + \frac{\hat{s}}{1 - \frac{n^0}{m} q(r)} \right) \right]}{1 + 2G^2(r)} \Bigg|_{r=r_{\mathrm{mode}}}$$

from Eq. (3.1.6) is also a quantity of order unity which takes the asymptotic value of $1/2$ as $n^0 \to \pm\infty$. In this limit, r_{mode} is given by $r_{\mathrm{mode}} \simeq -n/n'|_{r=r_{\mathrm{mode}}}$.

44

This value represents the localization of the mode as this limit is approached, and is too close to r_{MHD} to be of interest for calculation of the condition for overlap between resonances. This behavior is reproduced in figure [3.1], which graphs the dependence of r_{mode} on n^0 for fixed m, as determined by Eq. (3.1.2). The extreme values for $\delta r_W = r_{\mathrm{mode}} - r_{\mathrm{MHD}}$ occur as $|1 - n^0 q/m| \to 1$, corresponding to $n^0 = 0$, $2m/q$.

We can conclude that the relevant modes for our case are the quasi-flute modes and for a given m we can define a maximum displacement as

$$\delta r_{\mathrm{MAX}} \equiv r_{\mathrm{mode}}(n^0 = 0) - r_{\mathrm{mode}}(n^0 = 2m/q)$$

so that we find

$$\frac{\delta r_{\mathrm{MAX}}}{r_{\mathrm{MHD}}} \sim \frac{2}{(1 + (2n/n')')} \frac{m^2}{R_0^2} \frac{D_H^2}{v_A^2} \frac{\hat{s}}{q^2}\bigg|_{r = r_{\mathrm{MHD}}} \tag{3.1.8}$$

In the case where the full effective potential is considered, given by Eq. (3.1.2), the analysis is similar except that r_{MHD} is replaced by r_0, and

$$\frac{\delta r_{\mathrm{MAX}}}{r_0} \propto \frac{m^2}{R_0^2} \frac{D_H^2}{v_A^2} \frac{\hat{s}}{q^2}\bigg|_{r = r_0} \tag{3.1.9}$$

This effect becomes significant as $\delta r_{\mathrm{MAX}} > \Delta$, where Δ is the width of the mode. Figures [3.1],[3.2], [3.4]-[3.6] show the values of r_{mode} and ω that satisfy Eq. (3.1.2) for fixed values of m as n^0 changes, considering the set of parameters that is reproduced in Table A-I. Figure [3.3] shows the values of Δ for fixed values of m as n^0 changes, we only show the case $m = 25$ as in general Δ is almost unaffectes by changes in n^0. In figures [3.1], [3.3], [3.5], we plot the position of the mode localization r_{mode}/a against the toroidal mode number n_0 for a fixed value of the poloidal number m, we examine the cases $m = 25$, $m = 50$, $m = 100$. As expected from the previous analysis the localization for the oscillatory modes along the magnetic field ($n_0 > m/q$, $n_0 < 0$) is not sensitive to changes in n_0. We see that as the poloidal mode number increases δr_{MAX} increases too: the mode shifts mainly towards the interior of the plasma so that for example for $m = 100$ we have modes

localized around $r_{\text{mode}}/a = 0.6$. We find that $\delta r_{\text{MAX}} > \Delta$ corresponds to $m > 50$. We recall that as this effect becomes important, the mode localization goes further into the plasma and the mode particle interaction includes more of the α particle population.

For a fixed harmonic number ℓ, the set of modes resonating with $\ell\Omega_i$ will be contained in a range $r_{\text{left}} < r < r_{\text{right}}$. Thus the spectrum of this resonance will be given approximately by $\ell\Omega_i(R_0 + r_{\text{right}}) < \omega < \ell\Omega_i(R_0 + r_{\text{left}})$. Here, r_{left} is the solution to $\omega_{\text{mode}}(m_1, n_1^0) \simeq \omega$ for some pair of mode numbers (m_1, n_1^0) with the smallest corresponding value of r_{mode}, while r_{right} is the solution to $\omega_{\text{mode}}(m_2, n_2^0) \simeq \omega$ with the largest corresponding value of r_{mode}. A similar condition holds for the next higher resonance, $(\ell+1)\Omega_i(R_0 + r_{\text{right}}) < \omega < (\ell+1)\Omega_i(R_0 + r_{\text{left}})$, and thus a condition for overlap between harmonics is

$$\ell\Omega_i(R_0 + r_{\text{left}}) \geq (\ell+1)\Omega_i(R_0 + r_{\text{right}}) \qquad (3.1.10)$$

From this condition we can define an upper limit for the value ℓ_{trans} at which transition to a continuum must occur, and we find for the JET experiment that $\ell_{\text{trans}} \leq 18$. For the case $\ell = 18$, the corresponding m is given by $m \simeq 110$. Including the mode width and other terms in the resonance condition, in particular the possibility of having destabilizing interactions at $\theta \neq 0$, we will show that overlap can occur for smaller values of ℓ.
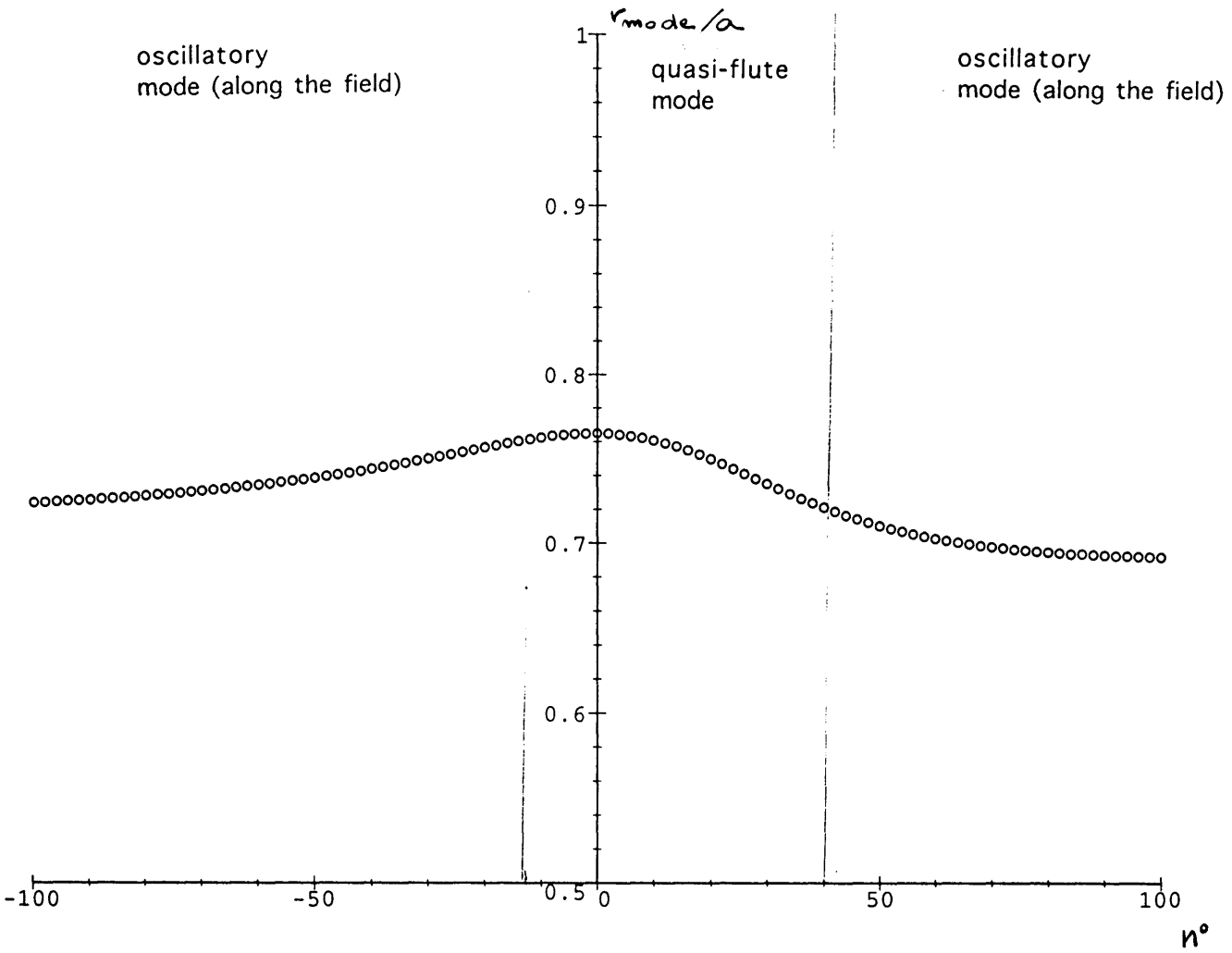
Figure 3.1 The localization of the mode r_{mode}/a is plotted against the toroidal mode number n^0 for fixed poloidal number $m = 25$. The change in localization is mostly sensitive to changes in n^0 for quasi-flute modes.
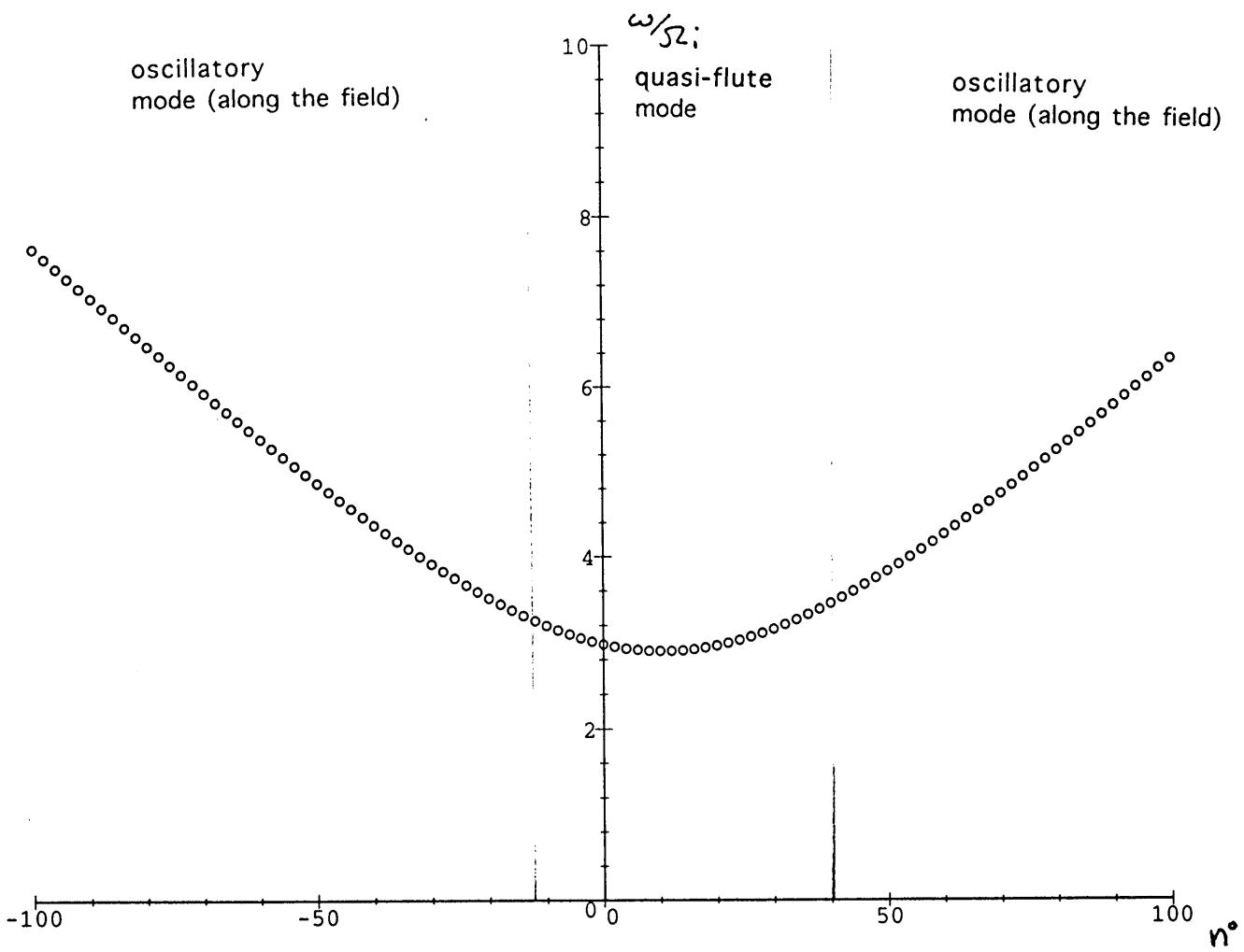
oscillatory
mode (along the field)

ω / Ω_i

quasi-flute
mode

oscillatory
mode (along the field)

Figure 3.2 The mode frequency, normalized to Ω_i, is plotted for the poloidal mode number $m = 25$, against the toroidal mode n^0.

48

oscillatory
mode (along the field)

quasi-flute
mode

oscillatory
mode (along the field)

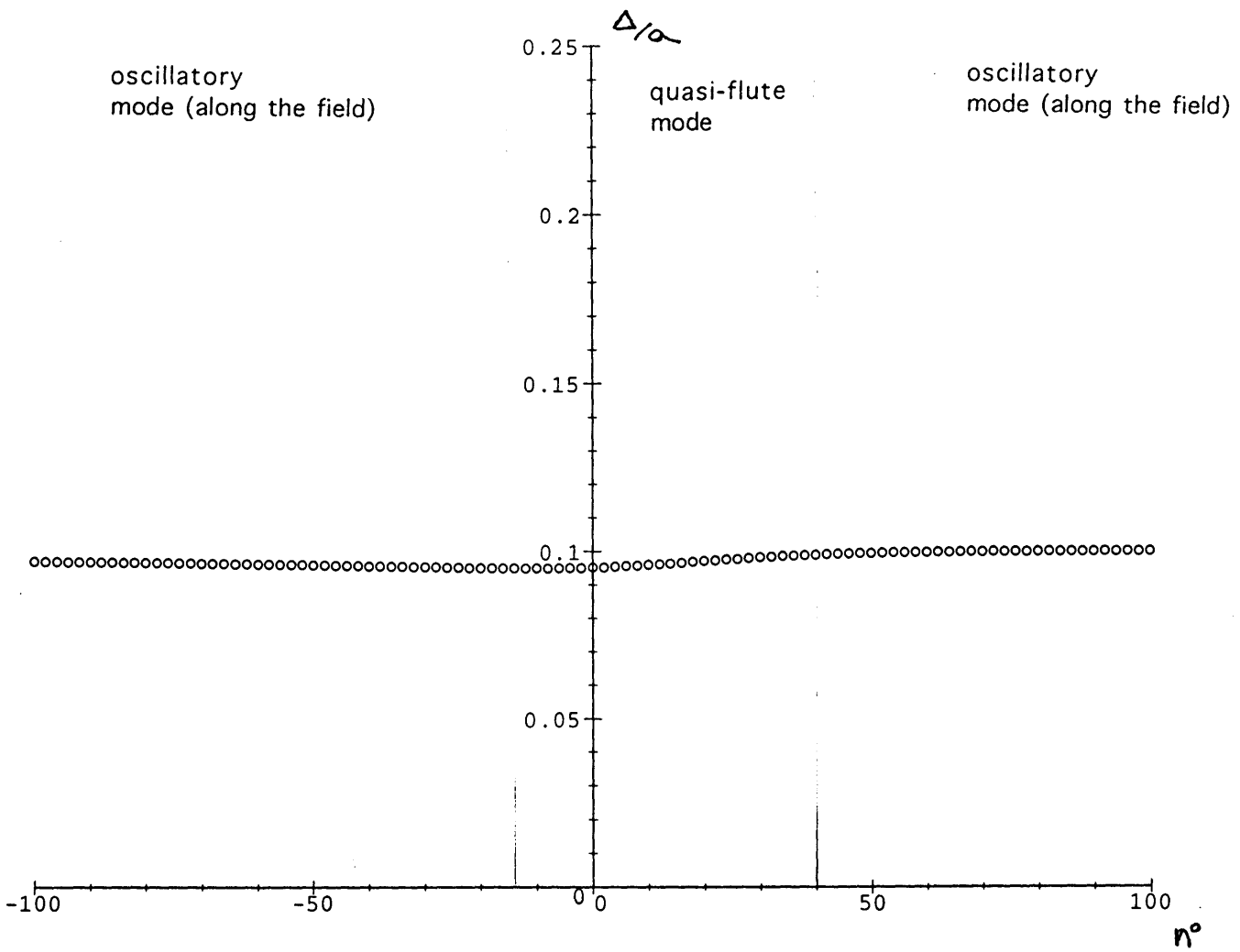Δ/a

n^o

Figure 3.3 The mode width Δ/a, for fixed poloidal mode number $m = 25$, against the toroidal mode n^o.
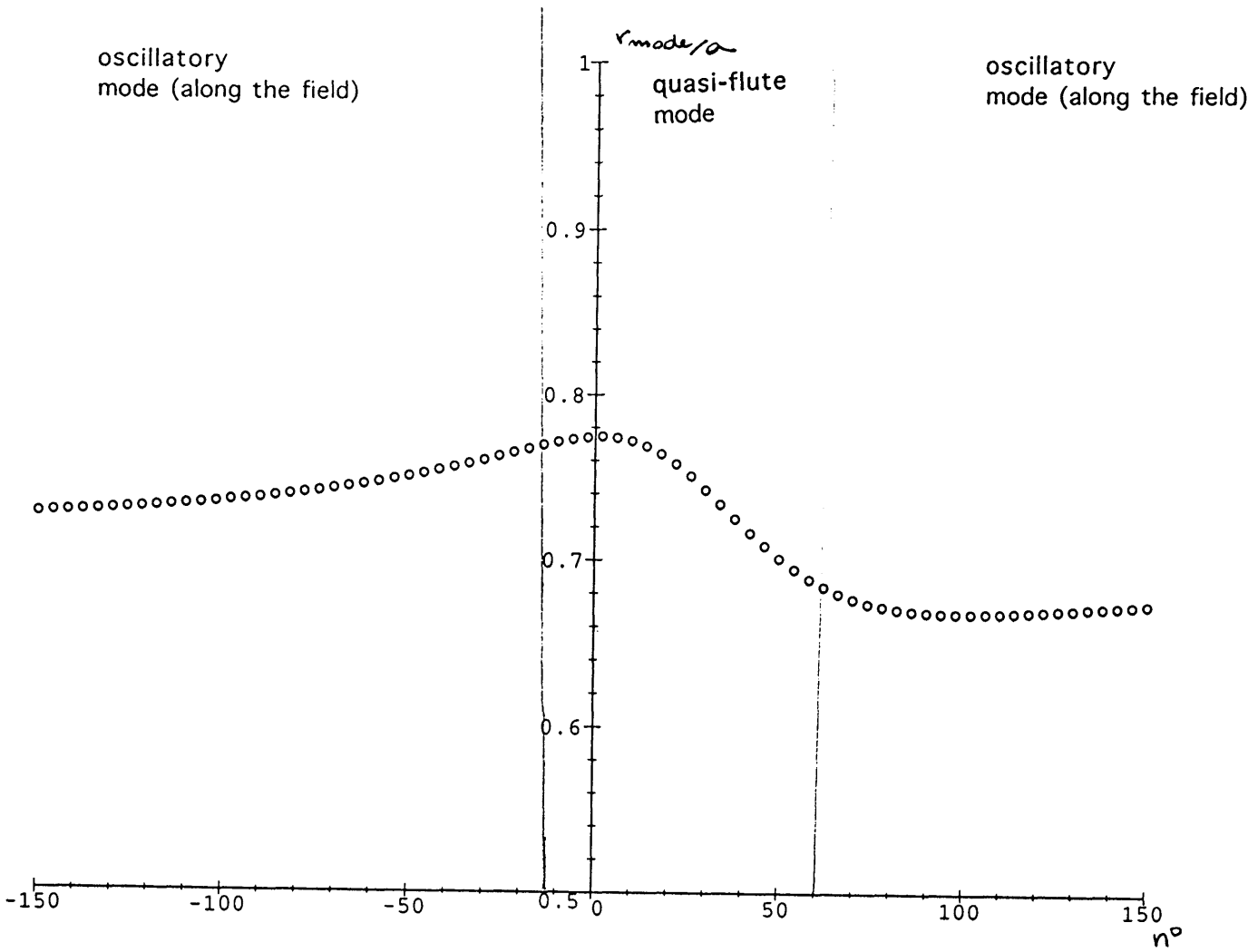
Figure 3.4 The localization of the mode r_{mode}/a is plotted against the toroidal mode number n^0 for fixed poloidal number $m = 50$. The change in localization is mostly sensitive to changes in n^0 for quasi-flute modes.
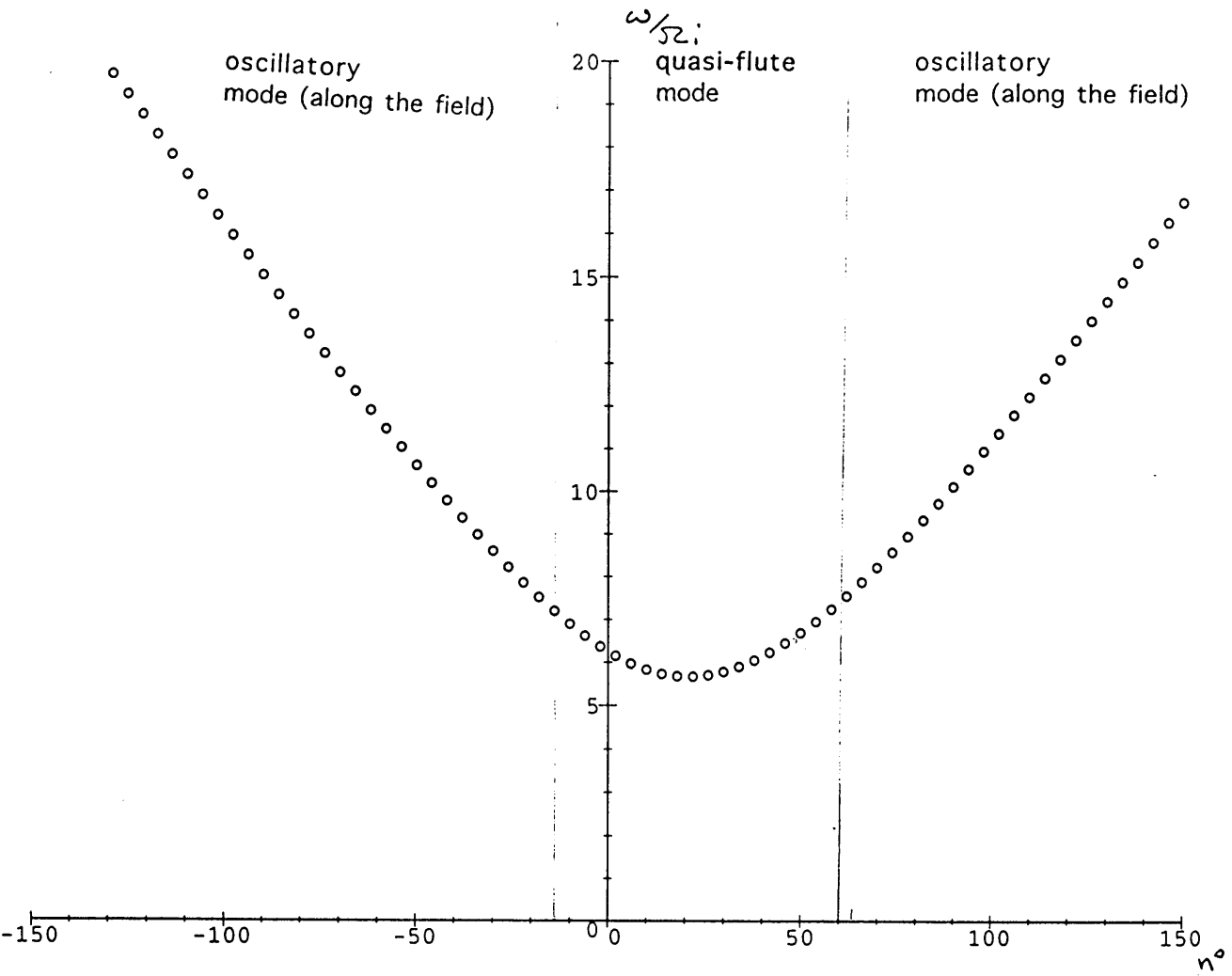
Figure 3.5 The mode frequency, normalized to Ω_i, is plotted for the poloidal mode number $m = 50$, against the toroidal mode n^0.
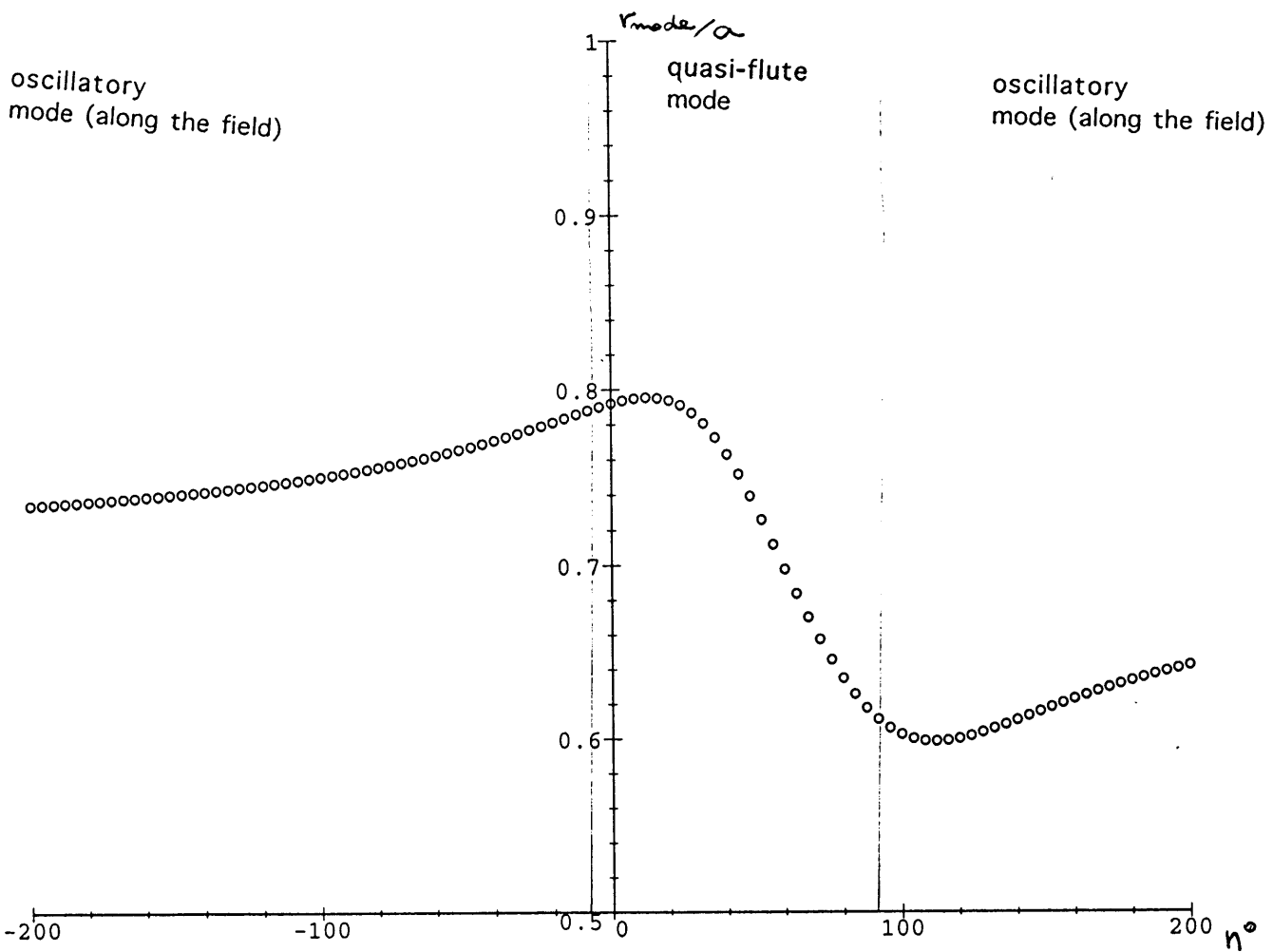
Figure 3.6 The localization of the mode r_{mode}/a is plotted against the toroidal mode number n^0 for fixed poloidal number $m = 100$. The change in localization is mostly sensitive to changes in n^0 for quasi-flute modes.
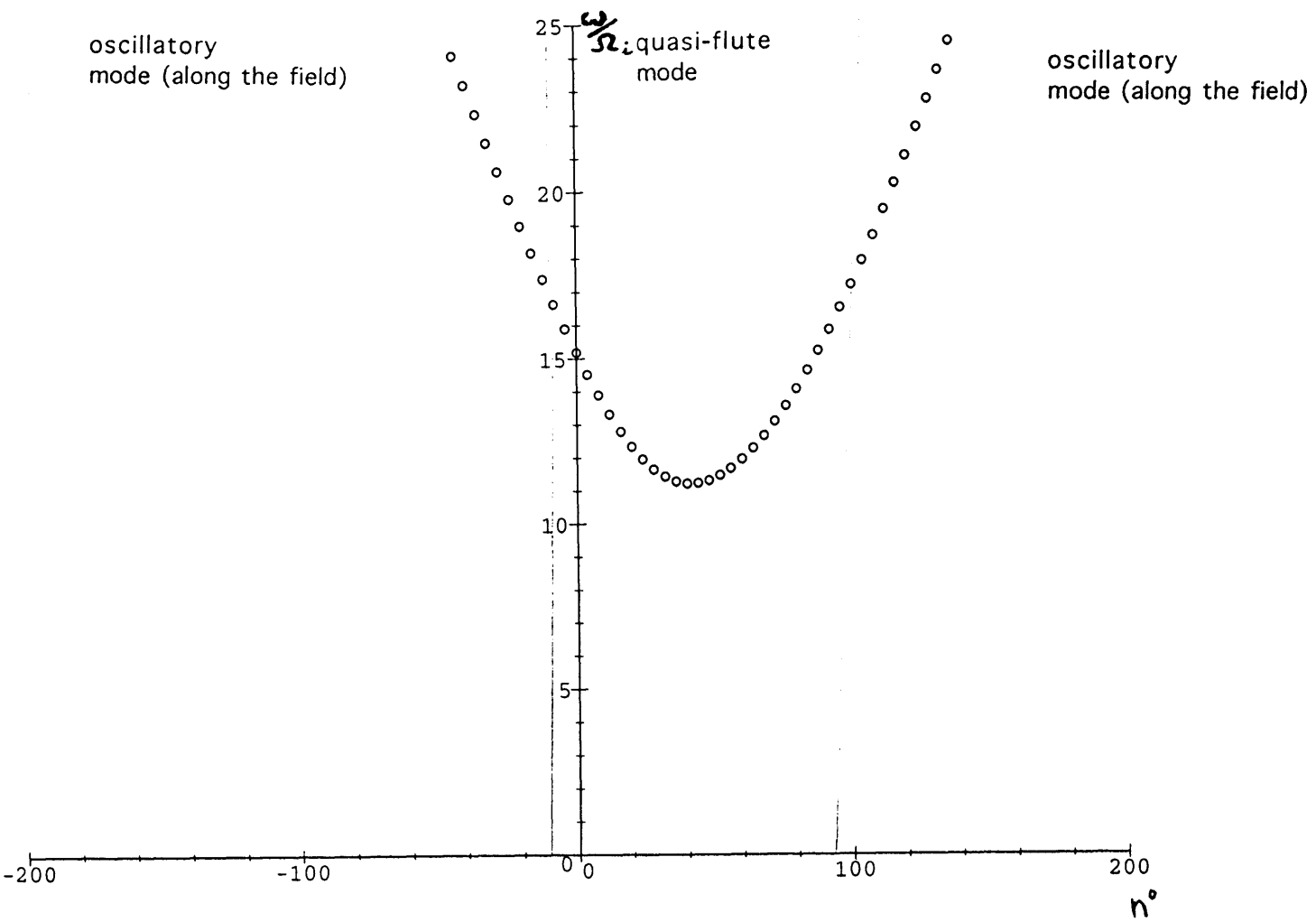
Figure 3.7 The mode frequency, normalized to Ω_i, is plotted for the poloidal mode number $m = 100$, against the toroidal mode n^0.

Chapter 4.

A Simple Picture of the Relevant Alpha-particles Orbits

Let us study the α-particles orbits in the case of azimuthal symmetry, that is for a system that does not depend on the ζ coordinate, as defined in appendix B.

For such a system we can identify the following constant of the motion, $\mathcal{E}$, μ, p_ζ, defined by:

$$\mathcal{E} = \frac{m}{2}(v_\parallel^2 + v_\perp^2) = \mathcal{E}_\alpha$$

$$\mu = \frac{1}{2}\frac{mv_\perp^2}{B} = const.$$

$$p_\zeta = mRv_\zeta + qRA_\zeta = const.$$

As shown in appendix C, the adiabatic invariant μ as defined above is a constant of the motion only to $O(\lambda)$, and if we consider the average over the gyroangle

to $O(\lambda/q)$, but from the point of view of the single particle orbits, this level of accuracy is enough. In this picture the spatial dependence is considered in the guiding center frame, so that the perpendicular motion is dominated by the drifts.

The constancy of the above quantities completely determines the orbit of a particle for a given set of initial conditions. We are interested in the projection of the motion in the perpendicular direction to the equilibrium magnetic field, so we can easily identify the function $r(\vartheta)$ that gives the shape of the orbit. In the case of energetic α-particles that are born mainly at the center of the plasma, the trapped particles that reach the outer edge of the plasma column will not follow the usual "banana orbit" limit ($\delta r << r$), as illustrated in figure [4.3] for the case of 10 keV deuterons, but due to their high energy they will have large radial excursions (potato orbits). This is illustrated in figure [4.4] for the case of 3.5 MeV α-particles. We thus include a brief review of the typical orbits for the case of large radial excursion, as it will give further insight into the final form of the distribution function for the α-particles, before the onset of the instability.

Section 4-1. Potato Orbits

We consider a sheared toroidal field of the form

$$\vec{B} = \frac{B_0}{1 + r/R_0 \cos\theta} \left(\hat{e}_\zeta + \frac{r}{R_0 q(r)} \hat{e}_\theta \right)$$

where we follow the notation of appendixB. We assume that $v_\parallel = v_\zeta + (B_\vartheta/B_0)v_\vartheta$ can be approximately taken as $v_\parallel \sim v_\zeta$. We expand in the small parameter $\epsilon = a/R$ and we keep toroidal corrections (i.e. $O(\epsilon)$) only in $v_\parallel$. By using these assumptions we can perform an approximate analytical calculation that can give us an estimate of the trapping condition and of the width of the orbit.

We fix the constants in such a way that $RA_\zeta(0,0) = 0$, and we consider as a reference case $q(r) \simeq (1 + 2.5(r/a)^2)$, $B_0 = 2.8\ T$, $a = 1.05\ m$, $R_0 = 3.15\ m$, that models the JET case. The subscript "0" labels quantities evaluated at the origin; we focus on orbits that pass through the origin ae most of the α-particles are produced in the core of the plasma. For this reference case we obtain that

55

$$RA_\zeta \simeq \frac{B_0 a^2}{5} \ln\left(1 + 2.5\frac{r^2}{a^2}\right) \tag{4.1.1}$$

and for a particle passing through $r = 0$, $\vartheta = 0$, we have, by imposing the constancy of p_ζ,

$$v_{\|0}\left(1 \mp \sqrt{1 + \frac{v_{\perp 0}^2}{v_{\|0}^2}\frac{r}{R_0}cos\vartheta}\right) = \frac{q}{mc}\frac{B_0}{R_0}\frac{a^2}{5}\ln\left(1 + 2.5\frac{r^2}{a^2}\right) \tag{4.1.2}$$

In Eq. (4.1.2) the minus sign is for circulating particles, while the plus sign is for trapped particles after the turning point.

If the parallel velocity at the origin is negative (where the positive direction is defined by the direction of the magnetic field B_0), there is no possibility of having a solution with trapped particles, since the right hand side of the above equality is always positive.

So only particles with $v_{\|0}$ can be trapped; this means that the local distribution function for trapped particles at the outer edge of the plasma column (after the turning point) will be such that the average value of the local parallel velocity will be some negative quantity.

As for the circulating particles, there can be a solution for negative values of $v_{\|0}$, but this requires $-\pi/2 < \vartheta < \pi/2$ so that the orbits of the particles with negative parallel velocity at the origin will be confined at the outer half of the plasma. With our choice of reference frame, the picture is the following:
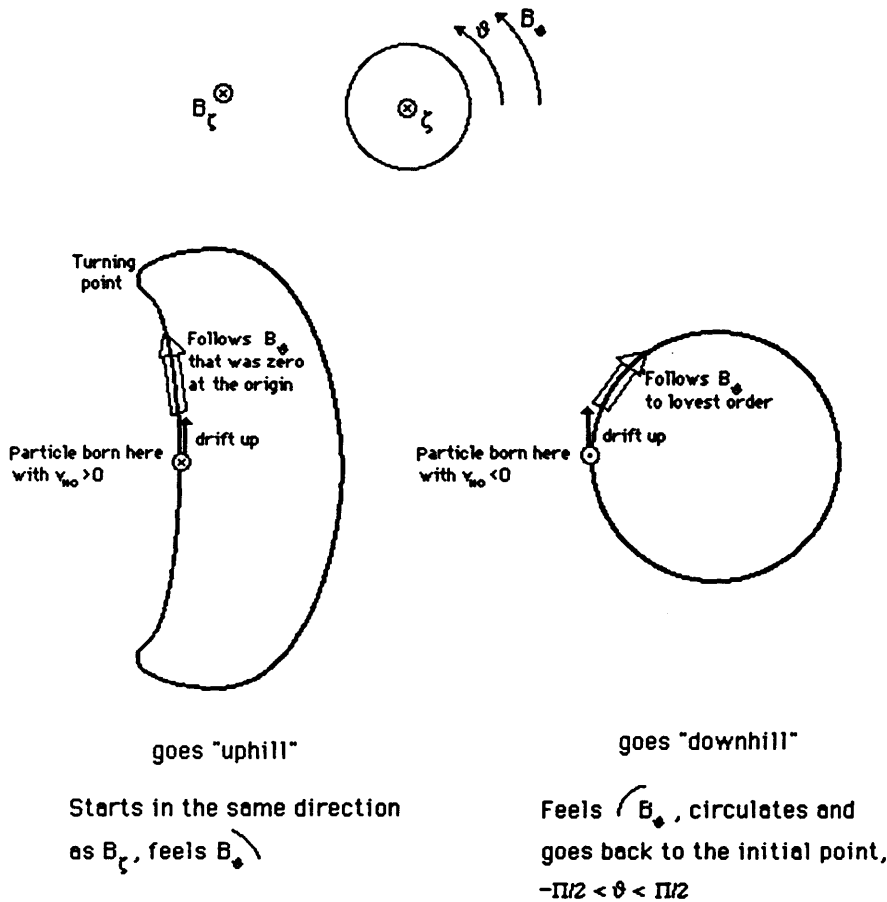
$$B_\zeta^{\otimes}$$

ϑ B_ϕ

$\otimes \zeta$

Turning
point

Follows B_ϕ
that was zero
at the origin

drift up

Particle born here
with $v_{\parallel 0} > 0$

Follows B_ϕ
to lowest order

drift up

Particle born here
with $v_{\parallel 0} < 0$

goes "uphill"

goes "downhill"

Starts in the same direction
as B_ζ, feels B_ϕ

Feels B_ϕ, circulates and
goes back to the initial point,
$-\Pi/2 < \vartheta < \Pi/2$

Figure 4.1 The orbits for energetic α-particles born at

the origin: two cases are shown, $v_{\parallel 0} > 0$ and $v_{\parallel 0} < 0$

It is clear from this picture why only orbits with $v_{\parallel 0} > 0$ can be trapped. Of course not all the particles with $v_{\parallel 0} > 0$ will be trapped, however we can easily identify the trapping condition that will finally correspond to a limit on the pitch angle. In figure [4.5] we show an example of a bifurcation orbit, i.e. the limiting case between a trapped orbit and a circulating orbit with $v_{\parallel 0} > 0$. The thick solid circle represents the location of the mode as found in chapters 2 and 3 and the dotted lines reproduce the width of the mode.

57

To find the condition on the pitch angle that corresponds to trapped particles, we recall that trapping occurs when $v_\parallel = 0$ at some point along the orbit. We will refer to this point as turning point or tip of the orbit. The extreme case is when the turning point is at $\vartheta = \pi$ so that the orbit is almost circulating, as in figure [4.5]. For a given set of initial conditions, $v_{\perp 0}$, $v_{\parallel 0}$, for a particle born at the origin, this will happen at a maximum radius compatible with the fact that the constancy of p_ζ is preserved. We can thus identify the trapping condition for $v_{\parallel 0}/v_{\perp 0} < v_{\parallel 0}/v_{\perp 0})_{limit} < 1$ where the limiting case corresponds to $v_\parallel(r_{MAX}, \vartheta = \pi) = 0$, i.e. $v_{\parallel 0}/v_{\perp 0} = \sqrt{r_{MAX}/R_0}$. Here r_{MAX} indicates the maximum radius where a turning point can lie. Since we expect $v_{\parallel 0}/v_{\perp 0} << 1$ and $v_{\parallel 0}^2 + v_{\perp 0}^2 = v_{th\alpha}^2$, we can use $v_{\perp 0} \simeq v_{th\alpha}$. We can then plug this inside the condition for p_ζ being constant, and we obtain:

$$v_{\parallel 0} R_0 = \frac{qB_0}{mc} \frac{a^2}{5} \ln\left(1 + 2.5 \frac{r_{MAX}^2}{a^2}\right) \qquad (4.1.3)$$

This equation can be approximated by using the above assumptions and gives

$$\frac{r_{MAX}}{a} \simeq \left(\frac{R_0(2\rho_\alpha)^2}{a^3}\right)^{1/3} \simeq 0.35 \qquad (4.1.4)$$

where the right hand side has been evaluated considering the parameters of Table A-I, and

$$\frac{v_{\parallel 0}}{v_{\perp 0}} \simeq \left(\frac{2\rho_\alpha}{R_0}\right)^{1/3} \simeq 0.34 \qquad (4.1.5)$$

instead of the usual assumption for deeply trapped particles, $v_{\parallel 0}/v_{\perp 0} \simeq \sqrt{a/R_0} = 0.54$.

An example of two trapped orbits not too far from the limiting condition is reproduced in figure [4.6], where $w = v_{\parallel 0}/v_\alpha$: we see how a small spread in the pitch angle results in a significant spatial spread. Again the solid thick line represents the localization of the mode as found in chapters 2 and 3.

A more exact calculation has been carried out nunerically in ref. [11,12] and the results are shown in the figure [4.5] for the sample case previously considered.

On the x axis we have the x axis of the section of the plasma column (so that for $x = 0$ we have $r = R_0$) and on the y axis we have the ratio $v_{\|0}/v_\alpha$. The lines reproduce the maximum radial excursion for particles born at $r = 0$, i.e. the intersection of the orbits with the x axis. In the case of trapped particles there are two lines that correspond respectively to the extreme on the x axis and the tip of the potato orbit, that in figure [4.6] are labelled by ◯ and ◯. We see that the numerical calculation agrees quite well with the analitycal approximation, since we have trapped particles only for $0 < v_{\|0}/v_\alpha < 0.34$.

It is worth to notice how the situation changes if we consider particles that are born further away from the center. Let us consider particles that are born at $r_b \neq 0$. To impose the conservation of p_ζ we need:

$$RA_\zeta(r) - RA_\zeta(r_b) = \int_{r_b}^r B_\theta R dr = \frac{qB_0}{mc}\frac{a^2}{5}\ln\left(\frac{1 + 2.5r^2/a^2}{1 + 2.5r_b^2/a^2}\right) \qquad (4.1.6)$$

The orbits are defined by:

$$v_{\|b}\left(1 \mp \sqrt{1 + \frac{v_{\perp b}^2}{v_{\|b}^2}\frac{r\cos\vartheta - r_b\cos\vartheta_b}{R_0}}\right) = \frac{qB_0}{mc}\frac{a^2}{5R_0}\ln\left(\frac{1 + 2.5r^2/a^2}{1 + 2.5r_b^2/a^2}\right) \qquad (4.1.7)$$

It is clear from this form that we can have trapped solutions for both $v_{\|b} < 0$ and $v_{\|b} > 0$. However if $v_{\|b} < 0$ we can have a trapped solution only if the turning points are such that $r < r_b$, so that for example for $\theta_b = 0$ we have the following picture.
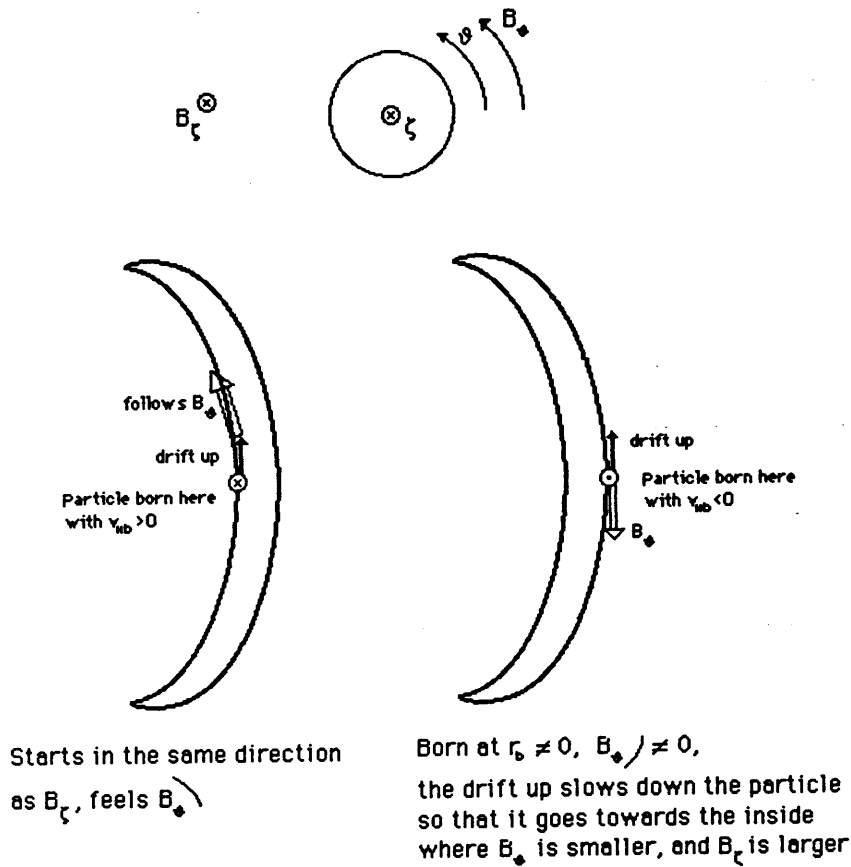
59

Figure 4.2 The orbits of two particles born at $r = r_b \neq 0$

with respectively $v_{\|0} > 0$ **and** $v_{\|0} < 0$.

A more precise and extended analysis has been carried numerically in ref. [11,12] and the results are reproduced in the figures [4.8] to [4.12]. This shows that the "banana orbit" with $\delta r << r$ and particles with parallel velocities in both directions can exist only for $r_b > r_{crit}$ [12], since if $r_b < r_{crit}$ the drift is so strong that we do not have $v_\| = 0$, for negative values of $v_{\|0}$. Figures [4.8] to [4.12] reproduce the maximum radial excursion plus, in the case of trapped orbits the "potato tip" for particles passing through the point $r = r_{mode}$ at different values

60

of ϑ. The quantity $r = r_{\mathrm{mode}}$ is represented by the solid straight line, and on the y axis is the ratio $v_\parallel(r = r_{\mathrm{mode}})/v_\alpha$. The striped region refers to particles that leave the plasma.

As expected the local value of $v_\parallel$ is within a narrow range $-0.45 < v_\parallel/v_\alpha < -0.2$ and is negative. If we assume that most of the particles are born between $\pm 30cm$, we have to restrict the allowed ratio to $-0.45 < v_\parallel/v_\alpha < -0.4$. In the next chapter we will see how the resulta presented here are consistent with the final form of the distribution function of fusion products before slowing down occurs.

The numerical analysis shows also how the orbit period changes for different classes of orbits: particularly in the standard bounce orbit calculation for banana orbits, assuming $\delta r << r$ (i.e. neglecting radial excursion) and $\vartheta \sim 0$, we obtain an estimate of the bounce time as:

$$\tau_b \simeq \frac{qR_0}{v_\alpha\sqrt{\epsilon}}2\pi \qquad (4.1.8)$$

while the circulating time is given by $\tau_c \sim 2\pi qR_0/v_\alpha$.

In our case since we have large radial excursions Eq. (4.1.8) does not hold, and we see that the orbit period can change significantly. An approximate form for the bounce time, for the case of JET and considering orbits that intersect $r = r_{\mathrm{mode}}$ at $\vartheta = \vartheta_0$, is given by

$$\Omega_\alpha\tau_b = 1506.3 - 345.7 \ \ln(1.33 \ \mathrm{rad} - \vartheta_0) \qquad (4.1.9)$$

where $\vartheta_{crit} = 1.33\mathrm{rad}$ is the critical angle for trapping, that is for $\vartheta_0 = \vartheta_{crit}$ the orbit period goes to infinity and we have a stationary orbit. For orbits that are confined inside the plasma ϑ_0 can take the value $0 < \vartheta_0 < \pi/3$. Eq. (4.1.9) gives a good approximation of the bounce time expecially for those particles that are closer to ϑ_{crit}. From this equation we find that $1407.5 < \Omega_\alpha\tau_b < 1946.0$ in the range of ϑ_0 of interest. Particularly the value of $\Omega_\alpha\tau_b$ at $\theta_0 = 0$ is 1407.5; so we can compare this value with the results[12] for the particles intersecting the mode at $\vartheta_0 = 0$, and we see that it's a good average estimate since the normalized period

takes values $1300 < \Omega_\alpha \tau_b < 1500$. We can compare this values with τ_b given by Eq. (4.1.8): for a trapped particle at the edge with $\epsilon = a/R_0 = 0.3$, $q = 3.5$, and $\rho_\alpha \simeq 8\ cm$ we obtain $\Omega_\alpha \tau_b \simeq 1581$.

We summarize our results by saying that if we look at a fixed radius $r = r_0$ where r_0 is towards the edge, almost all the particles that are able to reach this radius and have confined orbits, are born with positive parallel velocity and locally, at the mode layer, have negative parallel velocity. This will not hold only for a very small fraction of particles born at $r > r_0$. Only a small fraction of circulating particles will be able to reach the mode layer at $r = r_0$. An analytical approximate calculation gives an estimate for the limiting condition for trapping for particles born at the origin as $v_{\|0}/v_{\perp 0} \sim (2\rho_\alpha/R_0)^{1/3}$.
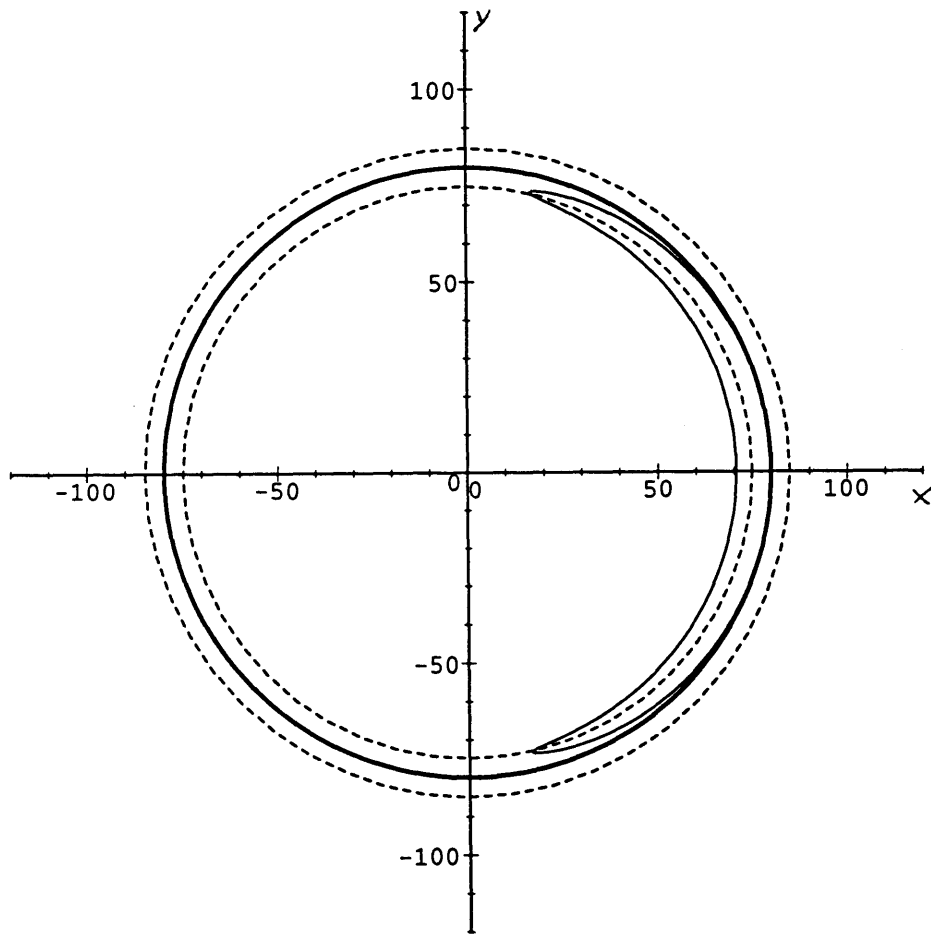
Figure 4.3 A typical "banana orbit" for a 10 keV deuteron. The thick line represents the localization of the mode, while the dotted line represent the width of the mode. For this orbit $v_{\parallel}/v_{\alpha}(r = r_{mode}) = -0.4$

Figure 4.4 A typical "banana orbit" for a 3.5 MeV α-particle. The thick line represents the localization of the mode, while the dotted line represent the width of the mode. For this orbit $v_\parallel / v_\alpha (r = r_{mode}) = -0.4$
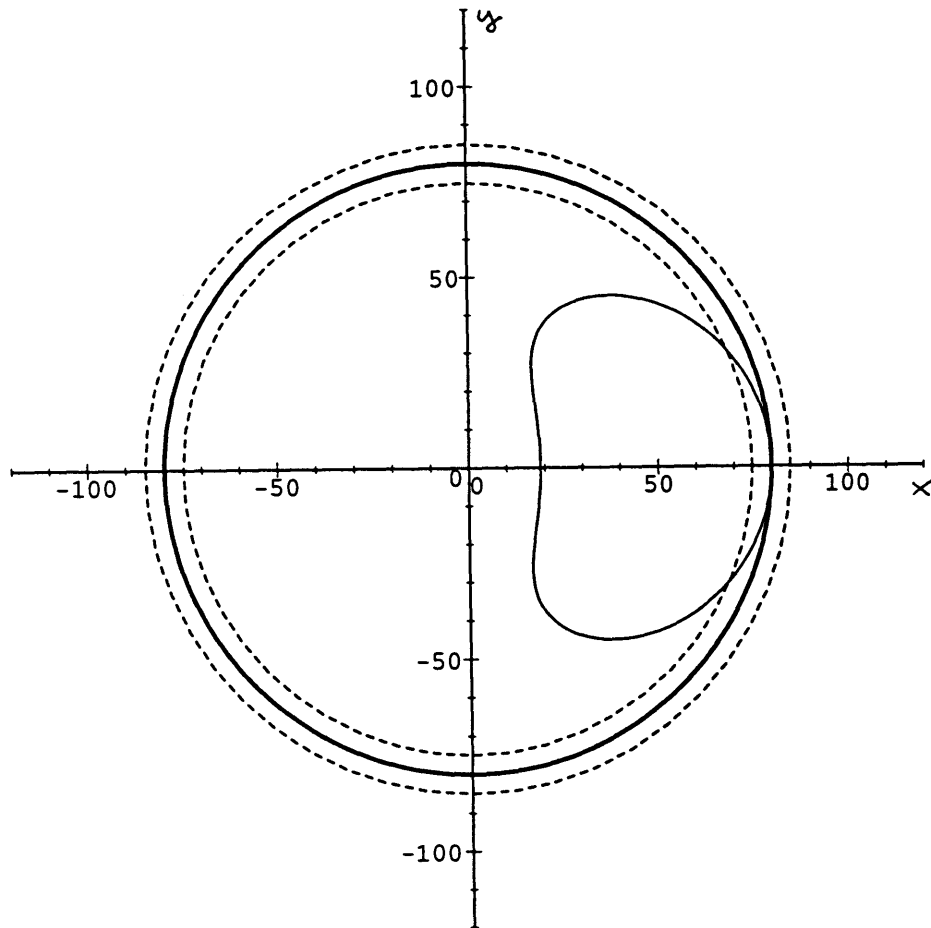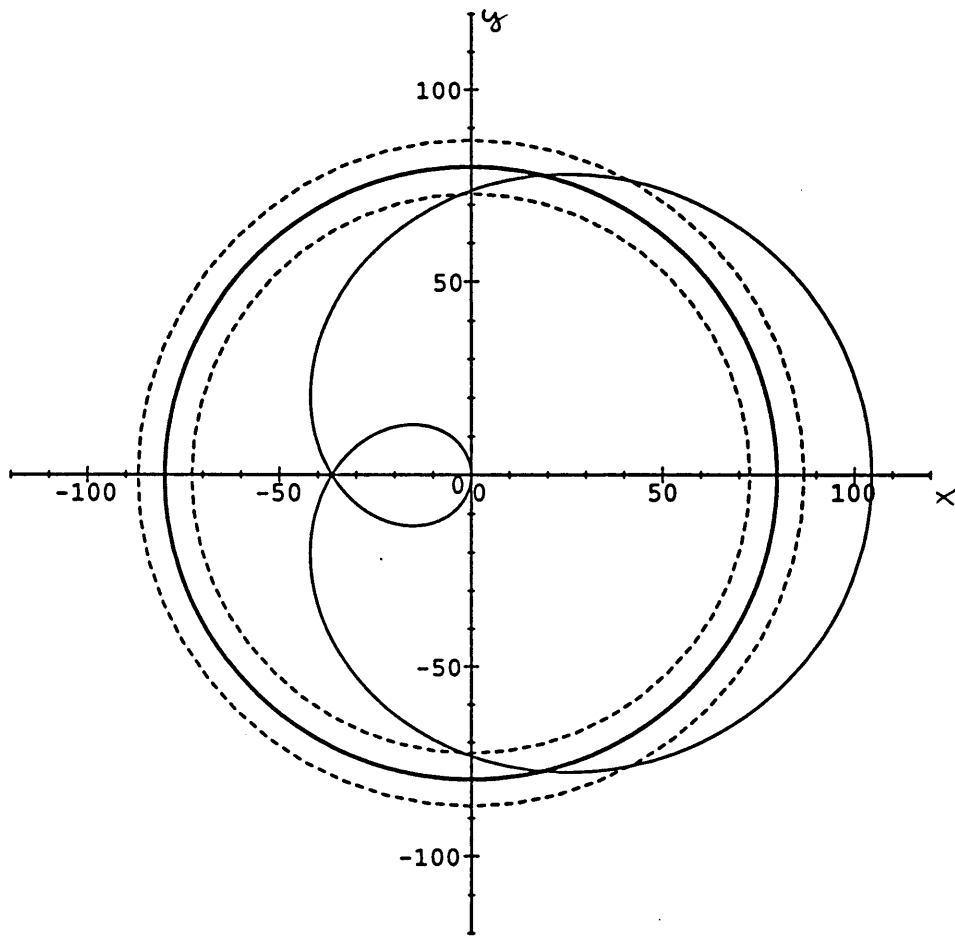
Figure 4.5 An example of a biforcation orbit for a particle passing trough the origin.
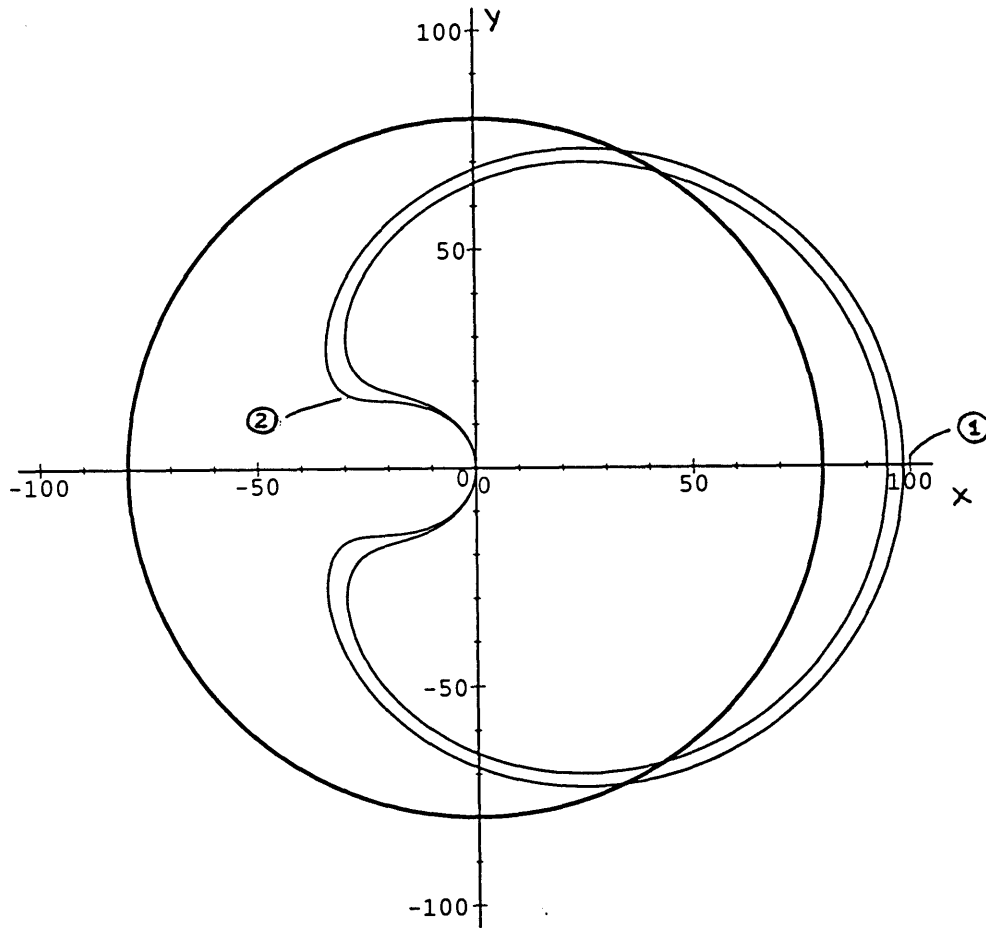
Figure 4.6 A small spread in pitch angle δw, where w is defined as $w = (v_{\parallel 0}/v_{\perp 0})$, results in a spatial spread. We label by ④ the intersection of the orbit with the x axis, and by ② the turning point of the orbit. In this case $w = 0.3$, $\delta w = 0.02$
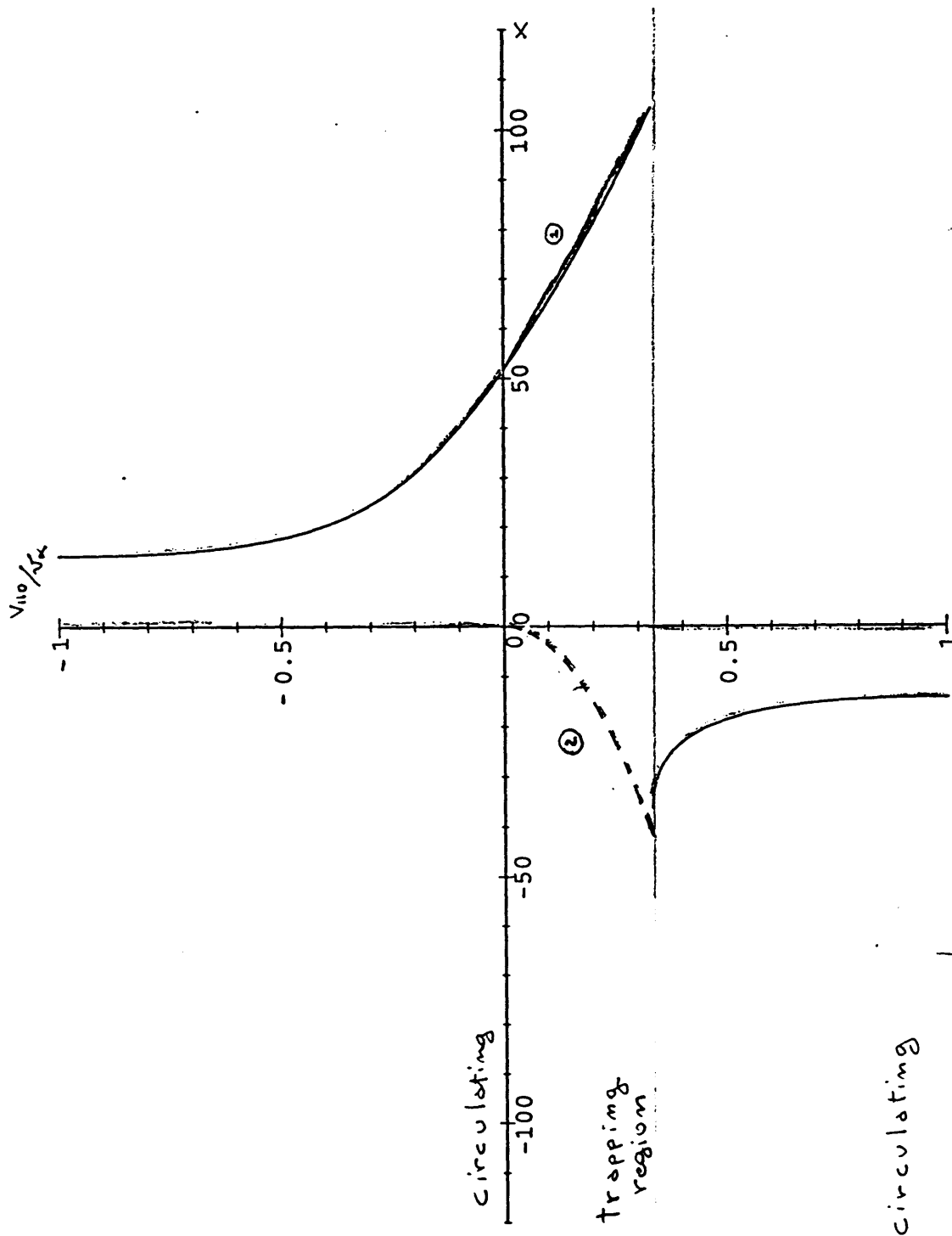
Figure 4.7 We can see from this figure the interval of values in velocity space that corresponds to trapped or circulating particles for particles born at the origin. On the y axis we have $v_{\|0}/v_\alpha$ The continuous line indicates the intersection of the orbit with the x axis, that for trapped particle is labelled by ①. The dotted line indicates the projection of the tip of the orbit on the x-axis, labelled by ② in Fig. 4.6

Figure 4.8 A plot of the orbits extremes for particles passing trough $r = r_{mode}$, $\vartheta = 0$ is represented: on the y axis is $v_{\parallel}(r_{mode})/v_\alpha$. The continuous line is the intersection of the orbit with the x axis, The dotted line, that identifies trapped particle, represents the the projection of the tip of the orbit on the x-axis. The striped region corresponds to particles that leave the plasma.

Figure 4.9 A plot of the orbits extremes for particles passing trough $r = r_{mode}$, $\vartheta = \Pi/4$ is represented: on the y axis is $v_{\parallel}(r_{mode})/v_{\alpha}$. The continuous line is the intersection of the orbit with the x axis, The dotted line, that identifies trapped particle, represents the projection of the tip of the orbit on the x-axis. The striped region corresponds to particles that leave the plasma.
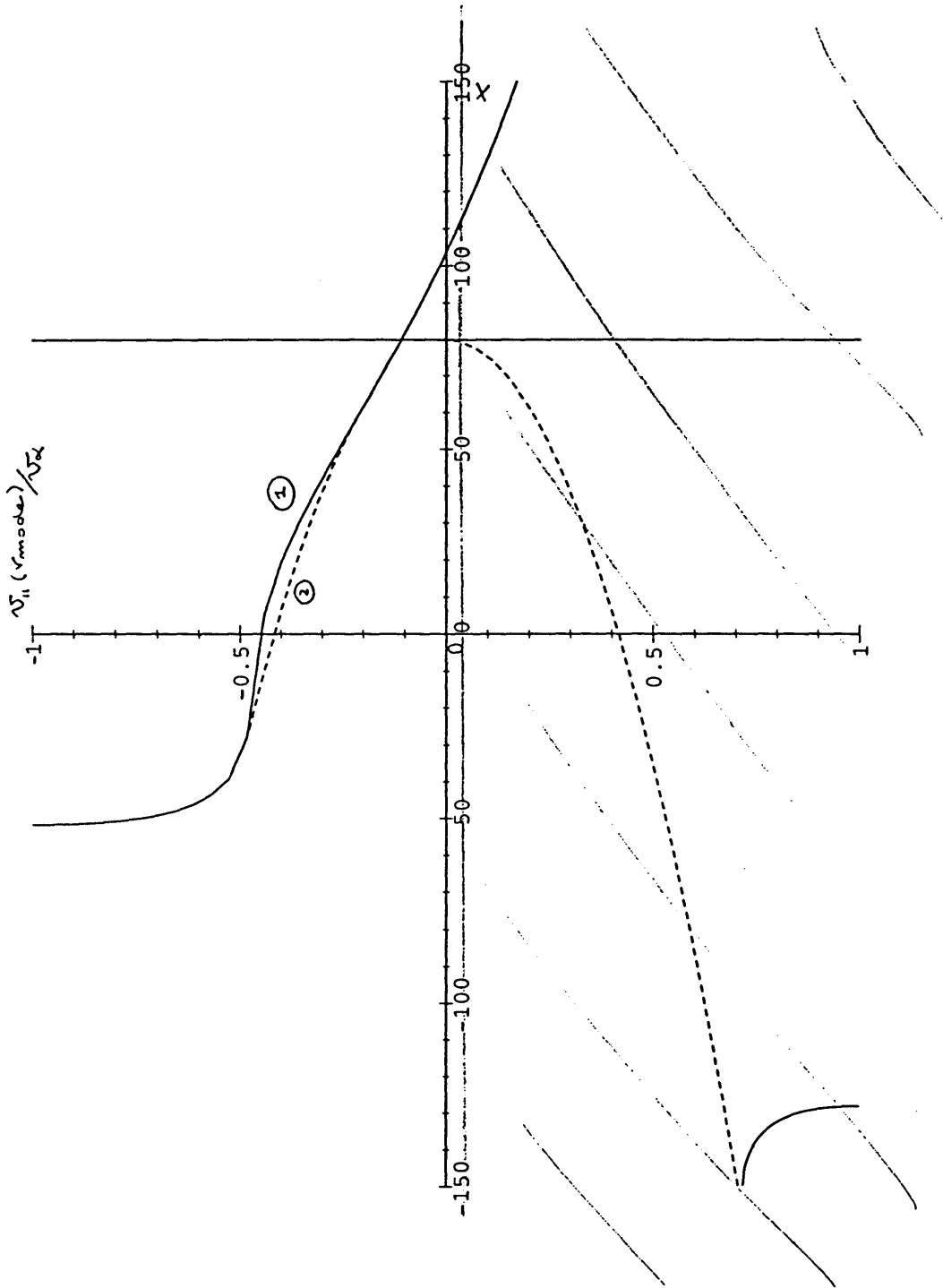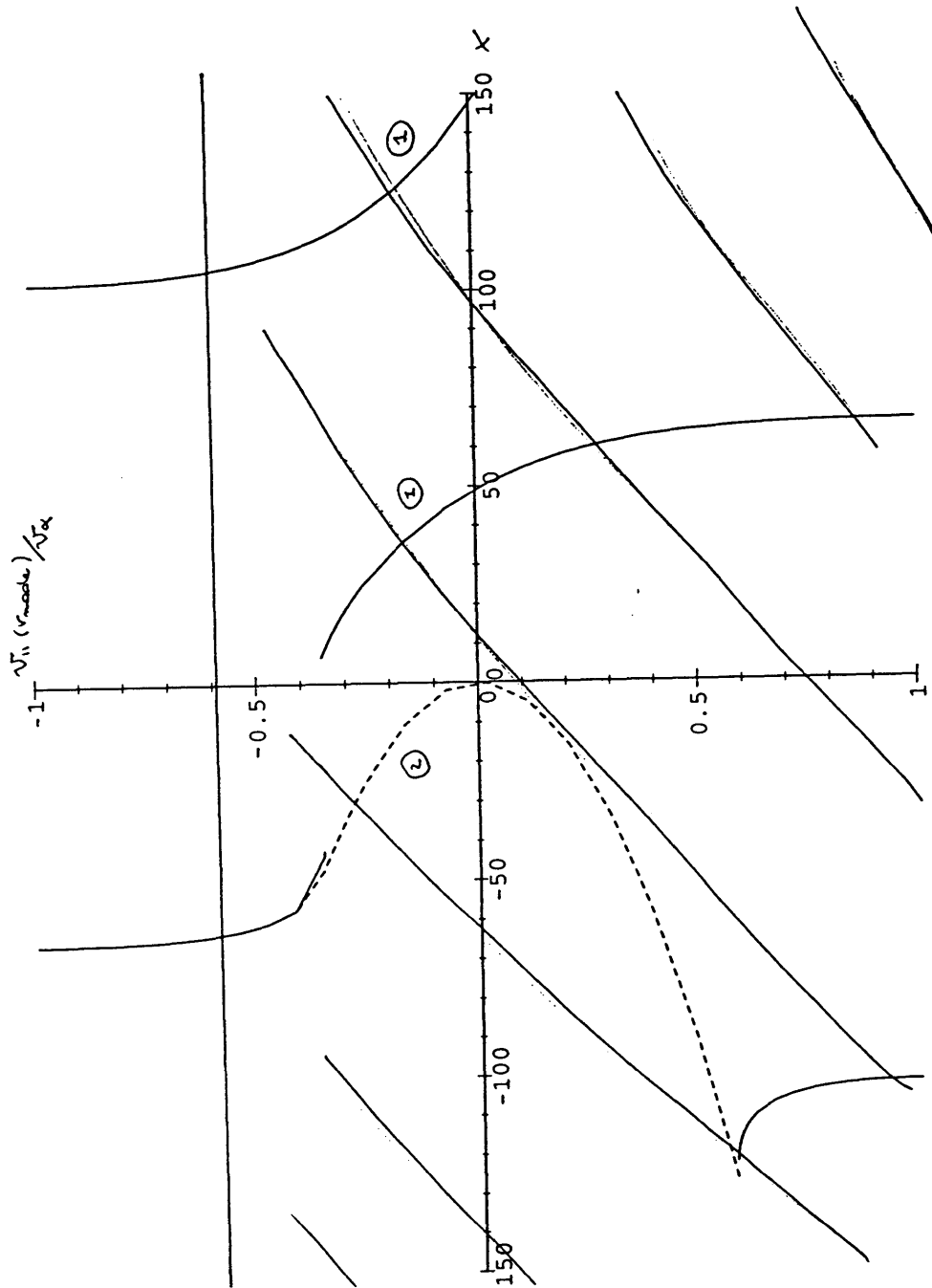
Figure 4.10 A plot of the orbits extremes for particles passing trough $r = r_{mode}$, $\vartheta = \Pi/2$ is represented: on the y axis is $v_{\parallel}(r_{mode})/v_\alpha$. The continuous line is the intersection of the orbit with the x axis, The dotted line, that identifies trapped particle, represents the projection of the tip of the orbit on the x-axis. The striped region corresponds to particles that leave the plasma.
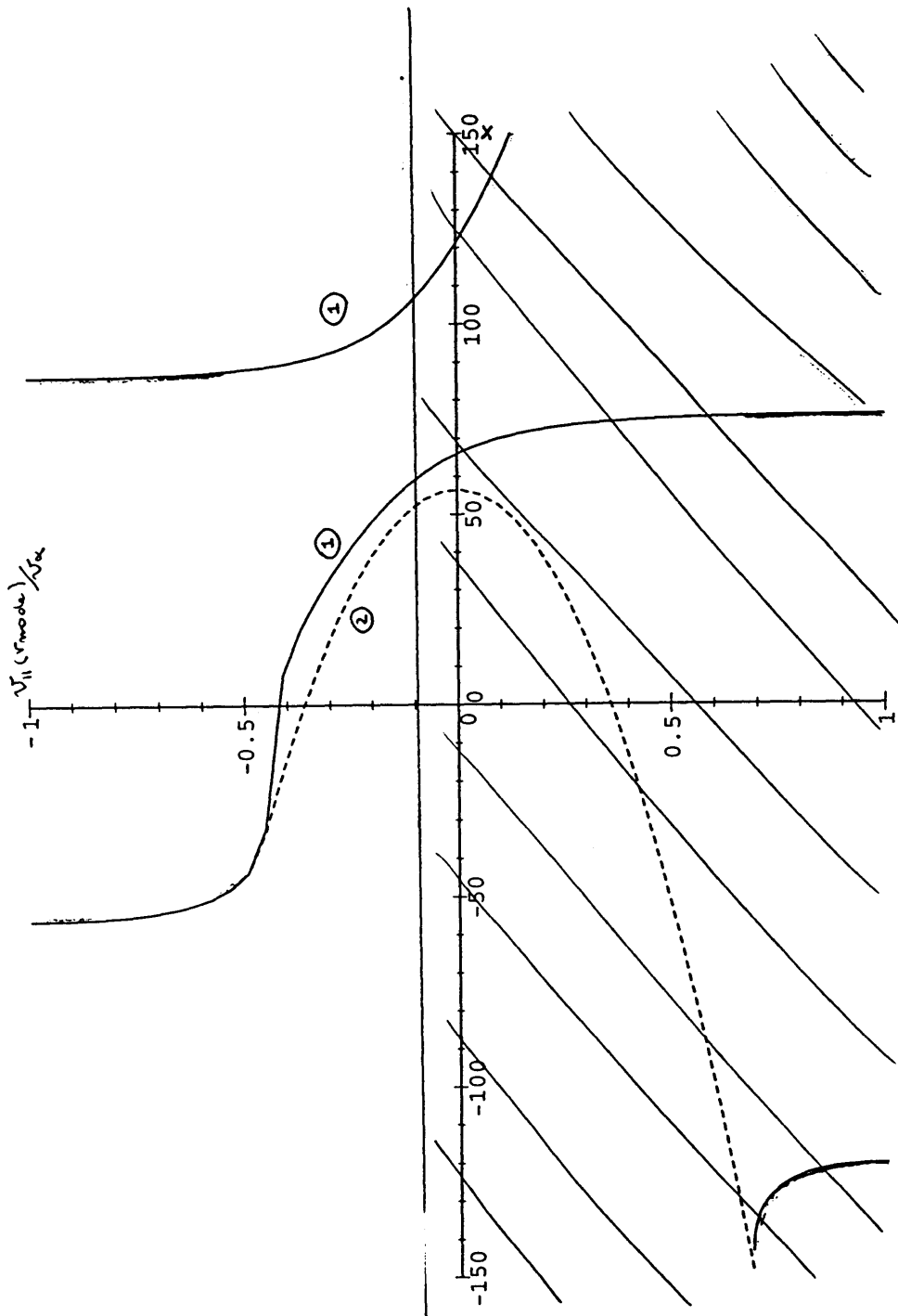
70
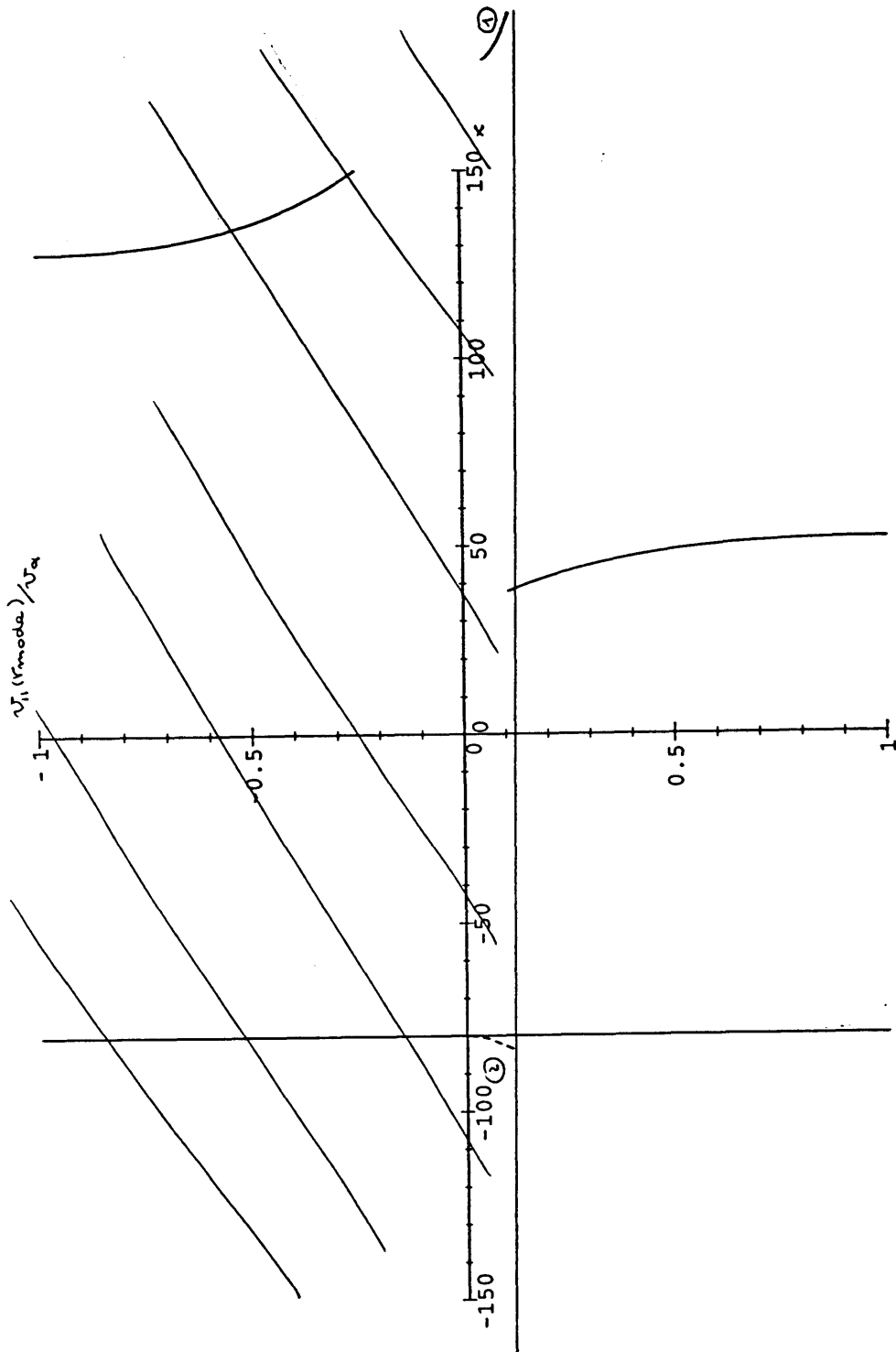
Figure 4.11   A plot of the orbits extremes for particles passing trough $r = r_{mode}$, $\vartheta = \Pi$ is represented: on the y axis is $v_{\parallel}(r_{mode})/v_\alpha$. The continuous line is the intersection of the orbit with the x axis, The dotted line, that identifies trapped particle, represents the projection of the tip of the orbit on the x-axis. The striped region corresponds to particles that leave the plasma.

71

Figure 4.12 A plot of the orbits extremes for particles passing trough $r = r_{mode}$, $\vartheta = 3\Pi/4$ is represented: on the y axis is $v_{\parallel}(r_{mode})/v_\alpha$. The continuous line is the intersection of the orbit with the x axis, The dotted line, that identifies trapped particle, represents the projection of the tip of the orbit on the x-axis. The striped region corresponds to particles that leave the plasma.
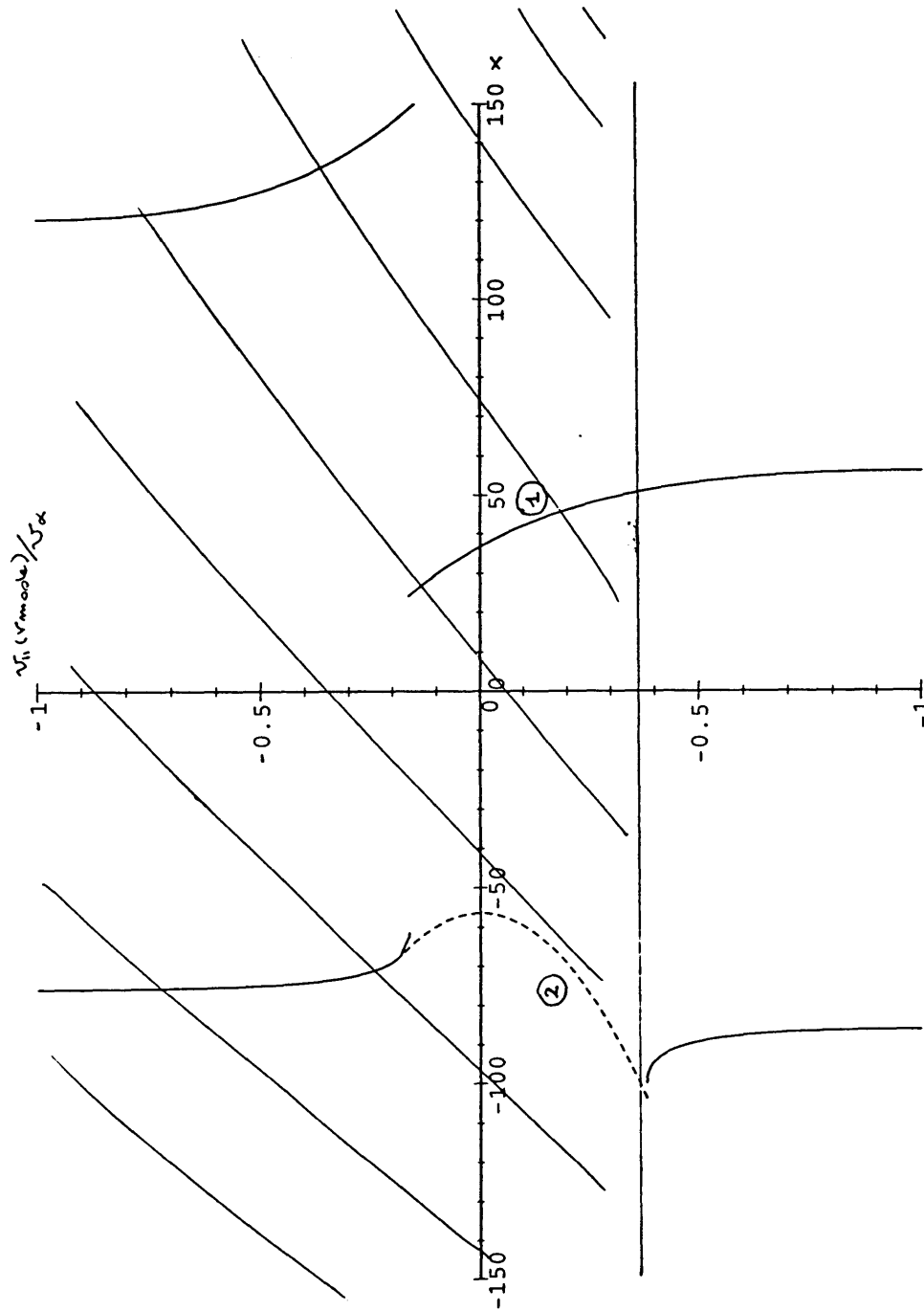
Chapter 5.

The Alpha-particles Distribution Function

In the previous chapter we analyzed the single particle orbits for energetic α-particles. From this analysis we saw that only trapped particles with large banana orbits (that is barely trapped particles) will be able to reach the mode and that particle born at the center of the plasma column will all have parallel velocity at the mode layer in the same direction, namely $v_\parallel(r_{mode}) < 0$. The situation does not change substantially if we consider particles that are produced by fusion reactions not too far from the center, as it happens in typical plasma profiles. In Fig. 5.1 we reproduce the source profile[13] using typical plasma parameters as listed in Table A-I, and and we see that most particles are produced in a range of 30 cm. from the center of the plasma column, so that we can restrict our analysis to this region. From the single particle picture we see that if we consider particles passing through the mode layer, but born at different points in the plasma, not too far from the center, they will all have the magnitude of $v_\parallel$ whitin a narrow range. This can be

seen explicitly by looking at figure [4.6] where particles born on the x-axis whitin 30 cm. from the center (the place of birth can be taken as to be represented by the place where the orbit crosses the x axis, that is by the x coordinate in the figure), all have velocities at the mode and at $\theta = 0$ given by $v_\parallel/v_\alpha \sim 0.45 \pm 0.02$. As it is clear from figure [4.7] the situation doesn't change significantly for $\theta = \pi/4$.

Thus we expect the local distribution function to be strongly anisotropic in velocity space. Furthermore, since the instability evolves on a time scale that is fast respect to the slowing down time, we expect the distribution function of the α-particles to be proportional to $\delta(\mathcal{E}_\alpha - \mathcal{E})$ where $\mathcal{E}_\alpha = 3.5$ MeV. This quantity will be multiplied by an anisotropic function that we find convenient to express as a function of μ and $\mathcal{E}_\alpha$ and that will be such that such that the average value of $v_\parallel(r_{\mathrm{mode}})$ will be some negative quantity consistent with the single particle results.

Section 5-1. An Analytic Form for the Distribution Function

To evaluate the distribution function we adopt the following procedure: since all the α-particles are produced by fusion, the source term for fusion products is the main factor to consider in order to obtain the final form for the distribution function before slowing down. Fusion particles are created at a rate determined by the plasma density and temperature profiles, which are roughly constant in time. For a given source, the distribution function F satisfies the equation

$$\frac{dF}{dt} = S$$

where F and S are normalized to the canonical phase space volume, and $\frac{d}{dt} = \frac{\partial}{\partial t} + \vec{v} \cdot \nabla + \vec{a} \cdot \nabla_v$ is the relevant convective derivative.

We define the orbit integral of the source to be

$$\bar{S} = \frac{1}{\tau_b} \oint d\tau S(\vec{x}(\tau), \vec{v}(\tau))$$

where τ is the "parametric time" according to which particles move along their orbits. Averaging over τ yields a function which is constant along orbits; therefore

74

$\bar{S}$ is a function only of the constants of the motion, $\mathcal{E}$, μ, P_ζ, which are needed to specify the orbits. This procedure replaces created particles with uniformly filled orbits.

If we assume $F = \bar{S}t$, we find that F satisfies

$$\frac{dF}{dt} = \bar{S}.$$

If $\tau_b << t$ and $\frac{\partial}{\partial t} << \vec{v} \cdot \nabla$, $\vec{a} \cdot \nabla_v$, then this estimate introduces only a small correction to the equation $dF/dt = S$ [14]. To understand the meaning of this approximation, and for the purpose of illustration, we examine in detail in appendix D a simpler case that allows an analytical treatment and vizualization. We consider in appendix D the case of the distribution function of particles in a constant magnetic field; so that the relevant periodic motion is the cyclotron motion, and we average over the orbits. We see how in that case orbit average leads from the distribution function of particles to the distribution function of giuding centers. In our case instead the periodic motion is the bounce motion of the guiding center of trapped particles and the difference between real space and guiding center space is neglected to lowest order, and, as we said, averaging along the orbits leads to a function of $\mathcal{E}$, μ, P_ζ.

With these assumptions we take

$$F = f(\mu, P_\zeta)\delta(\mathcal{E} - \mathcal{E}_\alpha)\frac{\bar{n}}{\sqrt{2\mathcal{E}_\alpha/m_\alpha^3}} \tag{5.1.1}$$

where μ and P_ζ are defined by

$$\mathcal{E} = \frac{1}{2}m_\alpha v^2$$

$$\mu = \frac{m_\alpha v_\perp^2}{2B}$$

$$P_\zeta = R\left[m_\alpha v_\zeta + qA_\zeta\right]$$

Here $RA_\zeta = \int_0^r RB_\theta \, dr$, the normalization $\bar{n}$ has dimensions of number of particles per unit volume, and f is dimensionless. We consider that $\bar{n}$ is roughly constant over the mode growth time that is about the orbit time.

75

Because we are interested in the interaction of α-particles with high frequency modes ($\omega \sim \ell\Omega_\alpha$) that require a gyrokinetic treatment, we shall incorporate corrections to Eq. (5.1.1) of the order of $\lambda \equiv \rho_\alpha/L_B$ as derived by L. Chen, S.T. Tsai[15] and X.S. Lee et al [16]. In this formalism a distribution function of the form of Eq. (5.1.1) is only the lowest order term in an expansion in the parameter λ. We notice that the guiding center coordinates perpendicular to the magnetic field are also constants of the motion, if we consistently neglect corrections of the order of λ. Thus we consider an equivalent form for the function f as given by

$$f = f(\mu, \theta, r) \tag{5.1.2}$$

where θ and r are the coordinates of the guiding centers. From here on, all spatial coordinates will refer to the location of the guiding center unless otherwise indicated. We can first numerically calculate $f(\mu, P_\zeta)$, and use the fact that P_ζ can be rewritten as a function $P_\zeta(\mathcal{E}, \mu, r, \theta)$. Then, setting $\mathcal{E} = \mathcal{E}_\alpha$, we infer the form of $f = f(\mu, \theta, r)$ that we consider at $r = r_{\text{mode}}$.

Considering the source function of α-particles and their motion in some given magnetic configuration, we can calculate the distribution at $r = r_{\text{mode}}$. As found in Chap. 4 only particles with $v_\parallel < 0$ at the point r_{mode}, θ, drift inwards from the mode layer towards the plasma core, allowing us to consider only that sign of $v_\parallel$. An appropriate model for the distribution is given by the function

$$f \simeq H(\theta_{cr} - |\theta|) \exp\left[-\frac{(\mu B/\mathcal{E}_\alpha - \Lambda_0)^2}{2\sigma^2}\right] \tag{5.1.3}$$

where H is a step function which vanishes for negative argument and is equal to 1 for positive argument. The magnetic field B is of the form

$$B \simeq \frac{B_0}{1 + r_{\text{mode}}\cos\theta/R_0}.$$

Using this model, $\bar{n}$ will be of the order of the volume averaged α particles density. A numerical evaluation of $\bar{S}$ [11,12], with parameters sampled from table A-I, is

76

consistent with the following values for the constants previously introduced: $\Lambda_0 = 0.8$, $\sigma = 3 \times 10^{-2}$, $\theta_{cr} = 2\pi/5$.

Notice that we do not include in these calculations first orbit losses to the wall, and discard all particles whose orbits extend beyond the plasma edge. This is the significance of the cutoff angle θ_{cr}. The ratio $\mu B(\theta)/\mathcal{E}_\alpha \simeq \Lambda_0$ corresponds to trapped particles whose orbits extend from the mode layer $r = r_{\text{mode}}$ well into the plasma core. At $r = r_{\text{mode}}$ and for $\theta > \theta_{cr}$, $\mu B(\theta)/\mathcal{E}_\alpha = \Lambda_0$ characterizes orbits which extend beyond the plasma edge.

The source term for fusion products, reproduced in figure [5.1] and valid for the range of temperatures attained in existing experiments, is represented approximately by[13] $S_\alpha \propto \frac{n_D n_T}{T^{3/2}} \exp\left(-\frac{20}{T^{1/3}}\right) \delta(\mathcal{E} - \mathcal{E}_\alpha)$, where T is in units of keV.

The considered profiles are given by

$$n = n_0(1 - r^2/a^2)^{1/2}$$
$$T = T_0 \frac{1 - 6r^2/a^2}{1 + 8r^2/a^2}$$
$$q = (1 + 2.5r^2/a^2)$$

where $q(r)$ is the magnetic field unwinding function and the values of the constants are taken from table A-I. The form for the distribution function used in Eq. (5.1.3) is sufficiently robust to model a wide variety of profiles, as long as the density and temperature are peaked at the center of the plasma. The values of the numerical constants used in this model are weakly dependent on the shape of the background profiles.
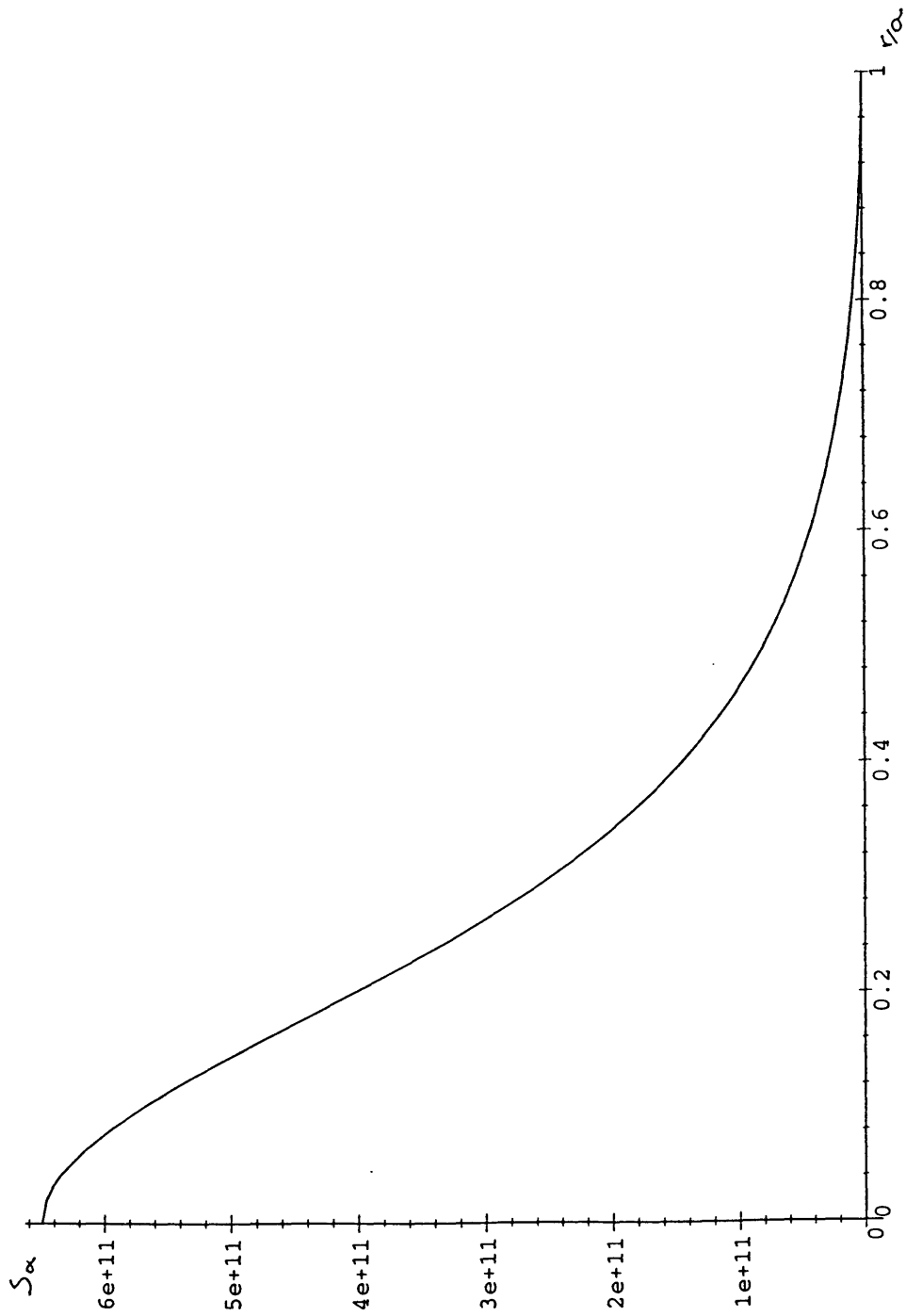
Figure 5.1 The production rate S_α in a typical D-T plasma discharge. On the y axis is S_α in units of $[cm^{-3}t^{-1}]$, and the x axis is r/a.

Chapter 6.

Quadratic Versus Linear Growth Rate

It has been shown[17] that α-particles can interact with magnetosonic modes, giving rise to a positive growth rate. In the case of a homogeneous plasma, for waves travelling mainly in the perpendicular direction, this growth rate is proportional to the square root of $n_\alpha/n_e \ll 1$, where n_α is the α-particles density[17] We labelthe growth rate with this dependence the "quadratic growth rate", γ_{quad}. The purpose of this chapter is to show how this dependence is typical of a "quasi-fluid" case, i.e. a case where all the particles partecipate to the wave-particle interaction, since they all resonate with the relevant harmonic. The interaction can produce damping or growth of the wave: the presence of an instability will obviously depend on the relative weight of the particles that give a positive contribution to the growth rate respect to the particles that damp the mode. The form of the distribution function plays a crucial role.

However if a significant Doppler shift is introduced, or toroidal effects[17,18] or other effects that allow only a fraction of the particles to resonate, this instability becomes a truly kinetic instability and the growth rate becomes linearly dependent

on the ratio n_α/n_e. We label this the "linear growth rate", γ_{lin}. In the next pages an analysis of the cases where we have the linear or quadratic growth rate depending on the value of the Doppler shift, will be presented: particularly we find that a "significant" Doppler shift that corresponds to a linear growth rate will be given by $k_\parallel v_{\parallel\alpha} > \Omega_\alpha (n_\alpha/n_e)^{1/2}$. Here $v_{\parallel\alpha}$ is the relevant velocity of the α particles in the parallel direction.

The condition presented above is the analogous of what found by Mikhailovskii in Ref.[17] studying the role of toroidal effects, in particular the variation of the magnetic field with radius. In his work it is found that "with increasing toroidicity, when $(n_\alpha/n_e)^{1/2} << a/R_0$, the trapped α-particle instability becomes kinetic, i.e., it is due to resonant interaction between a wave and α-particles with corresponding energy and pitch angle". In this chapter we wish to generalize this result by showing that we can identify a generic condition such that we can say that we have a linear growth rate, $\gamma_{lin} \sim n_\alpha/n_e$, when $(n_\alpha/n_e)^{1/2} < \delta\omega/\Omega_\alpha$. Here $\delta\omega/\Omega_\alpha$ can be related to toroidal effects, as the inhomogeneity of the magnetic field $\sim a/R_0$, or it can be due to the presence of toroidal drifts, appearing as $k_\perp v_D$ or to the Doppler shift in the parallel direction. In the opposite limit $(n_\alpha/n_e)^{1/2} > \delta\omega/\Omega_\alpha$ we have instead the quadratic growth rate $\gamma_{quad} \sim (n_\alpha/n_e)^{1/2}$.

Section 6-1. The Dispersion Relation with α-particles

Let us consider a homogeneous plasma with one ion species plus another species of energetic particles n_α such that $n_\alpha/n_e \ll 1$. In Section 1.2, we calculated the dispersion relation for magnetosonic-whistler waves for a perturbation of the form:

$$\vec{E}_1(t,y) = \vec{E}_1 e^{-i\omega t + i k_\perp y + i k_\parallel z}$$

with $k_\parallel \ll k_\perp$. We recall that $E_{1z} = 0$. For the purpose of this calculation we don't need to keep the contribution of $k_\parallel$ to the real part of the dispersion relation, so that the relevant mode to zeroth order in n_α/n_e, will be the one calculated in

section 1, with dispersion relation given by Eq. (1.1.13) and polarization given by Eq. (1.1.11).

If we include a population of α-particles in the plasma we only need to modify the current in Ampère's law so that Eq. (1.1.7) will have a term arising from the α-particles, $\delta \vec{J}_\alpha = en \int \vec{v} \delta F_\alpha d^3v$. We can define a conductivity tensor for α-particles so that $\delta \vec{J}_\alpha = \delta \overleftrightarrow{\sigma}_\perp \cdot \vec{E}_1$, and we can define the polarization of the wave as $\lambda = -i(E_{1y}/E_{1x})$ and the unit vector along the perturbed field as $\vec{\epsilon} = \vec{E}_1/|\vec{E}_1|$.

We write the dispersion relation is obtained by solving Eq. (1.1.7) with α-particles in terms of these quantities:

$$1 - \frac{\omega^2}{k^2 \bar{v}_A^2} - (1+\lambda^2)\frac{\omega^2}{k^2 c^2}\frac{i}{\epsilon_0 \omega}\vec{\epsilon}^* \cdot \delta \overleftrightarrow{\sigma}_\perp \cdot \vec{\epsilon} = 0 \qquad (6.1.1)$$

The explicit form of $\delta \overleftrightarrow{\sigma}_\perp$ is obtained by integration along the umperturbed orbits[27], and is given by

$$\delta \overleftrightarrow{\sigma}_\perp = -i\epsilon_0 \omega \frac{\omega_{p\alpha}^2}{\omega^2} \sum_{\ell=-\infty}^{+\infty} \int \frac{\overleftrightarrow{S}_\perp \mathcal{O}_\perp F_{\alpha 0}(v_\perp, v_\parallel)d^3v}{\omega - \ell \Omega_\alpha - k_\parallel v_\parallel} \qquad (6.1.2)$$

where

$$\overleftrightarrow{S}_\perp = \begin{pmatrix} v_\perp J_\ell'^2 & iv_\perp \frac{\ell}{\xi}J_\ell J_\ell' \\ -iv_\perp \frac{\ell}{\xi}J_\ell J_\ell' & v_\perp \left(\frac{\ell}{\xi}J_\ell\right)^2 \end{pmatrix}$$

and $\xi = k_\perp v_\perp/\Omega_\alpha$, $J_\ell = J_\ell(\xi)$, $\mathcal{O} = \omega \partial/\partial v_\perp + k_\parallel \mathcal{O}_a$. The operator $\mathcal{O}_a \equiv v_\perp \partial/\partial v_\parallel - v_\parallel \partial/\partial v_\perp$ is equal to zero for an isotropic distibution function. In the following treatment for semplicity we will neglect the contibution coming from this term, since it turns out to be only a small correction.

We can now evaluate

$$(1+\lambda^2)\frac{\omega^2}{k^2 c^2}\frac{i}{\epsilon_0 \omega}\vec{\epsilon}^* \cdot \delta \overleftrightarrow{\sigma}_\perp \cdot \vec{\epsilon} =$$

$$\frac{\omega_{p\alpha}^2}{k^2 c^2} \sum_{\ell=-\infty}^{+\infty} \omega \int \frac{\left[\frac{\ell}{\xi}\lambda J_\ell - J_\ell'\right]^2}{\omega - \ell \Omega_\alpha - k_\parallel v_\parallel} v_\perp \frac{\partial F_{\alpha 0}(v_\perp, v_\parallel)}{\partial v_\perp}d^3v \qquad (6.1.3)$$

81

Eq. (1.3) can be rewritten in a more convenient form by using the equality $\omega_{p\alpha}^2/(k_\perp c)^2 = (n_\alpha/n_e)(\Omega_\alpha\Omega_i/(k_\perp v_A)^2)$ that gives for the dispersion relation the form:

$$1 - \frac{\omega^2}{k_\perp^2 v_A^2} + \frac{n_\alpha}{n_e}\frac{\Omega_\alpha\Omega_i}{k_\perp^2 v_A^2}\omega \sum_{\ell=-\infty}^{+\infty}\left(\frac{\ell\Omega_\alpha}{k_\perp}\right)^2 \int \frac{\left[\lambda J_\ell - \frac{\xi}{\ell}J_\ell'\right]^2}{\omega - \ell\Omega_\alpha - k_\parallel v_\parallel}\frac{1}{v_\perp}\frac{\partial F_{\alpha0}}{\partial v_\perp}d^3v = 0 \quad (6.1.4)$$

For sake of simplicity and to enlighten the different role played by the parallel and perpendicular direction let us consider the equilibrium distribution function as the product of two functions, one dependent on $v_\parallel$ only, and the other dependent on $v_\perp$ only.

$$F_{\alpha0} = F_\parallel(v_\parallel) \times F_\perp(v_\perp)$$

This allows us to rewrite the dispersion relation in the form:

$$1 - \frac{k_\perp^2 v_A^2}{\omega^2} + \frac{n_\alpha}{n_e}\frac{\Omega_\alpha\Omega_i}{\omega^2}\omega \sum_{\ell=-\infty}^{+\infty}\left(\frac{\ell\Omega_\alpha}{k_\perp}\right)^2 2\pi \int_0^\infty dv_\perp \frac{\partial F_\perp}{\partial v_\perp}\left[\lambda J_\ell - \frac{\xi}{\ell}J_\ell'\right]^2 \times$$

$$\times \int_{-\infty}^{+\infty}dv_\parallel \frac{F_\parallel}{\omega - \ell\Omega_\alpha - k_\parallel v_\parallel} = 0 \quad (6.1.5)$$

It is convenient to define the quantities

$$\sigma_l = \frac{\Omega_i}{\Omega_\alpha}\sum_{\ell=-\infty}^{+\infty}\left(\frac{\ell\Omega_\alpha}{k_\perp}\right)^2 2\pi \int_0^\infty dv_\perp \frac{\partial F_\perp}{\partial v_\perp}\left[\lambda J_\ell - \frac{\xi}{\ell}J_\ell'\right]^2$$

and

$$I = \frac{n_\alpha}{n_e}\frac{\omega^2}{\omega}\int_{-\infty}^{+\infty}dv_\parallel \frac{F_\parallel}{\omega - \ell\Omega_\alpha - k_\parallel v_\parallel}.$$

In terms of these quantities Eq. (6.1.5) reads

$$1 - \frac{k_\perp^2 v_A^2}{\omega^2} + \sigma_l I = 0 \quad (6.1.6)$$

82

The quantity labelled σ_l is typically of order unity and can be positive or negative, depending on $F_\perp$. We will see that in order to have an instability we will need $\sigma_l > 0$. This term represent the source of "free energy" for the instability[10], and is going to be positive if $\partial F_\perp / \partial v_\perp$ is greater then zero somewhere, and particularly where the weight function $[\lambda J_\ell - \xi/\ell J'_\ell]^2$ takes the highest values. As expected we see immediately that for a maxwellian plasma in the perpendicular direction we don't have any instability. The driving term for the instability is thus the release of energy in the perpendicular direction. From now on we will just consider σ_l as some positive dimensionless quantity, and examine the role of I. Let us consider three different forms for $F_\parallel$:

i) delta function,

ii) lorentzian,

iii) maxwellian.

Section 6-2. The Quadratic Growth Rate.

i) $\quad F_\parallel(v_\parallel) = \dfrac{1}{2}[\delta(v_\parallel + v_0) + \delta(v_\parallel - v_0)]$

For this distribution function the quantity I is:

$$I = \frac{\Omega_\alpha^2}{\omega} \frac{n_\alpha}{n_e} \frac{\omega - \ell\Omega_\alpha}{(\omega - \ell\Omega_\alpha - k_\parallel v_0)(\omega - \ell\Omega_\alpha + k_\parallel v_0)} \tag{6.2.1}$$

and the dispersion relation becomes:

$$1 - \frac{k_\perp^2 v_A^2}{\omega^2} + \sigma_l \frac{\Omega_\alpha^2}{\omega} \frac{n_\alpha}{n_e} \frac{\omega - \ell\Omega_\alpha}{(\omega - \ell\Omega_\alpha - k_\parallel v_0)(\omega - \ell\Omega_\alpha + k_\parallel v_0)} = 0 \tag{6.2.2}$$

Since the ratio $n_\alpha/n_e << 1$ we can solve this equation by expanding in this small parameter, and we obtain to lowest order, defining $\omega = \omega_r + i\gamma$ with $\omega_r >> \gamma$,

$$\omega = \omega_r \simeq k_\perp v_A \tag{6.2.3}$$

83

The maximum contribution from the term proportional to n_α/n_e comes from $\omega \sim \ell\Omega_\alpha + k_\parallel v_0$ or $\omega \sim \ell\Omega_\alpha - k_\parallel v_0$, that is from the Doppler shifted cyclotron frequencies. Let us consider first the case $\omega \sim \ell\Omega_\alpha + k_\parallel v_0$, this resonance condition combined with Eq. (6.2.3) selects the values for $k_\parallel$ and $k_\perp$ that correspond to the maximum growth rate. The next order expansion of Eq. (6.2.2) gives

$$1 - \frac{k_\perp^2 v_A^2}{\omega_r^2}\left(1 - 2\frac{\delta\omega_r + i\gamma}{\omega_r}\right) + \sigma_l\frac{\Omega_\alpha^2}{\omega}\frac{n_\alpha}{n_e}\frac{k_\parallel v_0 + i\gamma}{(2k_\parallel v_0 + i\gamma)(i\gamma)} = 0 \qquad (6.2.4)$$

To find γ we equate the imaginary parts and we have:

$$2\gamma = \sigma_l\frac{\Omega_\alpha^2}{\omega}\frac{n_\alpha}{n_e}\frac{2k_\parallel^2 v_0^2 + \omega_i^2}{(4k_\parallel^2 v_0^2 + \omega_i^2)} \qquad (6.2.5)$$

This is a fourth order equation for γ, that we solve by considering the two extreme limits of interest:

i-1) $k_\parallel v_0 \gg \gamma$

$$\gamma^2 = \frac{\sigma_l}{4}\frac{n_\alpha}{n_e}\Omega_\alpha^2 \qquad (6.2.6)$$

i-2) $k_\parallel v_0 \ll \gamma$

$$\gamma^2 = \frac{\sigma_l}{2}\frac{n_\alpha}{n_e}\Omega_\alpha^2 \qquad (6.2.7)$$

We see that in both cases the instability requires $\sigma_l > 0$ and the growth rate goes as the square root of n_α/n_e. It is clear, by letting $v_0 \to -v_0$, that the same result holds for $\omega \sim \ell\Omega_\alpha - k_\parallel v_0$.

As expected with this kind of distribution function there is no "kinetic" instability, since either all the particles contibute to the instability or none, that is we always have a stronger, quadratic, instability. The different response for the limit $k_\parallel \to 0$ can be easily explained by looking at our choice for the distribution function: $F_\parallel(v_\parallel) = \frac{1}{2}[\delta(v_\parallel + v_0) + \delta(v_\parallel - v_0)]$. We see that if either $\omega \sim \ell\Omega_\alpha + k_\parallel v_0$ or $\omega \sim \ell\Omega_\alpha - k_\parallel v_0$ is considered, just one of the two beams interacts giving instability (i.e. half of the particles), but for $k_\parallel v_0 \ll \gamma \ll \omega_r$ the doppler shift is not

appreciable, so that all particle contribute to the instability resonating with $\ell\Omega_\alpha$. This accounts for the factor of 2.

Section 6-3. The Quadratic and the Linear Growth Rate

We consider both cases ii) and iii) together because the lorentzian distribution function allows to perform the integration and evaluate I, but exhibits a similar behavior to the case of the maxwellian in the parallel direction from the instability point of view.

ii) $\quad F_\parallel(v_\parallel) = \dfrac{a}{\pi}\dfrac{1}{v_\parallel^2 + a^2}$

Let us first evaluate the quantity I,

$$
\begin{aligned}
I &= \frac{\Omega_\alpha^2}{\omega}\frac{n_\alpha}{n_e}\int_{-\infty}^{+\infty}\frac{a}{\pi}\frac{dv_\parallel}{(v_\parallel^2 + a^2)(\omega - \ell\Omega_\alpha - k_\parallel v_\parallel)} \\
&= \frac{\Omega_\alpha^2}{\omega}\frac{n_\alpha}{n_e}\frac{1}{\omega - \ell\Omega_\alpha + i|k_\parallel|a}
\end{aligned}
\tag{6.3.1}
$$

with dispersion relation

$$
1 - \frac{k_\perp^2 v_A^2}{\omega^2} + \sigma_l\frac{\Omega_\alpha^2}{\omega}\frac{n_\alpha}{n_e}\frac{(\omega_r - \ell\Omega_\alpha) - i(\omega_i + |k_\parallel|a)}{(\omega_r - \ell\Omega_\alpha)^2 + (\omega_i + |k_\parallel|a)^2} = 0
\tag{6.3.1}
$$

We solve Eq. (6.3.1)) espanding in the small parameter n_α/n_e and as before the lowest order solution is given by Eq. (6.2.3) $\omega = k_\perp v_A$ and the next order can be used to determine the imaginary part that satisfies

$$
2\frac{\gamma}{\omega_r} \simeq \sigma_l\frac{\Omega_\alpha^2}{\omega}\frac{n_\alpha}{n_e}\frac{1}{(\gamma + |k_\parallel|a)}
\tag{6.3.3}
$$

Eq. (6.3.3) is a quadratic γ, $\gamma^2 + \gamma|k_\parallel|a - \sigma_l(\Omega_\alpha^2/2)(n_\alpha/n_e) = 0$ and again we are interested in the two extreme limits:

ii-1) if $\gamma \gg |k_\parallel|a$, the growth rate is

85

$$\gamma_{quad} \sim \left(\frac{\sigma_l}{2} \frac{n_\alpha}{n_e} \Omega_\alpha^2 \right)^{1/2} \tag{6.3.4}$$

ii-2) if $\gamma << |k_\parallel|a$, the growth rate is

$$\gamma_{lin} \sim \frac{\sigma_l}{2} \frac{n_\alpha}{n_e} \frac{\Omega_\alpha^2}{|k_\parallel|a} \tag{6.3.5}$$

As we see in both sub-cases the instability requires that $\sigma_l > 0$ and the growth rate will be quadratic (case 1) or linear (case 2) depending on the value of $k_\parallel$. Thus the quadratic growth rate requires $(\sigma_l/2)(n_\alpha/n_e)\Omega_\alpha^2 > (|k_\parallel|a)^2$, while the linear one requires $(\sigma_l/2)(n_\alpha/n_e)\Omega_\alpha^2 < (|k_\parallel|a)^2$.

To give a physical interpretation let us go back to the quantity I as defined by Eq. (6.3.1) before performing the integration. If we neglect in the denominator $k_\parallel v_\parallel$ respect to ω_i we have that

$$\frac{1}{\omega - \ell\Omega_\alpha - k_\parallel v_\parallel} \sim \frac{1}{\omega - \ell\Omega_\alpha}$$

can be factorized out of the integral so that

$$I = \frac{n_\alpha}{n_e} \frac{\Omega_\alpha^2}{\omega} \frac{1}{\omega - \ell\Omega_\alpha} \sim -i \frac{n_\alpha}{n_e} \frac{\Omega_\alpha^2}{\omega_r} \frac{1}{\gamma} \tag{6.3.6}$$

We see that in this case, for $\sigma_l > 0$, all the particles contribute to the instability, and we obtain a stronger growth rate. Let us now consider the limit $\gamma << |k_\parallel|a$ and use the Plemejely operator:

$$\frac{1}{\omega - \ell\Omega_\alpha - k_\parallel v_\parallel} \sim -i \frac{\pi}{|k_\parallel|} \delta \left(v_\parallel - \frac{\omega_r - \ell\Omega_\alpha}{k_\parallel} \right)$$

so that

$$I = -i \frac{n_\alpha}{n_e} \frac{\Omega_\alpha^2}{\omega_r} \frac{\pi}{|k_\parallel|} \frac{a}{\pi} \frac{1}{a^2 + ((\omega_r - \ell\Omega_\alpha)/k_\parallel)^2}$$

$$\sim -i \frac{n_\alpha}{n_e} \frac{\Omega_\alpha^2}{\omega_r} \frac{1}{|k_\parallel|a} \tag{6.3.7}$$

86

This leads to the same growth rate as in Eq. (6.3.5), that is the linear growth rate. Thus we see that for $|k_\parallel|a > \gamma$ not all the particles contribute to the instability, but only those one with $v_\parallel \sim (\omega - \ell\Omega_\alpha)/k_\parallel$, giving a "kinetic" growth rate.

Finally we consider the case of a maxwellian in the parallel direction.

$$\text{iii)} \quad F_\parallel(v_\parallel) = \frac{1}{\sqrt{\pi}v_{th}}e^{-\frac{v_\parallel^2}{v_{th}^2}}$$

This case is very similar to the previous one, so we just write the final result.

iii-1) if $\gamma \gg k_\parallel v_{th}$ the growth rate is

$$\gamma_{quad} \sim \left(\frac{\sigma_l}{2}\frac{n_\alpha}{n_e}\Omega_\alpha^2\right)^{1/2} \tag{6.3.8}$$

iii-2) if $\gamma \ll k_\parallel v_{th}$ the growth rate is

$$\gamma_{lin} \sim \frac{\sigma_l}{2}\frac{n_\alpha}{n_e}\frac{\Omega_\alpha^2\sqrt{\pi}}{|k_\parallel|v_{th}} \tag{6.3.9}$$

Here again the condition $\sigma_l > 0$ is required for instability and the two differnt responses depend on the condition

quadratic

$$\sigma_l\frac{n_\alpha}{n_e} \gtrless \frac{k_\parallel^2 v_{th}^2}{\Omega_\alpha^2} \tag{6.3.10}$$

linear

In our case, as detailed in the next chapter, for a realistic toroidal configuration we find that we need to keep not only the Doppler shift in the parallel direction, but also other toroidal corrections taht result in $\delta\omega/\Omega_\alpha$ larger then $(n_\alpha/n_e)^{1/2}$. We can thus conclude that we will have a growth rate that is linear in n_α/n_e.

Chapter 7.

The Growth Rate

In Chapter 2 and Chapter 3 we have studied the dispersion equation for the contained modes, considering only the background plasma. We can see how this is modified by the influence of fusion products through a perturbation of the dispersion relation in the quantity n_α, because $n_\alpha \ll n_i$. In Chapter 6 we exhamined the homogeneous case and we saw how the presence of n_α gives rise to an additional current contribution $\delta \vec{J}_\alpha$. We can thus extend the calculation carried out in Chapter 6, including the contribution of the α-particle current, yielding a new term in the dispersion equation proportional to n_α. In order to calculate the corrections related to the presence of the fusion products, it is convenient to analyze the problem in terms of the perturbed electric fields $\vec{E}_1$.

Section 7-1. The Perturbed Alpha-particles Distribution Function

Beginning with the original mode equation the dispersion relation can be written as $D_0(\omega, m, n) = 0$, where D_0 is related to the effective potential, defined in

Equation (2.2.4), by $D_0 = -V_{\text{eff}}(r_{\text{mode}})c^2/\omega^2$, correct to order $1/m$. The perturbed fields will have the form of Eq. (2.2.5)

$$\vec{E}_1(r) \simeq \vec{E}_1 H_s \left(\frac{r - r_{\text{mode}}}{\Delta} \right) e^{-\frac{(r-r_{\text{mode}})^2}{2\Delta^2}} e^{-i\omega t - im\theta + in^0\zeta} \qquad (7.1.1)$$

In terms of components, for the coordinate system defined in appendix B, $\vec{E}_{1\perp} = E_{1r}\hat{e}_r + E_{1\theta}\hat{e}_\theta = E_{1r}(\hat{e}_r - i\Lambda\hat{e}_\theta)$ with $\Lambda \equiv iE_{1\theta}/E_{1r} \simeq \omega/\Omega_i$. This is similar to the result Eq. (1.1.11) found in Chapter 1 for the polarization of the magnetosonic-whistler wave in a homogeneous plasma. The dispersion relation with α particles can be written as

$$D_0(\omega, k) + \delta D_\alpha(\omega, k) = 0 \qquad (7.1.2)$$

where

$$\delta D_\alpha(\omega, k) = \frac{i}{\omega\epsilon_0} \frac{< \vec{E}_1^* \cdot \delta\overleftrightarrow{\sigma} \cdot \vec{E}_1 >}{< \left| \vec{E}_1 \right|^2 >}$$

Here the brackets indicate spatial averages and the conductivity tensor $\delta\overleftrightarrow{\sigma}$ is defined by

$$\delta\vec{J}_\alpha = \int \vec{v}\, \delta F_\alpha\, d^3\vec{v} = \delta\overleftrightarrow{\sigma}_\perp \cdot \vec{E}_1 \qquad (7.1.3)$$

We recall that the mode solution given by Equation (7.1.1) is sharply localized about $r = r_{\text{mode}}$, and the average will later be replaced by the condition that quantities are evaluated at $r = r_{\text{mode}}$. This is justified by the fact that the scale length for variations in $\delta\overleftrightarrow{\sigma}$ is larger than the mode width.

Corrections to $\vec{E}_1$ only appear in the equation for δD_α to second order in terms of $\delta\vec{J}_\alpha$ and are not considered.

Solving perturbatively in terms of the imaginary part of the frequency, γ, yields

$$\gamma = -\Re\mathrm{e} \frac{< \vec{E}_1^* \cdot \delta\overleftrightarrow{\sigma} \cdot \vec{E}_1 >}{\omega\epsilon_0 \frac{\partial D_0}{\partial\omega} < \left| \vec{E}_1 \right|^2 >} \qquad (7.1.4)$$

89

To obtain $\delta\overset{\leftrightarrow}{\sigma}$, we begin with a full gyrokinetic calculation of δF_α, the perturbed alpha distribution due to the fields from the contained mode, for frequencies above Ω_α [15,16]. This level of detail is necessary due to the large radial excursions of the particled along the orbits, as seen in Chapter 4, and the large Larmor radii of the fusion-produced alpha particles. We model the magnetic field as

$$\vec{B} = \frac{B_0}{1 + (r/R_0)\cos\vartheta}\left(\hat{e}_\zeta + \frac{r}{R_0 q}\hat{e}_\vartheta\right)$$

and we consistently neglect effects related to β. We consider the limit of ω very close to a harmonic resonance with Ω_α, with harmonic number denoted as ℓ, so that only a single harmonic term contributes to each mode-particle interaction. The gyrokinetic calculation applies to systems where the magnetic field varies on a scale length considerably larger than the gyroradius of the particles. We expand in the parameter $\lambda = \rho_i/L_B$, and keep all terms in the interaction between the mode and the fusion products to first order in λ. For the sake of simplicity we neglect corrections of order λ/q, which means that we consider only the gradient and curvature drifts due to the toroidal field, which have the combined form

$$\vec{v}_d = \frac{1}{\Omega_\alpha R}(2\mathcal{E} - \mu B)[\hat{e}_\theta \cos\theta + \hat{e}_r \sin\theta]$$

For the following section, we introduce the notation that the vector $\vec{X}$ refers to the guiding center coordinates, while the relevant coordinates in velocity space are $\vec{V} = (\mathcal{E}, \mu, \varphi)$, where $\mathcal{E} = m_\alpha v^2/2$, $\mu = m_\alpha v_\perp^2/2B$, and φ is the gyroangle. In the following equations, all spatial coordinates refer to the guiding center location. For functions, the subscript g will indicate that the function dependence is expressed in terms of guiding center variables.

The unperturbed distribution function for the fusion products is approximately given by F_{g0} as obtained in Chapter 5 in Eq. (5.1.3). F_{g0} does not depend on φ but only on $\mathcal{E}$, μ, and the guiding center coordinates. However, because calculations of the mode-particle interaction are being carried out to first order in λ, the

first order correction to F_{g0} must also be included. As in Ref.s [15,16] this correction arises from the more precise form of $\mu = m_\alpha v_\perp^2/2B - m_\alpha \vec{v}_\perp \cdot \vec{v}_d/B + O(\mu\lambda/q)$, as examined in appendix C. Thus we take:

$$F_{g\alpha} = F_{g0} - (\vec{v}_\perp \cdot \vec{v}_d)\frac{1}{B}\frac{\partial F_{g0}}{\partial \mu}. \tag{7.1.5}$$

By using the results from the Chapter 5 we can take F_{g0} of the form Eq. (5.1.3).

The perturbed distribution function for the alpha particles under the effect of the contained mode will be given by the gyrokinetic version of the Vlasov kinetic equation[15,16], a detailed derivation leading to Eq. (7.1.6) is performed in appendix E.

$$\langle L_g \rangle_\ell \langle \delta F_{g\alpha} \rangle_\ell = - \langle S_g \rangle_\ell \tag{7.1.6}$$

where the gyroaverage of the Vlasov operator is given by:

$$\langle L_g \rangle_\ell = (v_\parallel \hat{e}_\parallel + \vec{v}_d) \cdot \nabla_X - i(\omega - \ell\Omega_\alpha(R_g))$$

For simplicity, in the above formula we neglect the correction to the resonant frequency, as shown in appendix E, of the form $\omega_\varphi = \langle \vec{v} \cdot \nabla_x\varphi \rangle_0$. This correction is estimated in appendix F to be $O((\lambda\Omega_\alpha)/q)$. The quantity $\langle S_g \rangle_\ell$ is related to the perturbed field operating on the unperturbed distribution function, acts as a source term, and is defined by

$$\langle S_g \rangle_\ell = \frac{q}{m}\left\langle \left[(\vec{E}_1 + \frac{1}{c}\vec{v} \times \vec{B}_1) \cdot \left(\vec{v}\frac{\partial}{\partial \mathcal{E}} + \frac{\vec{v}_\perp}{B}\frac{\partial}{\partial \mu} - \frac{\vec{v} \times \hat{e}_\parallel}{v_\perp^2}\frac{\partial}{\partial \varphi} \right) \right.\right.$$
$$\left.\left. + (\vec{E}_1 + \frac{1}{c}\vec{v} \times \vec{B}_1) \times \frac{\hat{e}_\parallel}{\Omega} \cdot \nabla_X \right] F_{g\alpha} \right\rangle_\ell \tag{7.1.7}$$

The harmonic components, which by definition are independent of gyrophase, are defined by the expansion

$$\delta F_{g\alpha} = \sum_\ell \exp(-i\ell\varphi) \langle \delta F_{g\alpha} \rangle_\ell$$

91

where φ is the gyrophase angle given by $\vec{v}_\perp = v_\perp(\cos\varphi\ \hat{e}_a + \sin\varphi\ \hat{e}_b)$. The unit vectors are chosen so that $\hat{e}_a \simeq \hat{e}_\theta$, $\hat{e}_b \simeq \hat{e}_r$ and they form an orthonormal system with $\hat{e}_\parallel = \vec{B}/B$.

Since we assume that the spatial structure of the mode determines the layer of the interaction, but that the nature of the interaction is determined mainly by the velocity distribution of the alpha-particles within the interaction layer, we can neglect the spatial derivatives of the unperturbed distribution function represented by the last term in Eq. (7.1.7). Thus the relevant terms in Eq. (7.1.6) are

$$\langle S_g \rangle_\ell = \langle L_{g1} \rangle_\ell F_{g0} - \left\langle \vec{E}_1 \cdot \vec{v}_d - \frac{i}{\omega}\left[\vec{v} \times (\nabla \times \vec{E}_1)\right] \cdot \vec{v}_d \right\rangle_\ell \frac{1}{B}\frac{\partial F_{g0}}{\partial \mu} \qquad (7.1.8)$$

where the perturbed Vlasov operator L_{g1} is given by:

$$L_{g1} = \frac{q}{m}\left\{ \vec{E}_{1g\perp} \cdot \vec{v}_\perp \left(\frac{\partial}{\partial\mathcal{E}} + \frac{1}{B}\frac{\partial}{\partial\mu} \right) + \frac{i}{\omega}\left[v_\parallel \left(\hat{e}_\parallel \cdot \nabla_x \vec{E}_1 \right) \cdot \vec{v}_\perp \right]_g \frac{1}{B}\frac{\partial}{\partial\mu} \right\}$$

We have set $E_{1\parallel} = 0$ in the above equation. We define the quantities $\overline{A}_\ell$, that is a function of the guiding center position, and $\overline{\overline{A}}_\ell$, that is convenient for field functions, as

$$\langle A_g \rangle_\ell = \overline{A}_\ell(r,\theta)\exp(-im\theta + in\zeta)$$

$$= \overline{\overline{A}}_\ell(r,\theta)\exp\left(-im\theta + in\zeta - i\frac{k_\perp v_\perp}{\Omega}\sin\varphi\right)$$

where r,θ,ζ are guiding center coordinates. Note that the guiding center position $\vec{X}$ is defined by $\vec{X} = \vec{x} + \frac{\vec{v}\times\hat{e}_\parallel}{\Omega}$.

By explicitly evaluating the components of $\langle S_g \rangle_\ell$ we find that $\overline{\delta F}_\ell$ has to satisfy the following equation:

$$\left[\frac{v_\parallel}{qR}\left(\frac{\partial}{\partial\theta} - i(m - nq(r)) \right) - i(\omega - k_{\perp\theta}v_{d\theta} - \ell\Omega_{g\alpha}) + v_{dr}\frac{\partial}{\partial r}\right]\overline{\delta F}_\ell$$

$$= \frac{iq}{m_\alpha}P_{\ell r}(F_{g0})\overline{\overline{E}}_{1r\ell} + \frac{iq}{m_\alpha}P_{\ell\theta}(F_{g0})\overline{\overline{E}}_{1\theta\ell} \qquad (7.1.9)$$

where

$$P_{\ell\theta}(F_{g0}) = \frac{\ell}{\xi} J_\ell(\xi)\sqrt{2\mu B m_\alpha}\left[\frac{\partial}{\partial \mathcal{E}} + \left(1 - \frac{k_\| v_\|}{\ell\Omega_\alpha} - \frac{k_\perp v_{d\theta}}{\ell\Omega_\alpha}\right)\frac{1}{B}\frac{\partial}{\partial\mu}\right]F_{g0}$$

$$P_{\ell r}(F_{g0}) = i J'_\ell(\xi)\sqrt{2\mu B m_\alpha}\left[\frac{\partial}{\partial \mathcal{E}} + \left(1 - \frac{k_\| v_\|}{\ell\Omega_\alpha} - \frac{k_\perp v_{d\theta}}{\ell\Omega_\alpha}\right)\frac{1}{B}\frac{\partial}{\partial\mu}\right]F_{g0}$$

with $\xi = k_\perp v_\perp/\Omega_\alpha$.

The operators $P_{\ell r}$ and $P_{\ell\theta}$ also contain corrections of order λ; these corrections are proportional to $(1/B)(\partial/\partial\mu)$, giving no contribution for an isotropic function. This equation has an integral solution

$$\overline{\delta F_\ell} = \int^\theta d\theta' \frac{iq}{m}\frac{q(r)R}{v_\|}\left(P_{\ell r}(F_{g0})\overline{\overline{E_{1r\ell}}} + P_{\ell\theta}(F_{g0})\overline{\overline{E_{1\theta\ell}}}\right) \qquad (7.1.10)$$

$$\times \exp\left\{-i\int_\theta^{\theta'} d\theta''\left[\frac{qR}{v_\|}\left(\omega - k_{\perp\theta}v_{d\theta} - \ell\Omega_{g\alpha}\right) + (m - nq)\right]\right\}$$

where the terms within the integral are evaluated at the guiding center $\theta', r(\theta')$, which defines particles orbits through

$$r(\theta') = \int^{\theta'} \frac{qRv_{dr}}{v_\|}\, d\theta''.$$

In terms of $\overline{\delta F_\ell}$, the slowly varying part of the current from Eq. (7.1.3) can be expressed as

$$\overline{\overline{\delta J_{\alpha\ell}}} = \int \overline{\delta F_\ell}\exp\left(-i\vec{k}_\perp \cdot \frac{\vec{v}_\perp \times \hat{e}_\|}{\Omega_\alpha}\right)\vec{v}\, d^3\vec{v} \qquad (7.1.11)$$

where the exponential factor arises from the difference between the quantities $\vec{k}_\perp \cdot \vec{x}$ and $\vec{k}_\perp \cdot \vec{X}$. For high mode numbers, it is appropriate to neglect poloidal coupling, and look at the θ-average of the energy flow from the particles to the mode, given by $\overline{\overline{E_{1\ell}}} \cdot \overline{\overline{\delta J_{\alpha\ell}}}$ evaluated at $r = r_{\text{mode}}$.

Section 7-2. The Local Growth Rate

We consider the case of $\gamma > \omega_b$, which we shall verify *a posteriori*, and use the "local approximation" which uses the form

$$\overline{\delta F}_\ell = \frac{-(q/m)\left[P_{\ell r}(F_{g0})\overline{\overline{E_{1r\ell}}} + P_{\ell\theta}(F_{g0})\overline{\overline{E_{1\theta\ell}}}\right]}{\omega - k_{\perp\theta}v_{d\theta} - \ell\Omega_\alpha + (v_\parallel/qR)\left[m - nq(r)\right]} \tag{7.2.1}$$

In the limit of $\gamma << (\omega - \ell\Omega_\alpha)$, the resonant particle contribution can be written in the form

$$\frac{1}{\omega - k_{\perp\theta}v_{d\theta} - \ell\Omega_\alpha + \frac{v_\parallel}{qR}(m - nq)} = -i\pi\delta\Big(\omega - k_{\perp\theta}v_{d\theta} - \ell\Omega_\alpha + \frac{v_\parallel}{qR}(m - nq)\Big)$$

The conductivity tensor, defined by Eq. (7.1.3) as $\delta\vec{J}_\alpha = \delta\overset{\leftrightarrow}{\sigma}\cdot\vec{E}_1$, takes the form

$$\delta\overset{\leftrightarrow}{\sigma} = -\frac{q^2}{m_\alpha^{5/2}}e^{-i\omega t - im\theta + in\zeta}\int \frac{4\pi^2\mu B^2\,d\mu\,d\mathcal{E}}{\sqrt{2(\mathcal{E} - \mu B)}}\delta(\omega - k_\parallel v_\parallel - k_\perp v_{d\theta} - \ell\Omega_\alpha) \tag{7.2.2}$$

$$\times \left[\frac{\partial}{\partial\mathcal{E}} + \left(1 - \frac{k_\parallel v_\parallel + k_\perp v_{d\theta}}{\ell\Omega_\alpha}\right)\frac{1}{B}\frac{\partial}{\partial\mu}\right]F_{g0}\begin{pmatrix} \left(\frac{\ell}{\xi}J_\ell\right)^2 & i\frac{\ell}{\xi}J_\ell J_\ell' \\ -i\frac{\ell}{\xi}J_\ell J_\ell' & J_\ell'^{\,2} \end{pmatrix}$$

The exlicit calculation for the conductivity tensor and a more complete form for it is carried out in appendix E. Through the delta function, each mode selects a class of orbits such that a particle can resonance with the mode as it passes through $r = r_{\text{mode}}$. The growth rate γ obtained by plugging Eq. (7.2.2) into (7.1.4) only has significant contributions from these resonant particles.

In terms of dimensionless variables the resonant condition is

$$\frac{\omega}{\Omega_{\alpha0}} - \frac{\ell}{1 + (r/R_0)\cos\theta} + K_\parallel\sqrt{\mathcal{E}/\mathcal{E}_\alpha - \mu B/\mathcal{E}_\alpha} + K_\perp(\mathcal{E}/\mathcal{E}_\alpha - \mu B/2\mathcal{E}_\alpha) = 0 \tag{7.2.3}$$

where $K_\parallel = -k_\parallel \sqrt{(2\mathcal{E}_\alpha/m_\alpha)}/\Omega_{\alpha 0}$, and $K_\perp = -(k_\perp 2\mathcal{E}_\alpha \cos\theta)/(m_\alpha \Omega_{\alpha 0}^2 R_0)$, that is defined so as to be a positive quantity.

The final form for the growth rate is:

$$\frac{\gamma}{\Omega_{i0}} = -\frac{\bar{n}_\alpha}{n_{e0}} \frac{\pi^2 \sqrt{2}}{1+\Lambda^2} H(\theta) \frac{\omega_{pi0}^2}{\Omega_{i0}^2} \frac{2}{\omega \partial D_0/\partial\omega}$$

$$\times \left\{ \left(\frac{\mu B/\mathcal{E}_\alpha - 0.8}{(0.03)^2} \right) \frac{W_\ell}{\sqrt{2(\mathcal{E}/\mathcal{E}_\alpha - \mu B/\mathcal{E}_\alpha)}} e^{-\frac{1}{2}\left(\frac{\mu B/\mathcal{E}_\alpha - 0.8}{0.03}\right)^2} \left(1 + \frac{\delta\omega}{l} \right) \right.$$

$$+ \mathcal{E}_\alpha \frac{\partial}{\partial\mathcal{E}} \left[\frac{W_\ell}{\sqrt{2(\mathcal{E}/\mathcal{E}_\alpha - \mu B/\mathcal{E}_\alpha)}} e^{-\frac{1}{2}\left(\frac{\mu B/\mathcal{E}_\alpha - 0.8}{0.03}\right)^2} \right]$$

$$\left. + \mathcal{E}_\alpha \frac{d\mu_{res}}{d\mathcal{E}} \frac{\partial}{\partial\mu} \left[\frac{W_\ell}{\sqrt{2(\mathcal{E}/\mathcal{E}_\alpha - \mu B/\mathcal{E}_\alpha)}} e^{-\frac{1}{2}\left(\frac{\mu B/\mathcal{E}_\alpha - 0.8}{0.03}\right)^2} \right] \right\}_{\mu=\mu_{res}} \quad (7.2.4)$$

Where $(\omega_{pi}^2/\Omega_i^2)[\omega\epsilon_0 \partial D_0/\partial\omega]^{-1} \sim O(1)$ is a positive quantity, and

$$W_\ell = \frac{2\mu B/\mathcal{E}_\alpha}{|-K_\parallel/2\sqrt{\mathcal{E}/\mathcal{E}_\alpha - \mu B/\mathcal{E}_\alpha} - K_\perp/2|} \left[\frac{\Lambda l}{\xi\sqrt{2\mu B/\mathcal{E}_\alpha}} J_l(\xi) - J_l'(\xi) \right]^2$$

In the "local interaction" limit, the growth rate as given by Eq. (7.2.4) is a function of the spatial coordinates; in our case, the localization of the mode allows us to set $r = r_0$, leaving a dependence on the resonant value of θ.

Since for the particles at birth the energy is fixed, for a given value of the frequency ω and the poloidal angle θ, Eq. (7.2.4) defines the acceptable values of $\mu = \mu_{res}$ at $r = r_{mode}$ for which there will be instability. The range of possible values for θ allows solutions with positive growth rate to be found within a range of frequencies; this justifies the width of the spectrum. We can have instability for different values of frequency, each corresponding to a single resonance in velocity space. Letting θ vary, and thus the resonant value of μ, results in a frequency spread that can be related to the width of the mode.

We find that there is a destabilizing interaction for those frequencies such that $\mu_{res}B < 0.8\,\mathcal{E}_\alpha$, i.e. the distribution function has positive slope for particles that

contribute to the instability. Notice that we can have more then one value of θ resonating at different points with the same frequencies, thus for a single mode, the θ-dependence can be averaged to determine a global growth rate. In figure [7.1], the global growth rate is plotted for modes in the discrete spectrum of contained modes as derived in Chapters 2 and 3 , for $k_\parallel/k_\perp < 0.1$. Assuming the emitted power produced by each mode to be proportional to the growth rate, figure [7.1] allows for a visualization of an observed spectrum. The peaks are located at multiples of $\Omega_\alpha(r_0, \theta = 0)$, that is found at the outer edge of the plasma column, consistent with experimental results. We see from the figure that not all of the first harmonics are excited. However we wish to point out that this result depends on the model distribution function that we have been using. In fact the growth rate appears to be very sensitive to the form of the distribution function in velocity space, and particularly for the function given by Eq. (5.1.3) on the values of the parameters σ and Λ_0. It is found that with smaller values of σ the lower harmonics are excited, while as $\sigma \to \infty$, the mode, in the limit considered in this chapter, becomes stable.

If we examine the growth rate given by Eq. (7.2.4), taking the limit of a uniform magnetic field and considering the electrostatic component of the mode as the dominant one, we see that our calculation agrees with the well established instability[17] for the homogeneous magnetosonic-whistler wave. The condition for the mode being dominated by the electrostatic component is that $\ell \gg 1$, as is clear from Eq. (1.1.11); this condition is commonly used in analytic calculation for ion cyclotron growth rate and does not alter substantially the nature of the interaction.

In a recent calculation of this instability, for $\ell \gg 1$ that includes finite banana-width effects[24], it is found that there are two contributions to the conductivity tensor, one of which is governed by finite Larmor radius effects, and another that is purely related to trapped orbit effects. The first term persists in the homogeneous limit, as shown in Chapter 6. However in ref. [24] the term which is related to FLR contributions has form equivalent to the homogeneous result, except that it has the opposite sign, reversing the role of finite Larmor radius effects in the instability.

Various models that try to explain ICE observations through a form of the magnetosonic cyclotron instability[17] have been proposed. Among these, some[19] consider a localized mode but without resolving the corrections coming from the Hall term. Our work incorporates the effects of the Hall term and propagation parallel to the magnetic field on the mode structure and the spectrum of excitation. Other models[20-24] consider a radially propagating mode and thus do not resolve the issue of the excessively weak growth rate when compared to the relevant radial convection rate. Localization also appears essential to justify why the observed emission peaks occur at frequencies corresponding to the cyclotron frequency at the outer edge of the plasma.
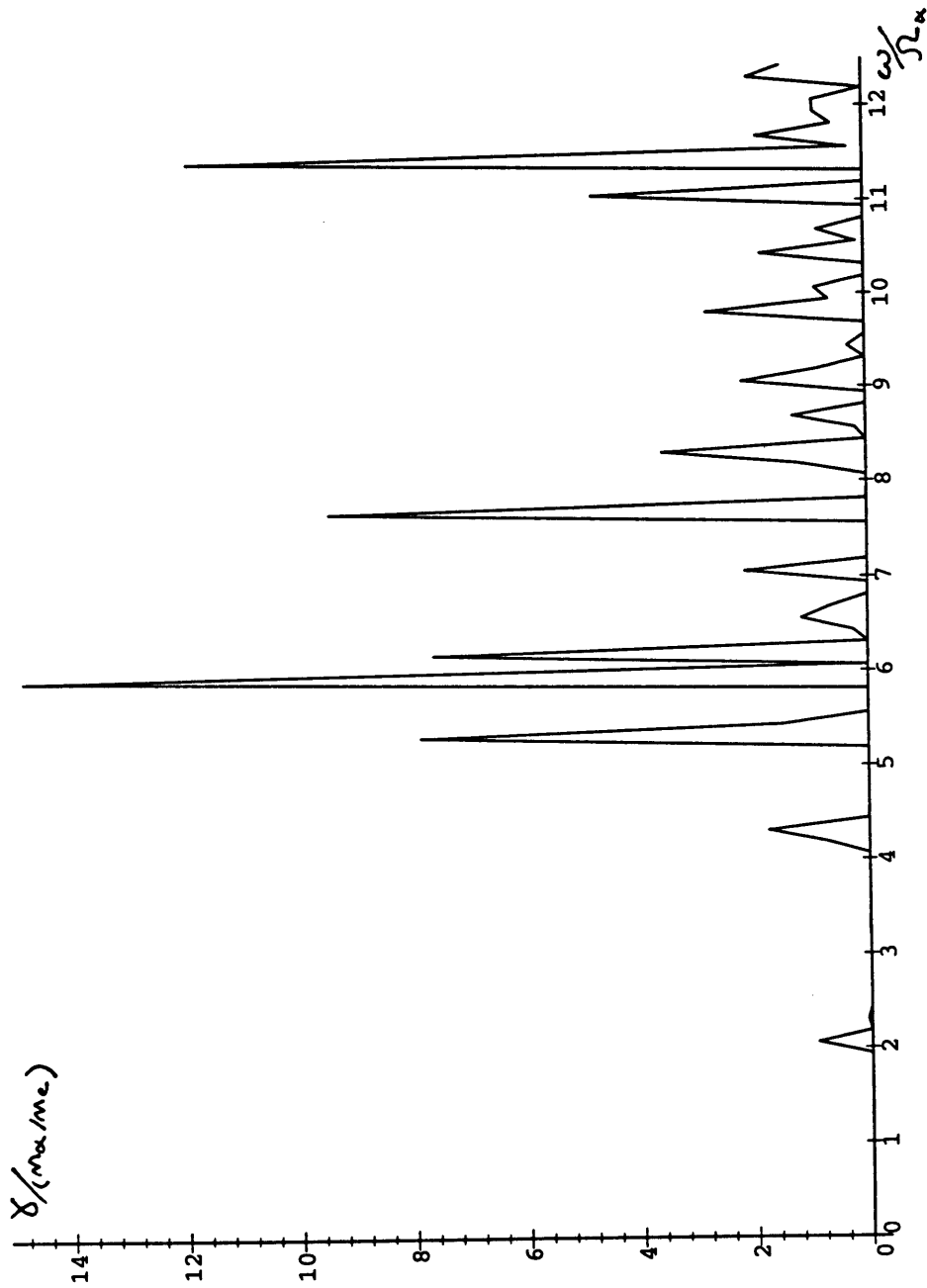
Figure 7.1 The growth rate γ as afunction of $\omega/\Omega_\alpha(r_{mode})$. Assuming that the emitted power produced by each mode is proportional to the growth rate, this figure allows for a visualizatioin of the observed spectrum.

Chapter 8.

Conclusions

In this thesis the interaction of fusion produced ions with the background plasma through collective modes has been studied. We identified a class of modes that can interact with energetic fusion products and be destabilized by them, giving rise to enhanced emission at harmonics of the cyclotron frequency of the particles. In the limit of a homogeneous plasma these modes are electomagnetic perturbations of the type of magnetosonic-whistler waves with dispersion relation $\omega^2 = k_\perp^2 (v_A^2 + k_\parallel^2 D_H^2)$ where $v_A^2 = B_0^2/(m_i n_i \mu_0)$, $D_H = B_0 c/(4\pi n_e q_e)$, and $k_\parallel$ and $k_\perp$ are respectively the wave vector along the equilibrium magnetic field and in the direction perpendicular to it.

These modes are studied in the limit of a cylindrical cold plasma that supports radially confined solutions, and they have the following characteristics: they propagate mainly in the poloidal direction ($k_\perp \sim k_\theta$); the mode solution is a sharply localized toroidal shell centered about a value $r = r_{\mathrm{mode}}$ near the periphery of the plasma colunm, and the mode width becomes smaller for higher frequencies. The range of frequency of interest $\omega \geq \Omega_\alpha$ requires poloidal numbers m that are above

10. Even if the mode propagation is primarily perpendicular to the equilibrium magnetic field we consider a small parallel component. We wish to point out that due to the small growth rate we find it of particular importance that the mode is contained so that there can be a substantial interaction betwee the particles and the mode.

As the problem is analyzed in the framework of the MHD equations, we have that the frequencies of interest are relatively high, thus we find that we need to keep the Hall term in Ohm's law: this term adds new characteristics to the modes. In fact the Hall term breaks the symmetry in the poloidal direction, since results in a term that depends linearly in the wave number m. We find different solutions for perturbed fields propagating along the poloidal direction or in the opposite direction. Particularly we find that contained solutions exist only for waves which propagate in the poloidal direction in the same direction as the ion cyclotron motion (that is $m > 0$ with our convention). In addition we find that there is only one mode localization for any poloidal mode number m and toroidal mode number n^0.

We find that for low multiples of Ω_i the mode localization is, with good approximation, independent of the mode numbers and thus of the frequency, but for higher frequencies the localization of the mode exhibits an increasing sensitivity on the mode numbers, that is in the direction of propagation of the mode along the equilibrium magnetic field. In particular, for a fixed small value of $k_\parallel/k_\perp$, we find a new class of modes localized from the edge up to halfway into the plasma column, that can be excited by the fusion products.

The resonance condition is $\omega \simeq \ell\Omega_\alpha(R)$, where R is determined by the mode localization and ℓ is the harmonic number. This suggests that the transition to a continuum spectrum, as observed in JET[1,2] for frequencies above $7\ \Omega_\alpha$, is caused by the change in location of the mode-particle interactions, in part dictated by the change in localization of the mode.

The discrete spectrum for the low harmonics is consistent with our finding that the localization of the mode is independent of the poloidal mode number, m, so that at lower frequencies modes will interact with the α-particles in roughly the

100

same region in space, and thus at a resonant cyclotron frequency determined by the same value for the magnetic field. However, if the surface of localization of resonant modes having the same harmonic number can vary, by an amount δR, the resonant modes will involve a frequency range $\ell\Omega_\alpha'\delta R = \ell\Omega_\alpha\delta R/R$. Different harmonics will overlap when $\ell \simeq R/\delta R$. For the lower harmonics, this is too small a range for there to be overlap between different harmonics.

For the higher harmonics, a significant contribution to δR comes from the dependence of the mode localization on $k_\parallel$; the strength of this dependence increases with mode frequency. Thus a sequence of modes localized at different radii inside the plasma will be excited. The condition for overlap among harmonics due to this mechanism alone is found to be $\ell \geq \ell_{\text{crit}} = (R/r)[n(r)q^2/n_0\hat{s}^2]^{1/3}$, where $\hat{s} = rq'/q$ is the shear parameter and $n(r)/n_0$ represents the density profile. For $\ell > \ell_{crit}$ the interval over which modes can be excited extends toward the center of the plasma column, so that more α-particles can interact with the mode. Thus the discrete part of the spectrum yields information specifically about the trapped, energetic particles with large orbits, while the continuum spectrum can give information about the average density of energetic particles inside the plasma column.

The α-particles produced by fusion slow down due to elctron collisions. The typical slowing down time is much larger than the typical time associated with the interaction thus we model the α-particles distribution function before slowing down occurs. Experimental evidence also support this hypotesis. By studying the single particle orbits for energetic fusion products we find that only trapped particles with large radial excursions in their orbits can reach the mode and thus have resonant interaction. An analysis of the values of the parameters in velocity space that correspond to orbits intersecting the mode, indicates that the relevant particles are barely trapped particles.

The distribution function of these particles is strongly anisotropic in velocity space, and is weighted towards the outer edge. This correlates with the experimental observation that the emission peaks are measured at multiples of the cyclotron frequency corresponding to the magnetic field strength at the outer edge[1,2,3].

We find that, for any realistic plasma configuration that includes variation of the magnetic field or Doppler shifted frequencies due to the particles' motion, the growth rate depends linearly on the ratio n_α/n_e for all harmonics. This is in contrast with the analogous growth rate for the case of a homogenous configuration that scales as the square root of n_α/n_e. Peak growth rates are higher than the bounce frequency, thus satisfying the condition for using the "local approximation."
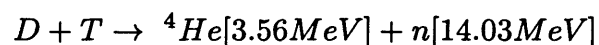
This growth rate is sufficient to maintain instability even including the various mechanisms for damping that affect the unperturbed mode, such as thermal damping.

An understanding of this phenomenon suggests the possibility of influencing α-particle transport through coupling with externally applied modes having frequencies in the range we have considered. The α-particle distribution and perpendicular energy may be manipulated through appropriately chosen injected waves.
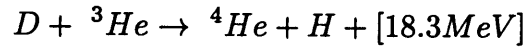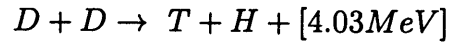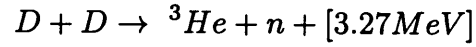
Appendix A.

A Brief Review of

Anomalous Ion Cyclotron Emission (ICE)

Observations in JET and TFTR

Enhanced ion cyclotron emission with peaks on the harmonics of the α-particles cyclotron frequency was observed in D-T discharges both in the JET (Joint European Torus) device[1,2] and in the TFTR (Tokamak Fusion Test Reactor) machine[3,4,5]. In this appendix we represent the typical parameters, taken from two sample discharges, that characterize these two machine, we describe the experimental observation of ICE, and we summarize the results of our theory when applied to these two different experiments. We recall that in a plasma made of deuterium and tritium, there will be a primary reaction that has the highest cross section

$$D + T \rightarrow {}^4He[3.56 MeV] + n[14.03 MeV]$$

the following secondary reactions can also occur

$$D + D \rightarrow {}^3He + n + [3.27 MeV]$$

$$D + D \rightarrow T + H + [4.03 MeV]$$

$$D + {}^3He \rightarrow {}^4He + H + [18.3 MeV]$$

We reproduce in table I the typical parameters for the JET and TFTR experiments as given in ref. [1,2] and ref. [3,4,5].

TABLE A-I - JET and TFTR Parameters

Plasma parameters	JET	TFTR
Plasma current	3.1 MA	2.7 MA
Toroidal Field	2.8 T	5.6 T
Central e^- density	2.5×10^{19} m^{-3}	7×10^{19} m^{-3}
Central ion temperature	18.8 keV	20 keV
Major radius of the torus	3.15 m	2.6 m
Minor radius of the torus	1.05 m	0.9 m

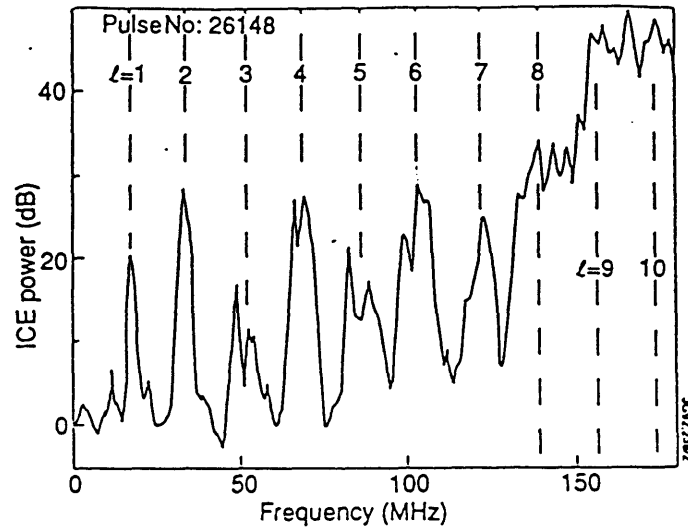Let us now examine the detected ICE spectrum of Jet.

Figure 1. The ICE spectrum measured in a DT discharge,

with $n_T/n_e = 7\%$, close to the time of the peak neutron emission

The spectrum reproduced in Fig. [1] presents the following characteristics: it shows peaks at the harmonics of $\Omega_\alpha = q_\alpha B(R = 4.02m)/m_\alpha = 1.05 \times 10^8 s^{-1}$ up to $\ell = 7$, where ℓ indicates the harmonic number. The detected power is of the order of μWatts, much larger ($\sim 10^2$) then the correspondent power level by thermal spontaneous emission. The spectrum becomes continuum and increases in power for $\ell \geq 8$, there are some additional peaks for $\omega < \Omega_\alpha$.

We can now examine the detected spectrum for TFTR, we consider two cases, in Fig. [2] we reproduce the spectrum for a plasma where only the tritium is injected as neutral beam, while the source of deuterium is the initial target plasma. In Fig. [3] there is both deuterium and tritium neutral beam injection.
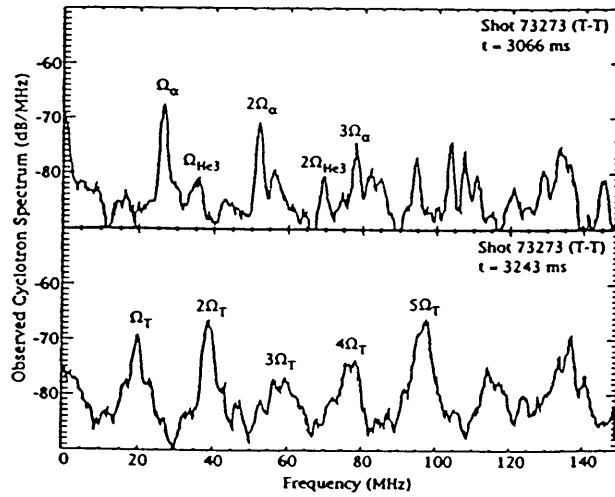
105

Figure 2. ICE spectra during T beam injection.

D-T fusion product α particle harmonics arise shortly after

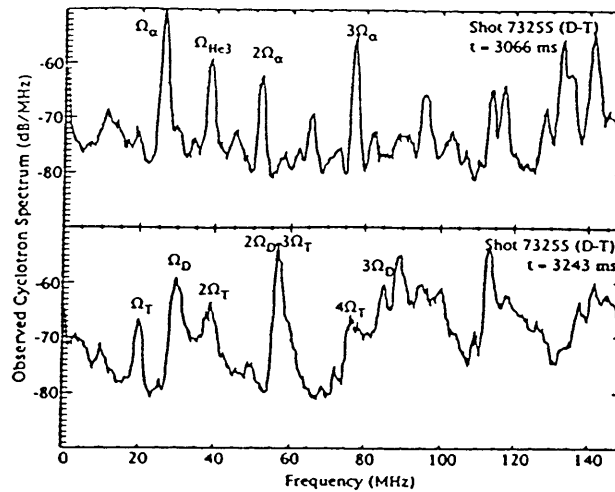the start of the beams. Later only Ω_T harmonics are present.

Figure 3. ICE spectra during D and T beam injection.

Immediatly after beam injection starts, both Ω_{He^3} and Ω_α are observed.

Later, both Ω_D and Ω_T harmonics are evident.

These figures show that in both cases the spectrum exhibits harmonics of Ω_α evaluated near the vessel wall, and Ω_{He^3} coming from D-D reactions. In Fig. [2] however the initial spectrum dies away after 100 ms, and the spectrum that arises has peaks at the harmonics of Ω_T evaluated at the plasma edge. In Fig. [3] less then 200 ms later, the initial spectrum has been replaced by harmonics of both Ω_D and Ω_T at the plasma edge. The detected spectrum at later times for harmonics of tritium, Fig. [2], or deuterium and tritium, Fig. [3], suggest the idea that the contained mode will be destabilized by beams.

In both experiments the emission is detected with values of the magnetic field corresponding to the outer edge of the plasma, but in JET the spectrum with peaks on the harmonics of α particles is detected during the whole time of the discharge. The fact that in TFTR at different times during the discharge two different spectra are detected reflects the characteristic of this experiment, in particular the fact that it has smaller values of the current and thus a less efficient mechanism of confinement of the α-particles with barely trapped orbits, that are the ones responsible for the instability.

Appendix B.

The Coordinate System

It is customary to define

$$\hat{e}_{\parallel} = \frac{B_{\zeta}}{B_0}\hat{e}_{\zeta} + \frac{B_{\theta}}{B_0}\hat{e}_{\theta}$$

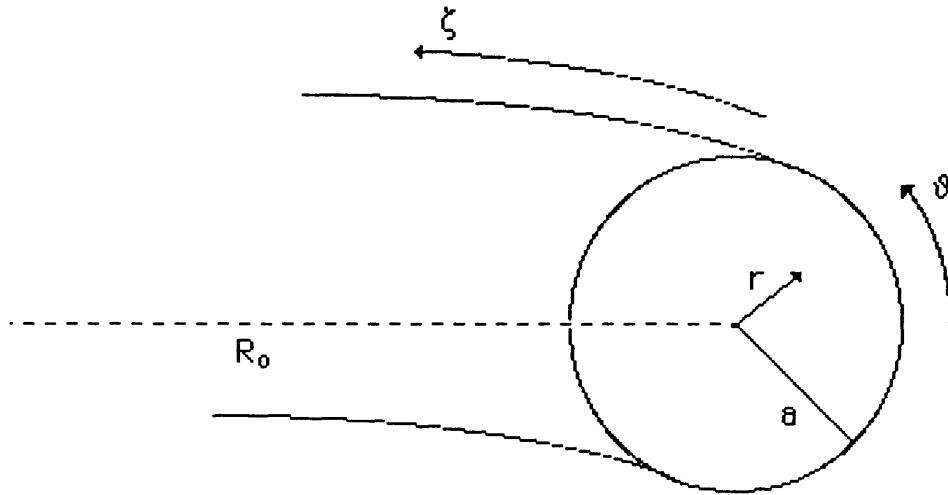$$\hat{e}_a = \hat{e}_{\theta} - \frac{B_{\theta}}{B_0}\hat{e}_{\zeta}$$

$$\hat{e}_b = \hat{e}_r$$

where r, ζ, θ, are defined by

$$x = (R_0 + r\cos\theta)\cos\zeta$$

$$y = (R_0 + r\cos\theta)\sin\zeta$$

$$z = r\sin\theta$$

therefore we have

$$\hat{e}_\zeta \times \hat{e}_\theta = \hat{e}_r$$

$$\hat{e}_r \times \hat{e}_\zeta = \hat{e}_\theta$$

$$\hat{e}_r \times \hat{e}_\theta = -\hat{e}_\zeta$$

moreover we define the following quantities, $\epsilon = r/R$, $q(r) = B_\zeta r/(B_\theta R_0)$, so that $B_\theta/B_\zeta = \epsilon/q$.

Apendix C.

Mu as an Adiabatic Invariant

If there is periodic motion whose parameters are slowly varying, we can define an adiabatic invariant as the action associated with the motion, $I = \int p \, dq / 2\pi$. In our case, for cyclotron motion in a slowly changing magnetic field and approximating $\vec{p} = m\vec{v}$,

$$I_\mu = \int_0^{2\pi} m v_\perp r_\perp d\varphi / 2\pi = (m/e)(1/4\pi)\mu_0 \qquad (C-1)$$

where $\mu_0 = \mathcal{E}_\perp / B = m v_\perp^2 / 2B$.

If the magnetic field is constant in time, then this is a real constant of the motion, but only to lowest order in the expansion parameter ρ / L_B. For a time-varying magnetic field, μ_0 is slowly changing so long as $|\Omega| >> |(1/B)(\partial B / \partial t)|$

We can explicitly calculate $d\mu_0 / dt$ for μ_0 defined as above, in order to show that it is not an exact constant of the motion, even for $\partial B / \partial t \equiv 0$. We obtain

$$\frac{d\mu_0}{dt} = -\frac{\mu_0}{B}\left(\frac{\partial B}{\partial t} + \vec{v} \cdot \vec{\nabla}_{\vec{x}} B\right) - \frac{v_\parallel}{B}\left(\frac{\partial}{\partial t}\hat{e}_\parallel + \vec{v} \cdot \vec{\nabla}_{\vec{x}}\hat{e}_\parallel\right) \cdot \vec{v}_\perp \qquad (C-2)$$

however, averaging over the gyrophase φ denoted by $\vec{v}_\perp = v_\perp (\cos \varphi \, \hat{e}_1 + \sin \varphi \, \hat{e}_2)$ yields $\left\langle \frac{d\mu_0}{dt} \right\rangle_\varphi = -\frac{\mu_0}{B} \frac{\partial B}{\partial t}$.

This suggests the existence of a quantity μ which is always close in value to μ_0 and which is the true adiabatic invariant: μ varies only on the time scale of the magnetic field variations, and $d\mu/dt$ is exponentially small in $\left| \frac{1}{\Omega B} \frac{\partial B}{\partial t} \right|$ Also, note that despite the fact that $\left\langle \frac{d\mu_0}{dt} \right\rangle_\varphi = 0$ μ is not equal to $\langle \mu_0 \rangle_\varphi$.

In most textbook derivations of the invariance of μ, the average over gyromotion and the approximation that variations in space and time are neglected in a single gyroorbit are taken implicitly, by considering the motion of the guiding center. Coordinates of the guiding center are used even if not explicitly described as such, or only referred to as the "average position" of the particle. For example, in the case of $\partial B/\partial t = 0$, the force (written as if acting on the guiding center) may be expressed as $F_\parallel = -\mu \partial B/\partial s$. Thus,

$$m\frac{dv_\parallel}{dt} = -\mu \frac{\partial B}{\partial s} \Rightarrow \frac{d}{dt}\left(\frac{1}{2}mv_\parallel^2\right) = -\mu \frac{dB}{dt} \qquad (C-3)$$

and energy conservation yields

$$0 = \frac{d}{dt}(\mu B) + \frac{d}{dt}\left(\frac{1}{2}mv_\parallel^2\right) = B\frac{d\mu}{dt} \qquad (C-4)$$

if the difference between μ and μ_0 is neglected.

We see from Eq. (C-2) that the relevant expansion parameter is ρ/L_B, and we can calculate the first order correction μ_1 to the adiabatic invariant by using this equation perturbatively. The dominant term in the LHS arises from $\Omega \partial \mu/\partial \varphi$, and thus the correction to μ is determined up to a constant by integrating the right hand side of this equation over φ, yielding the rapidly varying term $\tilde{\mu}_1$. Then $\bar{\mu}_1 = \mu_1 - \tilde{\mu}_1$ can be determined from the constraint:

$$\langle \vec{v} \cdot \nabla \mu_1 \rangle_\varphi = 0$$

yielding

111

$$\tilde{\mu}_1 = -\frac{1}{B}\vec{v}_\perp \cdot \vec{v}_d$$

$$-\frac{v_\parallel}{4\Omega B} \times \left\{ (\vec{v}_\perp \cdot \nabla \hat{e}_\parallel) \cdot (\vec{v}_\perp \times \hat{e}_\parallel) + [(\vec{v}_\perp \times \hat{e}_\parallel) \cdot \nabla \hat{e}_\parallel] \cdot \vec{v}_\perp \right\} \qquad (C-5)$$

$$\tilde{\mu}_1 = -\frac{v_\parallel v_\perp^2}{2B\Omega}\hat{e}_\parallel \cdot \nabla \times \hat{e}_\parallel \qquad (C-6)$$

Appendix D.

The Distribution Function Obtained Through an Orbit Average of the Source. The Example of the Cyclotron Motion

Let us first summarize the case of interest for us: trapped particles in a magnetic configuration whose motion is dominated by curvature and gradient of the magnetic field drift. Explicitly in this model the source will be dependent on the initial position and velocity of the particles (at $t = t_0 = t_b$, that is the time of birth of the particle), r_b, θ_b, $\mathcal{E}$, μ. Herte the subscript b refers to quantities at birth and let us recall the relevant definitions: $\mathcal{E} = v^2/2$, $\mu = v_\perp^2/2B$, $p_\zeta = R[v_\parallel - q/mA_\zeta]$, $RA_\zeta = \int_0^r RB_\theta dr$. In our case the source function depends only on r_b, is multiplied by $\delta(\mathcal{E} - \mathcal{E}_\alpha)$ since all particles are born with fixed energy, and is isotropic with respect to μ and θ_b. However if we restrict our analysis to trapped particles, and we study the local distribution function at some radius, we see that this introduces an anisotropy in velocity space, as well as a θ dependence. We notice also that, as the particles move along the orbits, the distribution function for the specific

position of the particle will be time dependent and finally giving more information that we need: by time averaging along the orbits, in the way explained below, we can substitute single particles with uniformly filled orbits.

The orbits of the particles are completely determined by three constants of the motion, for example μ, $\mathcal{E}$, and p_ζ, so of the four quantities that we have above, one is redundant if we are only interested at the orbit and not at the specific position of the particle. To eliminate this constant we rewrite $r_b, \theta_b, \mu, \mathcal{E}$ in terms of p_ζ, $\mathcal{E}$, μ, θ_b and we notice that the time average is equivalent to an average over θ_b and gets rid of the explicit dependence on this quantity (since three constats determine the orbit and the position of the particle on the orbit at any given time depends on the fourth constant). For sake of clarity, we will describe this procedure for a simple example.

We work out the details for a simple example by choosing a case where you can easily obtain the equation of motion of the single particle. We consider a periodic motion. In our case the motion is the motion of the guiding centers, and the periodic orbit is the bounce orbit (banana or better "potato" orbit).In this example the motion is the motion of the actual particle and the periodic orbit is the gyromotion, so that we study the distribution function of a particle created at some point and time in a constant magnetic field. In this case a particle born at $t = t_0$ with $x = x_0$, $y = y_0$, $v_\perp = v_{\perp 0}$, $\varphi = \varphi_0$ with $v_x = v_\perp \cos\varphi$, $v_y = v_\perp \sin\varphi$ follows the orbits defined by:

$$v_x = v_\perp \cos(\varphi_0 - \Omega\tau) \qquad\qquad (D-1)$$

$$v_y = v_\perp \sin(\varphi_0 - \Omega\tau) \qquad\qquad (D-2)$$

$$x = x_0 - \frac{v_\perp}{\Omega}\sin(\varphi_0 - \Omega\tau) + \frac{v_\perp}{\Omega}\sin\varphi_0 \qquad\qquad (D-3)$$

$$y = y_0 + \frac{v_\perp}{\Omega}\cos(\varphi_0 - \Omega\tau) - \frac{v_\perp}{\Omega}\cos\varphi_0 \qquad\qquad (D-4)$$

114

where $\tau = t - t_0$. It is also convenient to define the guiding centers, that are constants of the motion, so that

$$x_g = x + \frac{v_\perp}{\Omega} \sin \varphi = x_{g0} \qquad (D-5)$$

$$y_g = y - \frac{v_\perp}{\Omega} \cos \varphi = y_{g0} \qquad (D-6)$$

The source function is given by

$$S = s(t_s)\delta(x_b - x_0)\delta(y_b - y_0)\delta(v_{\perp b} - v_{\perp 0})\delta(\varphi_b - \varphi_0) \qquad (D-7)$$

Where the subscript 0 indicates the position in real space, or the position at birth from which the particle is moving away and is a constant of the motion. We thus have:

$$S = s(t_s)\delta(x - x_0 + \frac{v_\perp}{\Omega} \sin(\varphi 0 - \Omega \tau) - \frac{v_\perp}{\Omega} \sin \varphi 0)$$
$$\delta(y - y_0 - \frac{v_\perp}{\Omega} \cos(\varphi 0 - \Omega \tau) + \frac{v_\perp}{\Omega} \cos \varphi 0)$$
$$\delta(v_\perp - v_{\perp 0})\delta(\varphi + \Omega \tau - \varphi_0) \qquad (D-8)$$

If we time average over one period τ we obtain:

$$\bar{S} = \frac{s(t_s)}{\tau_b \Omega}\delta(x - x_0 + \frac{v_\perp}{\Omega} \sin(\varphi) - \frac{v_\perp}{\Omega} \sin \varphi 0)$$
$$\delta(y - y_0 - \frac{v_\perp}{\Omega} \cos(\varphi) + \frac{v_\perp}{\Omega} \cos \varphi 0)$$
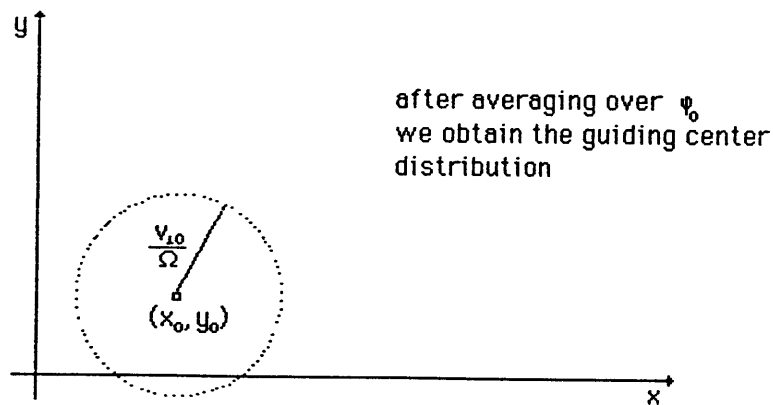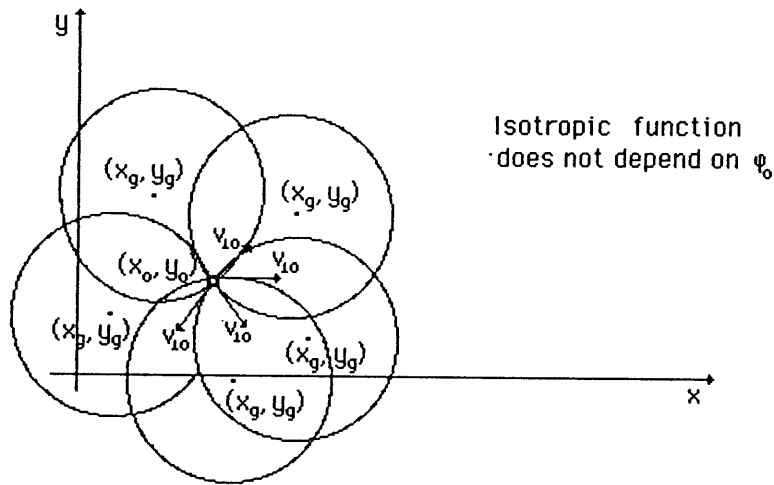$$\delta(v_\perp - v_{\perp 0}) \qquad (D-9)$$

where $0 < \varphi < 2\pi$. We finally obtain f as:

$$f = \left[\int_s^t dt_s \frac{s(t_s)}{\tau_b \Omega}\right] \delta(x - x_0 + \frac{v_\perp}{\Omega} \sin(\varphi) - \frac{v_\perp}{\Omega} \sin \varphi 0)$$
$$\delta(y - y_0 - \frac{v_\perp}{\Omega} \cos(\varphi) + \frac{v_\perp}{\Omega} \cos \varphi 0)$$
$$\delta(v_\perp - v_{\perp 0})$$
$$= \left[\int_s^t dt_s \frac{s(t_s)}{\tau_b \Omega}\right] \delta(x_g - x_{g0})\delta(y_g - y_{g0})\delta(v_\perp - v_{\perp 0}) \qquad (D-10)$$
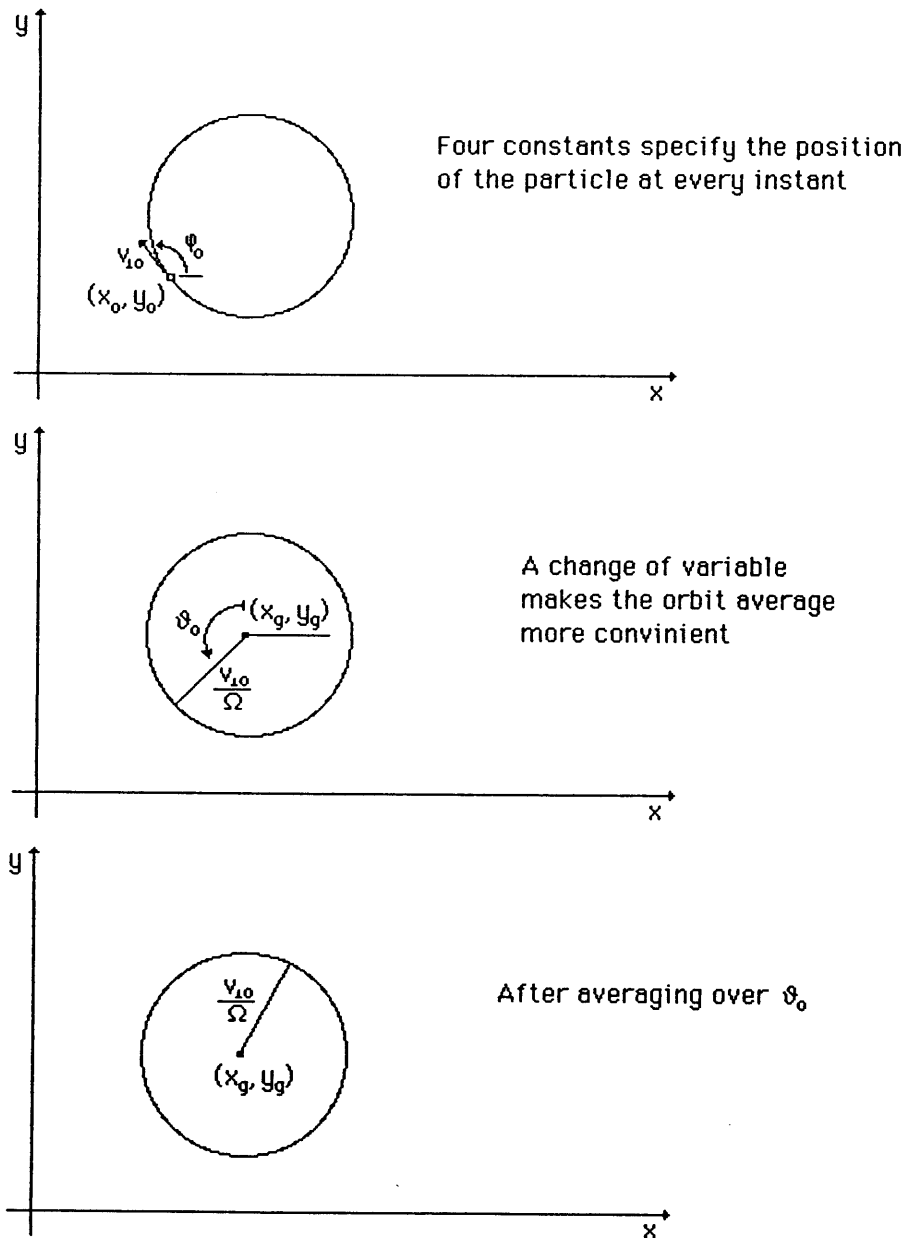
To find the equation for f we have considered particles all born with some initial value of $\varphi = \varphi_0$, but if we want to consider a realistic case where particles are produced at random values of φ_0, we can further average over φ_0 to obtain what is finally the distribution of all the different possible guiding centers with a given $v_{\perp 0}$

This gives

$$\bar{f} = \frac{1}{2\pi} \int_s^t dt_s \frac{s(\hat{t}_s)}{2\pi} \delta(v_\perp - v_{\perp 0}) \delta((x - x_0)^2 + (y - y_0)^2 - (v_\perp/\Omega)^2) \qquad (D-11)$$

Isotropic function
does not depend on φ_0

after averaging over φ_0
we obtain the guiding center
distribution

117

We see that the information about where the particle was at any given time is now lost, and being substituted by the orbit: all the particles are on the circle $x = x_{g0} + v_\perp/\Omega \sin\varphi$, $y = y_{g0} + v_\perp/\Omega \cos\varphi$ for all $0 < \varphi < 2\pi$. Notice that all the points in the orbit are equivalent, i.e. we assume that the particles uniformle fill the orbit.

Four constants specify the position
of the particle at every instant

A change of variable
makes the orbit average
more convinient

After averaging over ϑ_0

Appendix E.

A Detailed Calculation of the Conductivity Tensor with O(λ) Corrections

The perturbed α-particles distribution function δF_α has to satisfy the linearized Vlasov equation, where we assume that the perturbed fields are the fields of the Contained Modes, as found in Chapter 2, and we are interested in frequencies above Ω_α.

The linearized equation is:

$$\left[\frac{\partial}{\partial t} + \vec{v} \cdot \vec{\nabla}_{\vec{x}} + (\vec{v} \times \vec{\Omega}_\alpha) \cdot \vec{\nabla}_{\vec{v}}\right] \delta F_\alpha =$$

$$= -\frac{q}{m_\alpha}\left(\vec{E}_1 + \frac{\vec{v}}{c} \times \vec{B}_1\right) \cdot \vec{\nabla}_{\vec{v}} F_\alpha \qquad (E-1)$$

where we consider the case of $\vec{E}_0 = 0$, and we model the equilibrium magnetic field as

$$\vec{B} = \frac{B_0}{1 + (r/R_0)\cos\vartheta}\left(\hat{e}_\zeta + \frac{r}{R_0 q}\hat{e}_\vartheta\right)$$

118

We want to expand this equation for small values of the quantity $\lambda = \rho_\alpha/L_B$, where $L_B \equiv (d\ln B)^{-1} \sim R$, so it is more comvenient to perform a change of coordinates and consider to the guiding center phase space that is defined by:

$$\vec{X} = \vec{x} + \frac{\vec{v} \times \hat{e}_\parallel}{\Omega_\alpha}$$

$$\vec{V} = (\mathcal{E}, \mu, \varphi)$$

with $\mu = v_\perp^2/2B$, $\mathcal{E} = v^2/2$, and φ is defined by $\vec{v}_\perp = v_\perp(\hat{e}_a \cos\varphi + \hat{e}_b \sin\varphi)$, we have set $m_\alpha = 1$ and the subscript parallel is the projection along the direction of the magnetic field.

We use the following local orthogonal system, $\hat{e}_\parallel$, $\hat{e}_a$, $\hat{e}_b$, where $\hat{e}_a \times \hat{e}_\parallel = -\hat{e}_b$ and $\hat{e}_b \times \hat{e}_\parallel = \hat{e}_a$, as defined in appendix D. We will consider $\hat{e}_a \sim \hat{e}_\theta$, $\hat{e}_b \sim \hat{e}_r$.

The quantity F_α is the equilibrium distribution function and in the guiding center space we use the label g, $F_{g\alpha}$. We follow the formalism of Ref. [15], [16]. We keep corrections of order λ, but we neglect corrections of order λ/q, as explicitly evaluated in Appendix F. We consider

$$F_g = F_{g0}(\mathcal{E}, \mu, \vec{X}_\perp) + \tilde{\beta}\frac{1}{B}\frac{\partial F_{g0}}{\partial \mu} = F_{g0} + F_{g1} \qquad (E-2)$$

We recall here that $\hat{e}_\parallel \cdot \vec{\nabla}_x F_{g0} = 0$ since the system is independent of $\vec{x}_\parallel$, and $\tilde{\beta} \sim -\vec{v}_\perp \cdot \vec{v}_d$ where $\vec{v}_d = \hat{e}_\parallel/\Omega_\alpha \times [v_\perp^2/2\vec{\nabla}_x \ln B + v_\parallel^2 \hat{e}_\parallel \cdot \vec{\nabla}_x \hat{e}_\parallel]$. Since we consider a low β plasma, we can used a simplified form for the drift velocity and consider $\vec{v}_d = 1/(\Omega_\alpha R)(2v_\parallel^2 + v_\perp^2)[\hat{e}_\theta \cos\theta + \hat{e}_r \sin\theta]$. The quantity $\tilde{\beta}$ should also be expressed as a function of the guiding center variables, but we find it more convenient to leave it as a function of real space variables. We note that by definition $(L_v F_v)_g = L_g F_g$, where L_v is the Vlasov operator in real space as in the left hand side of Eq. (E-1) while L_g is the corresponding operator in guiding center space. Thus we can write

$$L_{v1}(F_{v0} + F_{v1}) = L_{g1}F_{g0} + L_{v1}F_{v1} =$$
$$= L_{g1}F_{g0} + \frac{1}{B}\frac{\partial F_{g0}}{\partial v}\left[L_{v1}\tilde{\beta}\right]_g + (\tilde{\beta})_g L_{g1}\left(\frac{1}{B}\frac{\partial F_{g0}}{\partial \mu}\right)$$

119

The spatial structure of the mode and the polarization are determined by the "background" ions so that the perturbed electric field is of the form

$$E_{1\parallel} \simeq 0$$

$$E_{1\theta} = E_{1\theta}(r, \theta)e^{-i\omega t - im\theta + in_0\zeta}$$

$$E_{1r} = E_{1r}(r, \theta)e^{-i\omega t - im\theta + in_0\zeta}$$

and we have that $E_{1\theta}/E_{1r} = -i\Lambda$ where $\Lambda \sim \omega/\Omega_i$.

In the guiding center coordinates Eq. (1) is :

$$\left[\frac{\partial}{\partial t} + v_\parallel \hat{e}_\parallel \cdot \vec{\nabla}_x + \vec{v} \cdot (\lambda_{B1} + \lambda_{B2}) - \Omega_\alpha \frac{\partial}{\partial \alpha} \right] \delta F_{g\alpha} =$$

$$= L_{g1}F_{g0} + \frac{1}{B}\frac{\partial F_{g0}}{\partial v}\left[L_{v1}\tilde{\beta} \right]_g + (\tilde{\beta})_g L_{g1}\left(\frac{1}{B}\frac{\partial F_{g0}}{\partial \mu} \right) \qquad (E-3)$$

where $\lambda_{B1} = \vec{v} \times \vec{\nabla}_x(\hat{e}_\parallel/\Omega_\alpha) \cdot \vec{\nabla}_X$, $\lambda_{B2} = \vec{\nabla}_x\mu(\partial/\partial\mu) + \vec{\nabla}_x\varphi(\partial/\partial\varphi)$ and $\vec{\nabla}_x\mu = -(\mu\vec{\nabla}_x B + v_\parallel \vec{\nabla}_x \hat{e}_\parallel \cdot \vec{V}_\perp)/B$, $\vec{\nabla}_x\varphi = (\vec{\nabla}_x \hat{e}_b) \cdot \hat{e}_a + (v_\parallel/v_\perp^2)\vec{\nabla}_x \hat{e}_\parallel \cdot (\vec{v}_\perp \times \hat{e}_\parallel)$. The perturbed fields will be evaluated in the guiding center coordinates system, and labelled as $\vec{E}_{1g}$, $\vec{B}_{1g}$.

We can now evaluate all the different terms in the right hand side of Eq. (3), for the case $E_{1\parallel} = 0$. First we consider L_{g1},

$$L_{g1} = -\frac{q}{m}\left[\left(\vec{E}_{g\perp} \cdot \vec{v}_\perp \frac{\partial}{\partial \mathcal{E}} + \vec{E}_{g\perp} \cdot \frac{\vec{v}_\perp}{B}\frac{\partial}{\partial \mu} \right) + \left(\frac{\vec{v} \times \vec{B}_1}{c} \right)_g \cdot \frac{\vec{v}_\perp}{B}\frac{\partial}{\partial \mu} \right.$$

$$\left. + \left(\vec{E}_{1g} + \frac{\vec{v} \times \vec{B}_1}{c} \right)_g \times \frac{\hat{e}_\parallel}{\Omega_\alpha} \cdot \vec{\nabla}_x \right] \qquad (E-4)$$

where we have used the fact that in our calculation L_{g1} acts only on F_{g0} and $\partial F_{g0}/\partial\varphi = 0$. We can further simplify this expression by using $\vec{\nabla}_x \times \vec{E}_1 = (i\omega/c)\vec{B}_1$, so that

$$\left(\frac{\vec{v} \times \vec{B}_1}{c}\right)_g \cdot \frac{\vec{v}_\perp}{B}\frac{\partial}{\partial\mu} = \frac{i}{\omega}\frac{1}{B}\frac{\partial}{\partial\mu}\left[\left(\vec{v}_\perp \cdot \vec{\nabla}\vec{v}_\parallel\right)\cdot\vec{E}_1 - (\vec{v}_\parallel\cdot\vec{\nabla}_x)\vec{E}_1\cdot\vec{v}_\perp\right]_g$$

We can thus write:

$$
\begin{aligned}
L_{g1} = &-\frac{q}{m}\Bigg\{\vec{E}_{g\perp}\cdot\vec{v}_\perp\left(\frac{\partial}{\partial\mathcal{E}} + \frac{1}{B}\frac{\partial}{\partial\mu}\right)\\
&+\frac{i}{\omega}\left(\left(\vec{v}_\perp\cdot\vec{\nabla}\vec{v}_\parallel\right)\cdot\vec{E}_1 - (\vec{v}_\parallel\cdot\vec{\nabla}_x)\vec{E}_1\cdot\vec{v}_\perp\right)_g\frac{1}{B}\frac{\partial}{\partial\mu}\\
&+\left[\vec{E}_{1g} + \frac{\vec{v}\times\vec{B}_1}{c}\right]_g\times\frac{\hat{e}_\parallel}{\Omega_\alpha}\cdot\vec{\nabla}_X\Bigg\}
\end{aligned}
\qquad (E-5)
$$

Let us now evaluate the term $(L_{v1}\tilde{\beta})_g$, to do so we can use

$$\vec{\nabla}_v[-\vec{v}\cdot\vec{v}_d] = -(\vec{\nabla}_v\vec{v})\vec{v}_d - (\vec{\nabla}_v\vec{v}_d)\cdot\vec{v} = -\left[\vec{v}_d - \tilde{\beta}\frac{\vec{v}_\perp + 2\vec{v}_\parallel}{v_\perp^2/2 + v_\parallel^2}\right]$$

so that, again for $E_{1\parallel} = 0$,

$$
\begin{aligned}
\left[L_{v1}\tilde{\beta}\right]_g = &-\Bigg[\vec{E}_{1\perp}\cdot\vec{v}_d - \frac{i}{\omega}(\vec{v}\times(\vec{\nabla}_x\times\vec{E}_{1\perp}))\cdot\vec{v}_d\\
&-\tilde{\beta}\frac{\vec{v}_\perp\cdot\vec{E}_{1\perp}}{v_\perp^2/2 + v_\parallel^2} + i\frac{\tilde{\beta}}{\omega}\frac{(\vec{v}\times(\vec{\nabla}_x\times\vec{E}_{1\perp}))\cdot\vec{v}_\parallel}{v_\perp^2/2 + v_\parallel^2}\Bigg]_g
\end{aligned}
\qquad (E-6)
$$

It is convenient to define

$$E_{g1} = \overline{E}_{g1}e^{-i\int^{\vec{X}}(\vec{k}_\perp\cdot d\vec{X})} \simeq \overline{E}_1 e^{-i\vec{k}_\perp\cdot\frac{\vec{v}\times\hat{e}_\parallel}{\Omega_\alpha}}$$

where $\vec{k}_\perp \sim -\frac{m}{r}\hat{e}_\theta$, so that $E_{g1} = \overline{E}_1\exp(-i(k_\perp v_\perp/\Omega_\alpha)\sin\varphi)$ and

$$E_{g1} = \overline{\overline{E}}_{g1}(\vec{X},\mathcal{E},\mu,\varphi)e^{-i\omega t - im\varphi_g - i\frac{k_\perp v_\perp}{\Omega_\alpha}\sin\varphi + in_0\zeta_g} \qquad (E-7)$$

In the previous expression $\zeta_g = \zeta$ and we look for a solution for $\delta F_{g\alpha}$ of the same form of Eq. (E-7). We can cosider a Fourier expansion respect to the φ variable, and define

$$\delta F_{g\alpha} = \sum_{\ell'=-\infty}^{+\infty} \langle \delta F_{g\alpha} \rangle_{\ell'} e^{-i\ell'\varphi}$$

$$\langle \delta F_{g\alpha} \rangle_\ell = \frac{1}{2\pi} \int_0^{2\pi} d\varphi e^{i\ell\varphi} \delta F_\alpha(\vec{X}, \mu, \mathcal{E}, \varphi) e^{-i\omega t - im\theta_g + in_0\zeta_g - i\frac{k_\perp v_\perp}{\Omega_\alpha}\sin\varphi}$$

To obtain an equation for $\langle \delta F_{g\alpha} \rangle_\ell$, we multiply Eq. (E-3) by $e^{i\ell\varphi}$ and integrate over φ, using the notation

$$\langle \delta F_{g\alpha} \rangle_\ell = \left\langle \overline{\delta F}_{g\alpha} \right\rangle_\ell e^{-i\omega t - im\theta_g + in_0\zeta_g}$$

that is

$$\left\langle \overline{\delta F}_{g\alpha} \right\rangle_\ell = \frac{1}{2\pi} \int_0^{2\pi} d\varphi \delta F(\vec{X}, \mu, \mathcal{E}, \varphi) e^{-i\frac{k_\perp v_\perp}{\Omega_\alpha}\sin\varphi + i\ell\varphi}$$

and

$$\delta F(\vec{X}, \mu, \mathcal{E}, \varphi) = \sum_{\ell=-\infty}^{\infty} \left\langle \overline{\delta F}_{g\alpha} \right\rangle_\ell e^{i\frac{k_\perp v_\perp}{\Omega_\alpha}\sin\varphi - i\ell\varphi}$$

In terms of these quantities, we can rewrite Eq. (E-3) as:

$$\left[-i\omega + \left\langle v_\parallel \hat{e}_\parallel \cdot \vec{\nabla}_X \right\rangle_0 + \langle \vec{v}(\lambda_{B1} + \lambda_{B2}) \rangle_{\ell 0} + i\ell\Omega_\alpha \right] \left\langle \overline{\delta F}_{g\alpha} \right\rangle_\ell e^{-i\omega t - im\theta_g + in_0\zeta_g}$$
$$+ \sum_{\ell' \neq \ell} \tilde{L}_{g\ell,\ell'} \left\langle \overline{\delta F}_{g\alpha} \right\rangle_{\ell'} e^{-i\omega t - im\theta_g + in_0\zeta_g}$$
$$= \langle L_{g1} F_{g0} \rangle_\ell + \left\langle \frac{1}{B} \frac{\partial F_{g0}}{\partial \mu} [L_{v1}\tilde{\beta}]_g \right\rangle_\ell + \left\langle \tilde{\beta} L_{g1} \frac{1}{\beta} \frac{\partial F_{g0}}{\partial \mu} \right\rangle_\ell \qquad (E-8)$$

Here $\left\langle v_\parallel \hat{e}_\parallel \cdot \vec{\nabla}_X \right\rangle_0 = v_\parallel \hat{e}_\parallel \cdot \vec{\nabla}_X$, $\langle \vec{v}(\lambda_{B1} + \lambda_{B2}) \rangle_{\ell 0} = \vec{v}_d \cdot \vec{\nabla}_X + (v_\perp^2/(2\Omega_\alpha))\hat{e}_\parallel \cdot \vec{\nabla}_x \times \hat{e}_\parallel)\hat{e}_\parallel \cdot \vec{\nabla}_x - i\ell\omega_\varphi = \vec{v}_d \cdot \vec{\nabla}_X + O((\lambda\Omega_\alpha)/q)$, and $\omega_\varphi = \left\langle \vec{v}_\perp \cdot \vec{\nabla}_x \varphi \right\rangle_0 = v_\parallel[\hat{e}_a(\hat{e}_\parallel \cdot \vec{\nabla}_x \hat{e}_b) - \hat{e}_\parallel(\vec{\nabla}_x \times \hat{e}_\parallel)/2]$. In appendix F we evaluate explicitly the terms $O((\lambda\Omega_\alpha)/q)$ that we are neglecting in the perturbed operator acting on the umperturbed function. We perform the calculation using the following assumptions: we keep the φ dependence only in the exponent, that is we consider the difference

between gyrocenter coordinates and regular coordinates only in the fast poloidal variation and the double barred quantities are taken as independent of φ and we use the well known equality[25]

$$e^{-i\frac{k_\perp v_\perp}{\Omega_\alpha}} = \sum_p e^{-ip\varphi} J_p(\frac{k_\perp v_\perp}{\Omega_\alpha})$$

By using this equality we can easily evaluate the three integrals

$$\frac{1}{2\pi} \int_0^2 \pi e^{-i\frac{k_\perp v_\perp}{\Omega_\alpha} \sin\varphi + i\ell\varphi} d\varphi = J_\ell(k_\perp v_\perp \Omega_\alpha)$$

$$\frac{1}{2\pi} \int_0^2 \pi e^{-i\frac{k_\perp v_\perp}{\Omega_\alpha} \sin\varphi + i\ell\varphi} \sin\varphi \, d\varphi = i\frac{\partial}{\partial\left(\frac{k_\perp v_\perp}{\Omega_\alpha}\right)} J_\ell(k_\perp v_\perp \Omega_\alpha)$$

$$\frac{1}{2\pi} \int_0^2 \pi e^{-i\frac{k_\perp v_\perp}{\Omega_\alpha} \sin\varphi + i\ell\varphi} \cos\varphi \, d\varphi = \frac{\ell\Omega_\alpha}{k_\perp v_\perp} J_\ell\left(\frac{k_\perp v_\perp}{\Omega_\alpha}\right)$$

Using these formulas, recalling that $k_\perp = -\frac{m}{r}$, $\vec{v}_\perp = v_\perp(\cos\varphi \hat{e}_\theta + \sin\varphi \hat{e}_r)$, and defining $k_\parallel \equiv n/(Rq(r))(q(r) - m/n_0)$, we obtain

$$\langle L_{g1}F_{g0}\rangle_\ell = -\frac{q}{m} e^{-i\omega t - im\theta_g + in_0\zeta_g}$$
$$\left\{ \left(\overline{\overline{E}}_{g1\theta}\frac{\ell}{\xi} J_\ell(\xi) + \overline{\overline{E}}_{g1r} iJ_\ell'(\xi) \right) v_\perp \left(\frac{\partial}{\partial\mathcal{E}} + \frac{1}{B}\frac{\partial}{\partial\mu} \right) F_{g0} \right.$$
$$- \frac{k_\parallel v_\parallel}{\omega} \left(\overline{\overline{E}}_{g1\theta}\frac{\ell}{\xi} J_\ell(\xi) + \overline{\overline{E}}_{g1r} iJ_\ell'(\xi) \right) \frac{v_\perp}{B}\frac{\partial F_{g0}}{\partial\mu}$$
$$+ J_\ell(\xi) \left[-\overline{\delta E_{g\theta}}\hat{e}_b + \overline{\overline{E}}_{g1r}\hat{e}_a \right] \cdot \vec{\nabla}_X F_{g0}$$
$$- \frac{i}{\omega} \left[J_\ell(\xi)\frac{v_\parallel}{\Omega_\alpha}(\vec{\nabla} \times \vec{E}_{1g}) \cdot \vec{\nabla}_X F_{g0} \right.$$
$$\left. + v_\perp\hat{e}_\parallel \cdot (\vec{\nabla} \times \vec{E}_{1g}) \left(\frac{\ell}{\xi} J_\ell(\xi)\hat{e}_\theta + iJ_\ell'(\xi)\hat{e}_r \right) \cdot \vec{\nabla}_X F_{g0} \right] \right\} (E-9)$$

where $\xi = (k_\perp v_\perp/\Omega_\alpha)$. To evaluate the next term, we use explicitly $\vec{\nabla}_x \sim i\vec{k}$. As it turns out for this term, we actually only need to consider $\vec{k} \sim k_\perp\hat{e}_\theta$ since the corrections related to $k_\parallel$ are of higher order in a term that is already $O(\lambda)$. Consistently we can neglect corrections proportional to $\partial/(\partial r)$. We find:

$$\left\langle \frac{1}{B}\frac{\partial F_{g0}}{\partial \mu}[L_{v1}\tilde{\beta}]_g \right\rangle_\ell = -\frac{q}{m}\frac{v_\perp}{B}\frac{\partial F_{g0}}{\partial \mu}\Bigg\{$$

$$\left(-\frac{k_\perp v_{d\theta}}{\omega}\left(\overline{\overline{E}}_{g1\theta}\frac{\ell}{\xi}J_\ell(\xi)+\overline{\overline{E}}_{g1r}iJ'_\ell(\xi)\right)\right)\frac{v_\perp}{B}\frac{\partial F_{g0}}{\partial \mu}$$

$$-\frac{v_\perp}{v_\perp^2/2+v_\parallel^2}\Bigg[\overline{\overline{E}}_{g1\theta}v_{d\theta}\left(J_\ell+J''_\ell\right)+\frac{1}{i}\left(\overline{\overline{E}}_{g1\theta}v_{dr}+\overline{\overline{E}}_{g1r}v_{d\theta}\right)$$

$$\times\left(\frac{\ell}{\xi^2}J_\ell-\frac{\ell}{\xi}J'_\ell\right)-\overline{\overline{E}}_{g1r}v_{dr}J''_\ell\Bigg]\Bigg\}\qquad (E-10)$$

The last term that has to be evaluated is

$$\left\langle \tilde{\beta}L_{g1}\frac{1}{B}\frac{\partial F_{g0}}{\partial \mu}\right\rangle_\ell = \frac{q}{m}v_\perp^2\Bigg\{$$

$$\overline{\overline{E}}_{g1\theta}\left[v_{d\theta}(J_\ell+J''_\ell)+\frac{v_{dr}}{i}\left(\frac{\ell}{\xi^2}J_\ell-\frac{\ell}{\xi}J'_\ell\right)\right]$$

$$+\overline{\overline{E}}_{g1r}\left[\frac{v_{d\theta}}{i}\left(\frac{\ell}{\xi^2}J_\ell-\frac{\ell}{\xi}J'_\ell\right)-v_{dr}J''_\ell\right]\Bigg\}\times$$

$$\times\left(\frac{\partial}{\partial \mathcal{E}}+\frac{1}{B}\frac{\partial}{\partial \mu}\right)\frac{1}{B}\frac{\partial F_{g0}}{\partial \mu}\Bigg\}\qquad (E-11)$$

We can now go back to Eq. (E-8), and note that if we consider resonance, that is $\omega \sim \ell\Omega_\alpha$, the terms $\tilde{L}_{g\ell,\ell'}$ can be neglected as higher order contributions. To proceed with the calculation we make the further assumption that we can use the "local" approximation, and thus we neglect gradients acting on $\langle \delta F_{g\alpha}\rangle_\ell$. Given this we obtain:

$$\langle \delta F_{g\alpha}\rangle_\ell = \frac{i}{\omega-k_\parallel v_\parallel-k_\perp v_d-\ell\Omega_\alpha}\{R.H.S.\}$$

where $ik_\parallel \equiv \hat{e}_\parallel \cdot \vec{\nabla}_X$, and $ik_\perp \equiv \hat{e}_a \cdot \vec{\nabla}_X$. We can now calculate $\delta \vec{J}_\alpha = q\, n_\alpha \int d^3v\ \vec{v}\ \delta F_\alpha$ and perform the φ integration, in order to find an expression for the conductivity $\delta \vec{J}_\alpha \equiv \overset{\leftrightarrow}{\delta\sigma}_\perp \cdot \vec{E}_{1\perp}$. It is convenient to define $\overset{\leftrightarrow}{\delta\Sigma}$ such that

$$\overset{\leftrightarrow}{\delta\sigma}_\perp = \int v_\perp^2 dv_\perp dv_\parallel 2\pi^2\delta(\omega-k_\parallel v_\parallel-k_\perp v_d-\ell\Omega_\alpha)\overset{\leftrightarrow}{\delta\Sigma}$$

The variuos components of the tensor $\overset{\leftrightarrow}{\delta\Sigma}$ are

$$\delta\Sigma_{\theta\theta} = a_\theta \frac{\ell}{\xi} J_\ell$$

$$\delta\Sigma_{\theta r} = a_r \frac{\ell}{\xi} J_\ell$$

$$\delta\Sigma_{r\theta} = a_\theta(-iJ'_\ell)$$

$$\delta\Sigma_{rr} = a_r(-iJ'_\ell)$$

where

$$
\begin{aligned}
a_\theta =& \frac{\ell}{\xi} J_\ell v_\perp \left[\frac{\partial}{\partial \mathcal{E}} + \left(1 - \frac{k_\parallel v_\parallel}{\omega} - \frac{k_\perp v_{d\theta}}{\omega}\right) \frac{1}{B}\frac{\partial}{\partial \mu} \right] F_{g0} \\
&- \left[v_{d\theta}\left(J_\ell + J''_\ell\right) + \frac{v_{dr}}{i}\left(\frac{\ell}{\xi^2}J_\ell - \frac{\ell}{\xi}J'_\ell\right) \right] \times \\
&\left(\frac{v_\perp^2}{v_\perp^2/2 + v_\parallel^2} + v_\perp^2\left(\frac{\partial}{\partial \mathcal{E}} + \frac{1}{B}\frac{\partial}{\partial \mu}\right)\right) \frac{1}{B}\frac{\partial F_{g0}}{\partial \mu}
\end{aligned}
\qquad (E-12)
$$

$$
\begin{aligned}
a_r =& iJ'_\ell v_\perp \left[\frac{\partial}{\partial \mathcal{E}} + \left(1 - \frac{k_\parallel v_\parallel}{\omega} - \frac{k_\perp v_{d\theta}}{\omega}\right) \frac{1}{B}\frac{\partial}{\partial \mu} \right] F_{g0} \\
&- \left[\frac{v_{d\theta}}{i}\left(\frac{\ell}{\xi^2}J_\ell - \frac{\ell}{\xi}J'_\ell\right) - v_{dr}J''_\ell \right] \times \\
&\left(\frac{v_\perp^2}{v_\perp^2/2 + v_\parallel^2} + v_\perp^2\left(\frac{\partial}{\partial \mathcal{E}} + \frac{1}{B}\frac{\partial}{\partial \mu}\right)\right) \frac{1}{B}\frac{\partial F_{g0}}{\partial \mu}
\end{aligned}
\qquad (E-13)
$$

We notice that $\delta\Sigma_{r\theta} = (\delta\Sigma_{\theta r})^*$ only to lowest order in λ.

Appendix F.

Example of an Explicit Calculation for an $O(\lambda/q)$ Term

As a result of the considered choice of variables and gyrokinetic average, we have that the equilibrium distribution function includes corrections proportional to the quantity

$$\tilde{\beta} = - \left[\vec{v}_\perp \cdot \vec{v}_d + \int^\varphi \frac{d\varphi'}{\Omega_\alpha} v_\| \left(\vec{v}_\perp \cdot \vec{\nabla}_x \hat{e}_\| \cdot \vec{v}_\perp - \frac{v_\perp^2}{2} \vec{\nabla}_x \cdot \hat{e}_\| \right) \right]$$

$v_\|$ has to be replaced by

$$\tilde{v}_\| = v_\| + \frac{v_\perp^2}{2\Omega_\alpha} \hat{e}_\| \cdot \nabla_x \times \hat{e}_\|$$

and we have a new resonant frequency

$$\omega_\varphi = \left\langle \vec{v}_\perp \cdot \vec{\nabla}_x \varphi \right\rangle_0 = v_\| [\hat{e}_a (\hat{e}_\| \cdot \vec{\nabla}_x \hat{e}_b) - \hat{e}_\| (\vec{\nabla}_x \times \hat{e}_\|)/2]$$

The correction to the parallel velocity, as well as the quantity ω_φ come from performing the average on the local gyrophase and the local parallel unit vector.

We can estimate the $\vec{v}_\perp \cdot \nabla_x \hat{e}_\parallel \cdot \vec{v}_\perp$ term in the $\tilde{\beta}$ correction, as well as the terms related to the $\tilde{v}_\parallel$ and ω_φ corrections. All these terms are of same order, so we just perform the calculation for one as an example and we look at $\hat{e}_\parallel \cdot \vec{\nabla}_x \times \hat{e}_\parallel$. We will show that these terms are corrections of order λ/q so that we can neglect them. Consistently we can neglect terms like $\vec{v}_\perp \cdot \nabla_x \vec{v}_\parallel \cdot \vec{E}_{1g}$ that are of the same order.

The leading order term in the curvature drift velocity is:

$$\hat{e}_\parallel \cdot \nabla_x \hat{e}_\parallel \simeq \hat{e}_\zeta \cdot \nabla_x \hat{e}_\zeta = -\frac{1}{R}\cos\theta \hat{e}_r + \frac{1}{R}\sin\theta \hat{e}_\theta$$

Let us evaluate and compare with this term the quantity

$$\hat{e}_\parallel \cdot \vec{\nabla}_x \times \hat{e}_\parallel = \hat{e}_\parallel \cdot \vec{\nabla}_x \times \hat{e}_\zeta + \hat{e}_\parallel \cdot \vec{\nabla}_x \times \left(\frac{B_\theta}{B_0}\hat{e}_\theta\right) =$$

$$= \hat{e}_\zeta \cdot \vec{\nabla} \times \hat{e}_\zeta + \frac{B_\theta}{B_0}(\nabla \times \hat{e}_\zeta)_\theta + \frac{B_\theta}{B_0}(\nabla \times \hat{e}_\zeta)_\zeta - \hat{e}_\parallel \cdot \left(\hat{e}_\theta \times \nabla\frac{B_\theta}{B_0}\right) =$$

$$= \frac{B_\theta}{B_0}\frac{\cos\theta}{R} - \frac{B_\theta}{B_0}\frac{1}{r} - \hat{e}_\parallel \cdot \left(\hat{e}_\theta \times \nabla\frac{B_\theta}{B_0}\right)$$

In this expression the highest order term is $B_\theta/(B_0 r)$ that is $O(1/qR)$ respect to the curvature drift velocity corrections. It is clear from this that we are consistently neglecting the curvature of the poloidal field.

Appendix G

The Omega Star Contribution to the Perturbed Vlasov Operator

In performing the growth rate calculation we have neglected the terms proportional to the spatial gradient of the equilibrium α-particles distribution function, since our instability is mainly a velocity space instability and we concentrated our efforts into evaluating the velocity dependence of the equilibrium α-particle distribution function, loosing specific infomations about the spatial gradients. However for sake of completeness we can evaluate the gyroaverage of the terms proportional to the spatial gradients of the alpha particles, for the mode that we are considering. We recall that in our case $E_{1\parallel} \simeq 0$, $\hat{e}_{\parallel} \cdot \vec{\nabla}_X = 0$, and the electric fields are radially confined modes , with high poloidal numbers, so that $k_{\perp} \simeq -m/r$. We find:

$$\left\langle (\vec{E}_1 + \frac{1}{c}\vec{v} \times \vec{B}_1) \times \frac{\hat{e}_{\parallel}}{\Omega} \right\rangle_0 \cdot \vec{\nabla}_X F_{g\alpha} = -\frac{q}{m}e^{-i\omega t - im\theta_g + in^0\zeta_g} \times$$

$$\left\{ \frac{J_{\ell}}{\Omega_{\alpha}} \left[-\overline{\overline{E}}_{g1\theta}\hat{e}_r + \overline{\overline{E}}_{g1r}\hat{e}_{\theta} \right] \cdot \vec{\nabla}_X F_{g\alpha} \right.$$

$$- \frac{i}{\omega} J_\ell \frac{v_\parallel}{\Omega_\alpha} \left[(\vec{\nabla}_x \times \vec{E}_{1\perp}) - (\hat{e}_\parallel \cdot (\vec{\nabla}_x \times \vec{E}_{1\perp}))\hat{e}_\parallel \right] \cdot \vec{\nabla}_X F_{g\alpha}$$

$$- \frac{i}{\omega} \frac{v_\perp}{\Omega_\alpha} \hat{e}_\parallel \cdot (\vec{\nabla}_x \times \vec{E}_{1\perp}) \left[\frac{\ell}{\xi} J_\ell \hat{e}_\theta + i J_\ell' \hat{e}_r \right] \cdot \vec{\nabla}_X F_{g\alpha} \Bigg\} \qquad (G-1)$$

If we assume that the highest order contribution is from $\vec{\nabla}_x \times \vec{E}_{1\perp} \simeq \hat{e}_\parallel(-im/r E_{1r})$ we have that

$$\left\langle (\vec{E}_1 + \frac{1}{c}\vec{v} \times \vec{B}_1) \times \frac{\hat{e}_\parallel}{\Omega} \right\rangle_0 \cdot \vec{\nabla}_X F_{g\alpha} = -\frac{q}{m\Omega_\alpha} e^{-i\omega t - im\theta_g + in^0 \zeta_g}$$

$$\left\{ \left[-J_\ell \overline{\overline{E}}_{g1\theta} + i\frac{k_\perp v_\perp}{\omega} J_\ell' \overline{\overline{E}}_{g1r} \right] \hat{e}_r \cdot \vec{\nabla}_X F_{g\alpha} \right.$$

$$\left. + \left[J_\ell \left(1 + l\frac{\Omega_\alpha}{\omega} \right) \overline{\overline{E}}_{g1r} \right] \hat{e}_\theta \cdot \vec{\nabla}_X F_{g\alpha} \right\} \qquad (G-2)$$

REFERENCES

[1]. JET Team, Phys. of Fluids B5 (1993) 3

[2]. J. Cottrell et al., Nucl. Fusion 33 (1993) 1365

[3]. G. J. Greene, Proceeding of the 17th International Conference on Controlled Fusion and Plasma Heating, European Physical Society, Amsterdam, 14B (IV), (1994) p. 1540

[4]. J.D. Strachan et al., Nucl. Fusion 72 (1994) 3526

[5]. S. Cauffman, R. Majeski, Rev. Sci. Instrum. 66 (1995) 817

[6]. B. Coppi, S. Cowley, R. Kulsrud, P. Detragiache, F. Pegoraro, Phys. of Fluids, 29 (1986) 4060

[7]. B. Coppi, Phys. Lett. A 172 (1993) 439

[8]. B. Coppi, Fusion Tech. 25 (1994) 326

[9]. B. Coppi, AIP Conference Proceedings 311(1993) 47

[10]. M.N. Rosenbluth, Microinstabilities,Plasma Physics, IAEA, Vienna (1965) Section IV, p.485

[11]. "Excitation of Contained Modes by High Energy Nuclei and Correlated Cyclotron Emission", B. Coppi, G. Penn, C. Riconda, PTP-96/02, LOG-10386, M.I.T.

[12]. G. Penn, M.I.T. Thesis

[13]. T.S. Stringer, Plasma Phys. 16 (1974) 651

[14]. C.M. Bender, S.A. Orszag, Advanced Mathematical Methods for Scientists and Engineers, McGraw-Hill (1987)

[15]. L. Chen, S.T. Tsai, Plasma Phys. 25 (1983) 349

[16]. X.S. Lee, J.R. Myra, P.J. Catto, Phys. Fluids 26 (1983) 223

[17]. A.B. Mikhailovskii, Rev. of Plasma Phys., ed. Leontovich, N.Y., (1986) Vol. 9, p. 103

[18]. A.B. Mikhailovskii, Theory of Plasma Instabilities, Consultants Bureau, N.Y. (1974) Vol. 2, p. 271

[19]. N.N. Gorelenkov, C.Z. Cheng, Phys. Plasmas 2 (1995) 1

[20]. Ya. I. Kolesnichenko, Nucl. Fus. 20 (1980) 727

[21]. V.S. Belikov, Ya. I. Kolesnichenkov Fusion Tech. 25 (1983) 259

[22]. R.O. Dendy, C.N. Lashmore-Davies, K.G. Mc Clemens, G.A. Cottrell, Phys. Plasmas 1 (1994) 1918

[23]. K.G. McClemens, R.O. Dendy, C.N. Lashmore-Davies, G.A. Cottrell, S. Cauffman, R. Majeski, Phys. Plasmas 3 (1996) 543

[24]. Y.P. Chen, S.T. Tsai, Phys. Plasmas 2 (1995) 3049

[25]. I.S. Gradshteyn, I.M. Ryzhik, Tables of Integrals and Sums, Series and Products, Revised Edition, Academic Press, San Diego, (1980)

[26]. J.P. Freidberg, Ideal Magnetohydrodynamics, Plenum Press, N.Y. (1987)

[27]. N.A. Krall, A. W. Trivelpiece, Principles of Plasma Physics, San Francisco Press, San Francisco (1986)

[28]. N. Sckopke et al., J. Geophys. Res. 95 (1990) 6337

[29]. V.D. Shapiro, K.B. Quest, M. Okolicsanyi, Bulletin of the APS, 38th Meeting of the Division of Plasma Physics, Denver, Colorado, Vol. 41 (1996) 7Q 16 p. 1544